2292E

ENVIRONMENTAL RESEARCH

RESEARCH AND TECHNOLOGY BRANCH

MODELLING CONCENTRATION FLUCTUATIONS IN THE ATMOSPHERE

RAC 389C

FINAL REPORT

Ontario Environment Environnement

ISBN 0-7729-9790-X

MODELLING CONCENTRATION FLUCTUATIONS IN THE ATMOSPHERE

RAC 389C

FINAL REPORT

Report prepared by:

A. Ciccone, Ph.D., P.Eng.
E. Alp, Ph.D., P.Eng.
Concord Environmental Corporation

DECEMBER 1993

Cette publication technique n'est disponible qu'en anglais.
Copyright: Queen's printer for Ontario, 1993

This publication may be reproduced for non-commercial purposes with appropriate attribution.

PIBS 2292

ACKNOWLEDGEMENT AND DISCLAIMER

This report was prepared for the Ontario Ministry of Environment and Energy (formerly Ministry of the Environment) as part of a Ministry funded project. The views and ideas expressed in this report are those of the author(s) and do not necessarily reflect the views and policies of the Ministry of Environment and Energy, nor does mention of trade names or commercial products constitute endorsement or recommendation for use. The Ministry, however, encourages the distribution of information and strongly supports technology transfer and diffusion. Note, all references to the Ministry of Environment in the report should read Ministry of Environment and Energy.

Any person who wishes to republish part or all of this report should apply for permission to do so to the Research and Technology Section, Fiscal Planning and Information Management Branch, Ontario Ministry of Environment and Energy, 135 St. Clair Ave. W., Toronto, Ontario, M4V 1P5, Canada.

Copyright: Queen's printer for Ontario
This publication may be reproduced for non-commercial purpose with appropriate attribution.

TABLE OF CONTENTS

TABLE OF CONTENTS (Cont'd)

LIST OF TABLES

LIST OF FIGURES

LIST OF FIGURES (Cont'd)

LIST OF FIGURES (Cont'd)

LIST OF FIGURES (Cont'd)

LIST OF FIGURES (Cont'd)

EXECUTIVE SUMMARY

A mathematical modelling system to predict the magnitude and frequency of peak concentrations which make-up the time averaged mean concentration has been developed and implemented. The modelling system uses dispersion and meteorological parameters calculated via the Ontario Ministry of the Environment GAS model to drive the Empirical Gaussian Model (EGM) to estimate concentration intensity and plume intermittency. These results are used in a log-normal distribution model to determine "quasi" instantaneous concentrations at various percentile levels.

The modelling system was evaluated against recent full-scale experiments carried out in Alberta. The field experiments were carried out during low-wind stable atmospheric dispersion conditions. The results of the evaluation study indicate that the EGM should be used only under limited conditions. These conditions are for winds greater than 3 m/s and for crosswind distances less than σ_y.

A sensitivity analysis of the wind tunnel-derived constants in the EGM showed that the model is very sensitive to a constant used to determine the dissipation time scale. The model results seem linearly dependent to changes in the other constants.

The log-normal distribution was found to be inadequate as a model to predict peak concentrations. The exponential distribution was determined to be a better model performer in the current full-scale evaluation.

The EGM was assessed to be incompatible with the GAS convective dispersion model based on theoretical grounds. Recommendation for an appropriate convective concentration fluctuation model have been made as well as for further work.

ACKNOWLEDGEMENT

The Alberta Energy Resources Conservation Board (ERCB) is gratefully acknowledged for the use of the meteorological and tracer gas data. Special thanks to Linda Holizki for her support in allowing the use of the data.

Grateful acknowledgements to Mr. Mervyn Davis of Concord for his assistance and discussion in meteorology and the field experiments. Special thanks to Dr. David Wilson of the University of Alberta for many insightful discussions on modelling concentration fluctuations.

1 INTRODUCTION

This report documents the work carried out by Concord Environmental Corporation under contract to Ontario Ministry of the Environment (Purchase Order A-10521, Project No.: 389c) on "Modelling of Concentration Fluctuations in the Atmosphere".

1.1 BACKGROUND

The concentration of a contaminant at a fixed point in a plume in the atmosphere is highly variable, with a mean deviation comparable to the time average, and peaks reaching a factor of five or more times the average. A typical time trace of concentration is shown in Figure 1-1. Here, c is instantaneous concentration, $\bar{c}$ is a time average over period T, c' is the instantaneous deviation from the average. The plume can be highly intermittent which suggests that the concentration may drop to zero for short time periods during the total period T. An intermittency factor is typically used for describing the fraction of time non-zero concentrations are present at the measurement point.

A knowledge of the magnitude and frequency of the peaks is essential from a regulatory point of view if avoidance of significant occurrence of nuisance odours is desired.

Information on concentration peaks is also necessary for emergency planning purposes for accidental releases of toxic or flammable gases, since actual danger zones could be significantly larger than those estimated based on average concentrations alone. This situation is schematically shown in Figure 1-2, where a ground level hazard-threshold concentration isopleth based on time-averaged concentration is shown as the inner ellipse. This threshold can be exceeded instantaneously for a large percentage (30-50%) of the time. Actual danger levels, however, may persist down to much smaller time-averaged concentration levels, for example, where the hazard threshold is exceeded perhaps only 5% of the time.

FIGURE 1-1

Typical Time Variation of Instantaneous Concentration of a Contaminant in a Plume

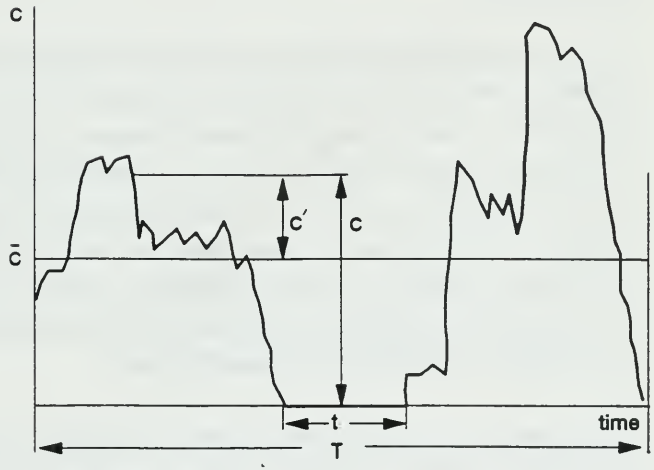

Intermittency : fraction of time non-zero concentration is present at the measurement point

$$\gamma = \frac{T-t}{T}$$

FIGURE 1-2

Hazard Zones of a Plume based on Different Exceedance Probabilities of a Hazard Threshold

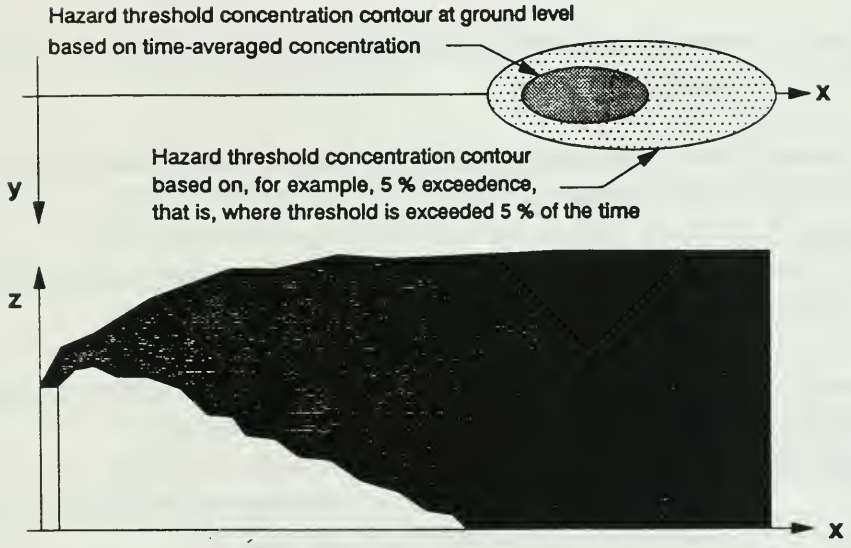

Such a level is shown in Figure 1-2 as the outer ellipse. Clearly, the actual hazard area could be significantly larger than that based on time-averaged concentrations.

1.2 STUDY OBJECTIVE

To predict the probability or risk of peak exposures, a modelling system is required to estimate the magnitude and frequency of concentration fluctuations under a variety of meteorological conditions and for different source types.

A modelling system for concentration fluctuations consists of three basic components:

1) a module to estimate the time-averaged concentrations at receptor points of interest,

2) a module to estimate the plume intermittency (γ) and the time-averaged fluctuation intensity ($\overline{c'^2}/\overline{c}^2$) at that receptor,

3) a model to estimate the shape of the frequency distribution of fluctuations that make up the time-average fluctuation intensity.

The objective of the present study is to develop a mathematical model which can provide estimates of the probability of peak exposures.

1.3 REPORT OUTLINE

After this brief introduction, a basic mathematical framework is established in Section 2 describing concentration fluctuations in mathematical terms, together with some definitions to set the stage for the remainder of the report.

In Section 3, examples found in the literature on modelling of concentration fluctuations are reviewed. The literature review presents the current state-of-the-art for the prediction of fluctuations from which an objective analysis can be made.

In Section 4, the framework of the model developed in this study, and the model components are described. The model, in its current form, uses OME Clean Air Program formulations, Wilson's Empirical Gaussian Model and a log-normal distribution, and is ready for immediate use by the OME for regulatory applications.

A description of the ERCB field program on which model evaluation will be based on is presented in Section 5.

Section 6 presents results of the sensitivity analysis on how model predictions vary in response to changes in input parameters as well as to changes in some of the empirical constants embedded in the model equations. This analysis is conducted to establish which input parameters and empirical model constants are of importance, so that more emphasis can be put in refining them in future work.

Comparison of model predictions to field experiments is presented in Section 7. These comparisons are done in two stages; one for examining and validating the fluctuation model component, and two for examining the complete model including the time-average model.

Conclusions of the study and recommendations for future work are presented in Section 8.

2 MATHEMATICAL DESCRIPTION OF CONCENTRATIONS FLUCTUATIONS: GENERAL DEFINITIONS NOMENCLATURE

Referring to Figure 1-1, the instantaneous concentration can be expressed in terms of a time average and an instantaneous deviation about this time average:

$$c = \bar{c} + c' \quad (c \geq 0) \qquad [2.1]$$

where:

- c = instantaneous concentration
- $\bar{c}$ = time average over period T
- c' = instantaneous deviation from the time average

The time-average concentration is defined by the integral:

$$\bar{c} = \frac{1}{T} \int_{t}^{t+T} c \, dt \qquad [2.2]$$

which is typically predicted with the aid of tradition dispersion models (i.e., the OME GAS model).

For instances when the plume (i.e., non-zero concentration) is present at the measurement point,

$$c = \overline{c_p} + c_p' \quad (c > 0 \text{ only}) \qquad [2.3]$$

where subscript p denotes in-plume or conditional values.

There is a relationship between unconditional and conditional statistics. By definition, the intermittency, γ, is the fraction of non-zero events in a time series and P(c) is the probability that the concentration c(t) exceeds c; thus, the cumulative distribution functions are coupled via,

$$P(c) = \gamma P_p(c) \quad ; \quad c \geq 0$$
$$= 1 \quad ; \quad c < 0 \qquad [2.4]$$

where $P_p(c)$ is the conditional cumulative distribution.

Further, the pdf is $p(c) = - dP(c)/dc$, so

$$p(c) = \gamma p_p(c) + (1 - \gamma)\delta(c) \quad (c \geq 0)$$
$$= 0 \qquad\qquad (c < 0) \qquad [2.5]$$

where the dirac function is the result of the discontinuity in p(c) at the origin. The n-th concentration moment is defined as

$$\overline{c^n} = \int_o^\infty c^n p(c)\, dc \qquad [2.6]$$

and the unconditional and conditional n-th moments are related via,

$$\overline{c^n} = \gamma \overline{c_p^n} . \qquad [2.7]$$

The first central moments or means are related via,

$$\bar{c} = \gamma \bar{c}_p . \qquad [2.8]$$

and the fluctuating components are

$$c' = c - \bar{c} . \qquad c \geq 0$$
$$c_p' = c - \bar{c}_p \qquad c > 0 \qquad [2.9]$$

Using (2.7), the second central moment or variance is,

$$\overline{c'^2} = \overline{(c - \bar{c})^2} = \gamma \overline{c'^2_p} + \gamma(1 - \gamma)\bar{c}_p^2 \qquad [2.10]$$

and the concentration intensity is,

$$i^2 = \frac{i_p^2}{\gamma} + \frac{(1 - \gamma)}{\gamma} \quad . \qquad [2.11a]$$

or

$$\gamma = \frac{i_p^2 + 1}{i^2 + 1} \qquad [2.11b]$$

where:

$$i^2 = \overline{c'^2} / \bar{c}^2 \qquad [2.12a]$$

and

$$i_p^2 = \overline{c'^2}_p / \bar{c}_p^2 \quad . \qquad [2.12b]$$

Similar relationships between higher-order moments can also be derived.

3 LITERATURE SURVEY AND MODEL SELECTION

Concentration fluctuations in a plume are a result of two physically distinct atmospheric processes. The first is related to small scale mixing and the second to large scale atmospheric motions.

Small scale mixing occurs within a marked volume of fluid or plume. Here parcels of fluid from various origins (i.e., contaminated and clean air) intermingle with each other to generate fluctuations in concentration at points relative to the centre of mass or centerline of the plume. These fluctuations are analogous to turbulent velocity or temperature fluctuations in a turbulent flow and are generally termed "in-plume" fluctuations.

The second process reflects the concentrations at a position which is fixed relative to the source. Here, fluctuations occur due to the varying relative distance between plume-centerline and the fixed position. The plume is physically moved by the large scale motions of the atmosphere and this has been termed "meandering".

The two processes can be superimposed onto each other to describe the atmospheric process of dispersion. Under high winds and neutral stability conditions, an elevated plume from a point source does not generally meander but stays in a well-defined "cone" shape as it travels downwind. Dispersion is a result of small-scale mixing. Meandering is most apparent under stable, low wind conditions where the plume oscillates in the cross-wind direction but does not spread very rapidly. Generally, the plume meandering component dominates the fluctuations from small sources at travel times less than one Lagrangian time scale ($t < T_L$) and the in-plume component dominates from broad sources at all times or from small sources at large travel times ($t >> T_L$).

Concentration fluctuation models can be classed as follows (Hanna, 1984):

1) K-models;
2) Empirical Gaussian models;
3) Similarity models;
4) Meandering plume models;
5) PDF models;
6) Statistical models; and
7) Second order closure and large eddy simulation models.

The first three adequately handle in-plume conditions, the fourth and fifth are primarily for meandering while the last two are capable of handling both.

3.1 UNCONDITIONAL CONCENTRATION FLUCTUATION MODELS

The following describes models which predict the unconditional concentration variances ($\overline{c'^2}$) or intensity (i).

3.1.1 K-Models

As mentioned above, concentration fluctuations can be regarded in a similar context as turbulent velocity fluctuations where the instantaneous concentration is given as

$$c = \bar{c} + c' \qquad [3.1]$$

In the same fashion as per turbulent kinetic energy, a conservation equation can be constructed for the mean square concentration fluctuation ($\overline{c'^2}$) or variance. The conservation equation contains an advection term, a production term which contains the product of the flux and its mean gradients, a divergence or diffusion of the flux term, and a dissipation term which represents the smoothing out of fluctuations by molecular action:

$$Q_A + Q_p + Q_D + Q_\epsilon = 0 \qquad [3.2]$$

advection:

$$Q_A = U_o \frac{\partial \overline{c'^2}}{\partial x} \qquad [3.2a]$$

production:

$$Q_p = +2\overline{v'c'}\,\frac{\partial \overline{c}}{\partial y} + 2\overline{w'c'}\,\frac{\partial \overline{c}}{\partial z} \qquad [3.2b]$$

diffusion:

$$Q_D = +\frac{\partial}{\partial y}\left(\overline{v'c'^2}\right) + \frac{\partial}{\partial z}\left(\overline{w'c'^2}\right) \qquad [3.2c]$$

dissipation:

$$Q_\epsilon = 2D\left[+\overline{\left(\frac{\partial c'}{\partial y}\right)^2} + \overline{\left(\frac{\partial c'}{\partial z}\right)^2}\right] \qquad [3\text{-}2d]$$

where v' and w' are the fluctuation velocity components in the y and z directions, respectively, and D is molecular diffusivity. As in the turbulent velocity fluctuation in boundary-layer, gradients along the x-axis are assumed small as compared to gradients in the lateral and vertical directions, and molecular diffusion is assumed negligible.

Csanady (1967, 1973) and subsequently Netterville (1979) considered the solution to the above with various simplifications and assumptions:

i) The turbulent flux of the mean and the variance are described by a gradient-transfer relationship with a common value of eddy diffusivity (K).

ii) This distribution of $\overline{c'^2}$ is self-similar in the x-direction as is $\bar{c}$. This implies a universal function of y/L where L is a length scale associated with the spread of $\bar{c}$.

iii) The dissipation rate of $\overline{c'^2}$ is assumed to be proportional to $\overline{c'^2}/T_d$, where T_d is the dissipation time scale which increases linearly with distance.

The above assumptions change the conservation equation to:

$$U_o \frac{\partial \overline{c'^2}}{\partial x} = K_y \frac{\partial^2 \overline{c'^2}}{\partial y^2} + K_z \frac{\partial^2 \overline{c'^2}}{\partial z^2} + 2 K_y \left(\frac{\partial \bar{c}}{\partial y}\right)^2 + 2 K_z \left(\frac{\partial \bar{c}}{\partial z}\right)^2 - \frac{\overline{c'^2}}{T_d} \qquad [3.3]$$

where the first and second terms on the right hand side are diffusion, the third and fourth terms are production and the last term is dissipation.

The above shows that variance production is greatest near the source where the mean concentration gradients are the largest. These gradients decrease with downwind distance indicating that the production term becomes negligible.

Assuming that $K_y = K_z = K$ (constant) and that production and dissipation levels are small, the solution to the above is equivalent to a Gaussian crosswind distribution (Csanady, 1973). Assuming that the vertical and cross-wind spreads (σ_y and σ_z) are proportional to $\sqrt{K_y t}$ and $\sqrt{K_z t}$ respectively, further manipulation of [3.3] leads to,

$$(\overline{c'^2})^{1/2} = (\overline{c'^2_o})^{1/2} \exp(-y^2/4\sigma_y^2) \exp(-z^2/4\sigma_z^2)$$

[3.4a]

$$or \quad i = \frac{(\overline{c'^2})^{1/2}}{\bar{c}} = \frac{(\overline{c'^2_o})}{\bar{c}_o} \exp(y^2/4\sigma_y^2) \exp(z^2/4\sigma_z^2)$$

where subscript o refers to centerline values, and

$$\bar{c} = \bar{c_o} \exp(-1/2 \frac{y^2}{\sigma_y^2})(\exp(-1/2\ z^2/\sigma_z^2) \qquad [3.4b]$$

is mean concentration.

The above shows that the fluctuations decrease at a slower rate than the mean concentration in the crosswind direction which subsequently maximizes the total concentration intensity (i) at the plume edges.

3.1.2 Empirical Gaussian Model

The above Gaussian formula forms the basis of the model developed by Wilson et al. (1982a, b) and Wilson (1982, 1986) to simulate concentration fluctuations from a continuous source. The model is ideally suited for in-plume fluctuations and does not directly deal with meandering.

The initial model proposed by Wilson et al. included a pair of point sources above and on either side of the plume axis which generated the variance source strength. This was done to account for the off-axis maximum in total variance production. Subsequently, Wilson and Simms (1985) revised this assumption to include a single variance point source above the plume axis. The following assumptions form the basis of the model:

1. The variation of $\overline{c'^2}$ in the cross-wind and vertical directions is a result of diffusion alone (using the same diffusivity as per the mean concentration $\bar{c}$).

2. Crosswind and vertical profiles of the variance are self-similar and only a function of the downwind distance.

3. The variance originates from a point source above the plume centerline where most of $\overline{c'^2}$ is observed to be produced due to the strong $\bar{c}$ gradients.

4. Surface dissipation of $\overline{c'^2}$ is approximated by an image sink with a strength equal to a fraction of the variance source.

5. The variance flux is not a conserved quantity like mass and decays with downwind distance due to dissipation by molecular diffusion. This "along-wind" dissipation is simulated based on balance between local advection and dissipation.

The Gaussian plume equation for $\overline{c'^2}$ is then

$$\overline{c'^2} = \left(\frac{q}{2\pi U \sigma_y \sigma_z}\right)^2 \left(\exp\left(1/2y^2/2\sigma_y^2\right)\right) \times \left[\left(\exp\left(-\frac{(z-h_v)^2}{2\sigma_z^2}\right) - \alpha \exp\left(-\frac{(z+h_v)^2}{2\sigma_z^2}\right)\right)\right] \quad [3.5]$$

where q is the variance source strength, α is the sink strength parameter and h_v is the variance source height given as

$$\left(\frac{h_v}{\sigma_z}\right)^2 = \left[\left(\frac{h}{\sigma_z}\right)^2 + \phi^2\right] \quad [3.6]$$

where h is the height of the plume centerline and ϕ is a constant.

Wilson et al. (1982b) argues that the upward displacement of the variance source term, above the release height, is reasonable because the zone of maximum $\overline{c'^2}$ production will drift upward as surface reflection flattens the mean concentration profile and reduces $\partial\bar{c}/\partial z$ near the ground. The above formulation is reasonable

since fluctuation levels are, intuitively, strongly dependent on the source size (laterally and vertically) and turbulent scale near the source and weakly dependent on source size further downwind.

The variance source strength (q) was developed from the conservation equation [3.3] and wind-tunnel observations showing advection in balance with dissipation. Wilson et al. (1982b) shows that the ratio of q to Q (mass emission rate) has a functional form

$$\frac{q}{Q} = \frac{C_2 \lambda}{(\lambda^2 + \lambda_0^2)^{C_1/2}} \qquad [3.7a]$$

$$\lambda_o = \frac{C_3}{C_4\left(\frac{L_w}{d} + 1\right)} \qquad [3.7b]$$

$$\lambda = \sqrt{\sigma_z \sigma_y}\ /H\ . \qquad [3.7c]$$

where C_1, C_2, C_3, and C_4, are wind-tunnel derived constants, d is the source diameter, H is the mixing layer depth and L_w is the average turbulent length scale felt by the plume. The term λ_o is a virtual origin which accounts for near source production. Wilson (1982) suggests

$$L_w = 0.6\ h \exp\left(-\left(\frac{\sigma_z}{h}\right)^2\right) \qquad [3.8]$$

as an appropriate formulation for turbulent length scale.

The above constants (α, ϕ, C_1, C_2, C_3 and C_4) were derived by Wilson via systematic curve fitting the wind tunnel data of Fackrell and Robins (1982a, b). Further development of the empirical Gaussian model will be discussed later.

3.1.3 Similarity Models

Similarity models are presently not well developed due to a lack of field data required to derive the generalized dimensionless relationships. Chatwin and Sullivan (1979) considered the relative diffusion of instantaneous puffs of dimension σ_o in explaining concentration fluctuations with the aid of similarity theory.

Neglecting the effect of molecular diffusion, Chatwin and Sullivan show that after a travel time t, the order of magnitude of $\overline{c}$ and $\overline{c'^2}$, for a cloud of initial size σ_o, are Q/σ^3 and $Q^2/\sigma_o{}^3\sigma^3$, respectively, in the bulk of the cloud where Q is the total emission and $\sigma = \sigma(t)$ is the mean current cloud dimension at time t after release. The asymptotic value for the concentration intensity (i) has an order of magnitude of

$$i \sim \left(\frac{\sigma(t)}{\sigma_o}\right)^{3/2} \sim \left(\frac{c_o}{c(t)}\right)^{1/2} \qquad [3.9]$$

where c_o is the initial cloud concentration and c is the cloud concentration at t.

3.1.4 Meandering Plume Model

Much of the work today on meandering plumes has its foundations on the work carried out by Gifford (1959) which dealt with concentration fluctuations brought about by oscillations or meandering of the instantaneous plume. This is often the dominant contribution to concentration fluctuations observed in field experiments. The concentration distribution within the instantaneous plume relative to its centerline is assumed to be constant. Gifford assumes that the plume is made up of a series of discs in the plane normal to the mean wind direction. Gifford decomposed the total variance $\overline{c'^2}$ into a variance $\overline{c'^2}_i$ which represents relative or instantaneous component of the disc centre and $\overline{c'^2}_m$ which is the variation of the displacement of disc centers from a fixed axis or the meandering component, i.e.,

$$\overline{c'^2} = \overline{c_I'^2} + \overline{c_M'^2} \qquad [3.10]$$

The above assumes that there are no in-plume fluctuations within the instantaneous plume.

The variance for the above under isotropic conditions was given as

$$\overline{c'^2} = \frac{Q^2}{(2\Pi u)^2} \frac{\exp\left(\frac{-(y^2+z^2)}{2\sigma_{ym}^2+\sigma_{yI}^2}\right)}{\sigma_{yI}^2(2\sigma_{ym}^2+\sigma_{yI}^2)} - \frac{\exp\left(\frac{-(y^2+z^2)}{\sigma_{ym}^2+\sigma_{yI}^2}\right)}{(\sigma_{ym}^2+\sigma_{yI}^2)} \qquad [3.11]$$

where σ_{yi} and σ_{ym} are instantaneous and meandering dispersion parameters.

Progress in further development has been hindered due to a lack of information regarding the dispersion parameters. Boundary layer theory does provide an estimate for these parameters under neutral and stable conditions (Hanna, 1984; Nappo, 1983; Lee and Stone, 1983; Wyngaard, 1982; Lamb, 1982). Under neutral conditions the dispersion parameters in the crosswind directions are

$$\sigma_y^2 = \sigma_{yo}^2 + \overline{v'^2}\, t^2 \qquad [3.12a]$$

$$\sigma_{yI}^2 = \sigma_{yo}^2 + C_1 t^2 (\varepsilon \sigma_{yo})^{2/3} \qquad [for\ t > t_1] \qquad [3.12b]$$

$$\sigma_{yI}^2 = C_2 \varepsilon t^3 \qquad [for\ t > t_1] \qquad [3.12c]$$

where σ_{yo} is the initial source size, ε is the dissipation rate, $\overline{v'^2}$ is the crosswind velocity fluctuations, t is time and C_1, C_2 are constants. The time t_1 is the point where the influence of σ_{yo} is no longer important.

After a sufficient amount of time or distance, the instantaneous plume dispersion will be equivalent to the meandering component. Lee and Stone (1983) show, theoretically, that this will occur at $t = C_3 T_L$ where T_L is the Lagrangian integral time scale.

There is sufficient experimental evidence that justifies further development of the meandering plume model. Specifically, more work is required in developing dispersion parameters under various atmospheric conditions.

3.1.5 Probability Density Function (PDF) Models

PDF models are based on the premise that the concentration fluctuations pdf is directly related to the turbulent velocity pdf. The individual air parcels follow straight line trajectories prescribed by the turbulent wind field which is similar to Gifford's meandering plume model. This techniques is valid for travel time (t) less than the turbulent Lagrangian integral time scale (T_L), and for averaging times (T_A), larger than T_L.

Defining all variables as functions of sampling time (t_1) and averaging time (t_2) (i.e., $c = c[t_1, t_2]$), the crosswind integrated ground level concentration over sampling time T_s and averaging time $T_A = 0$ is

$$C^y[T_s, O] = \frac{2Q}{\times\sqrt{2\Pi}\ \sigma_w[T_s, O]} \exp\left[\frac{-(w_s - w_o)^2}{2\sigma^2_w[T_s, O]}\right] \qquad [3.13]$$

where w_s is the vertical velocity which will bring a parcel of air to the ground in a straightline trajectory from an effective stack height (h_s), (i.e., $w_s = -U_o h_s/x$), w_o is the average vertical velocity over sampling time T_s, and σ_w is the standard deviation of the vertical velocity fluctuations $(w'^2)^{1/2}$.

Venkatram (1984) derives a formula for concentration fluctuations with the aid of a log-normal distribution and subsequently averaging over the sampling time (S). The two-dimensional form is given as:

$$\sigma_L^2[T_s, O] = \frac{1}{4}\frac{\sigma_w^4[S, T_s]}{\sigma_w^4[T_s, O]}\left(2 + \frac{4w_s^2}{\sigma_w^2[S, T_s]}\right) + \frac{1}{4}\frac{\sigma_v^4[S, T_s]}{\sigma_v^4[T_s, O]}\left(2 + \frac{4v_s^2}{\sigma_v^2[S, T_s]}\right) \quad [3.14]$$

where σ_L^2 is the variance of the natural log of the concentration ($\ln(c[T_s, O])$, σ_v^2 is the crosswind turbulent velocity of fluctuations (v'^2), and v_s and w_s are the velocities required to being a parcel of air from the source to the receptor. The ratio

$$\frac{\sigma_w^2[S, T_s]}{\sigma_w^2[S, O]}$$

is based on an exponential autocorrelation and given as

$$\frac{\sigma_w^2[S, T_s]}{\sigma_w^2[S, O]} = 2\left(\frac{T_2}{T_s}\right) \times 1 - \frac{T_2}{T_s}\left[\left(1 - \exp\left(-\frac{T_s}{T_2}\right)\right)\right] \quad [3.14a]$$

where sampling time (S) is much greater than the averaging time (T_s). A similar equation can be used for the lateral velocity variance. The above ratio can be related to the velocity ratios in 3.14 via

$$\frac{\sigma_w^4[S, T_s]}{\sigma_w^4[T_s, O]} = \left(\frac{\sigma_w^2[S, T_s]}{\sigma_w^2[S, O]} - 1\right)^{-2} \quad [3.14b]$$

The ratio of turbulent velocity fluctuations (LHS) in (3.14b) is the square of the ratio of the turbulent kinetic energy at large time scales (> T_s) to the turbulent energy at small scales (< T_s). This leads to an analogy with the meandering plume model. The ratio represents the portion of the turbulent spectrum which generates plume meandering to the spectrum which generates relative diffusion (Hanna, 1984).

This model is best suited for determining fluctuations from small size elevated sources when $T_s > T_L$.

Equation 3.14 relation can be transformed to the concentration intensity (Mage, 1975) via:

$$\frac{\overline{c'^2}}{\overline{c}^2} = i^2 = \exp\left(\sigma_L^2(T_s, O)\right) - 1 . \qquad [3.15]$$

3.1.6 Statistical Models

Statistical or Monte Carlo numerical models follow which the trajectory of thousands of air parcels from which a concentration pdf can be determined. Durbin (1980), Lamb (1982) and Sawford (1983), followed pairs of parcels, while Lee and Stone (1982) and Kaplan and Dinar (1988) followed a single parcel. Sawford applied a two-point covariance formula between parcel locations at time t_1 and t_2 to calculate the concentration intensity from the numerical model runs. His results show that at large times ($t > T_L$), the intensity approaches a constant value. This asymptotic value was reported to be a power function of ratio of the Eulerian length scale (L_E) to the source size (σ_o)

$$i \alpha \left(\frac{L_E}{\sigma_o}\right)^{1/3} \qquad [3.16]$$

Hanna (1984) suggests a good fit to the model results is

$$i = 0.56 \left(\frac{L_E}{\sigma_o}\right)^{0.3} \qquad [3.17]$$

and subsequently generalized the intensity as

$$i^2 = \left[0.56 \left(\frac{L_{EY}}{\sigma_{oy}}\right)^{0.3} \exp\left(\frac{y^2}{4\sigma_y^2}\right)\right]^2 + \left[0.56 \left(\frac{L_{EZ}}{\sigma_{oz}}\right)^{0.3} \exp\left(\frac{(z - h_e)^2}{4\sigma_z}\right)\right]^2 \qquad [3.18]$$

The above equation is applicable to $t > T_L$ and is thus a solution to the in-plume concentration field.

3.1.7 Numerical Models

Numerical solutions to the concentration fluctuation equation (3.3) have been carried out with the aid of second order closure models of diffusion (Sykes, et al., 1984; Lewellen, et al., 1986). Here, the variance is predicted directly.

In these models, the third order terms (e.g., $(\overline{w'c'^2})$) are parameterized by assuming that they are proportional to the gradients of the second order terms. Second-order closure models require much computer time and the results are questionable under convective conditions when transport is dominated by large eddies.

Large eddy simulations (LES) models have been exclusively used in computational fluid dynamics and are extremely computer extensive. The principal objective is to numerically simulate atmospheric diffusion such that the results have sufficient spatial and temporal resolution to estimate concentration fluctuation statistics (Lamb, 1982). The LES approach is actually a "surrogate" field study under controlled conditions to generate enough data for testing of the simpler models described above.

3.2 CONDITIONAL CONCENTRATION STATISTICS

The variability of the concentration at a receptor is the result of two mechanism which are distinguished according to the relative size of the plume to the turbulent eddies (i.e., meandering and in-plume). Generally, the occurrence and distribution of zero concentrations is determined by the large eddies while statistics of non-zero concentrations are determined by smaller eddies. While this connection is obviously not precise, it suggests that there might be more order in conditionally sampled statistics for which zero concentrations are ignored (roughly speaking, 'in-plume' statistics). Conversely, the intermittency (by convention the fraction of non-

zero concentrations) should reflect variations due to the large-scale inhomogeneous features of the concentration field.

As the plume meanders, it will pass over a fixed receptor for only a fraction, γ, of the time. It is not the mean concentration $\overline{c}$ or its variance $\overline{c'^2}$ that is important in determining the peak concentration but rather the mean $\overline{c}_p$ and variance that $\overline{c'^2_p}$ occurs when the plume is present over the receptor. These are called the "conditionally averaged" mean and variance. Most plume dispersion models predict the unconditional mean $\overline{c}$ and not the conditional value $\overline{c}_p$ and similarly, the models and formulae presented above deal with the variance unconditional or intensity rather than the conditional.

The conditional and unconditional statistics are coupled via the intermittency factor (2.7) but an appropriate pdf is required to determine the peak concentrations. A number of pdf's have been proposed and applied including the exponential, log-normal and clipped-normal (Figure 3-1).

Exponential

Csanady (1967), Barry (1975) and Hanna (1984) have shown that the exponential distribution,

$$p_p(c) = \frac{1}{\overline{c}_p} \exp(-c/\overline{c}_p) \qquad [3.19]$$

provides reasonable agreement with measured data within 100 m. Wilson (1982) suggest that this pdf is most appropriate for strongly intermittent ($\gamma << 1$) concentrations where events are likely uncorrelated due to long periods of zero concentrations, i.e., meandering conditions. It is of interest to note that with an exponential pdf, $\overline{c'^2_p} = \overline{c}_p^2$ which results in $i_p = 1$ under all conditions. This results in γ being a function of i only;

FIGURE 3-1

Conditional Log-Normal and Exponential PDF's

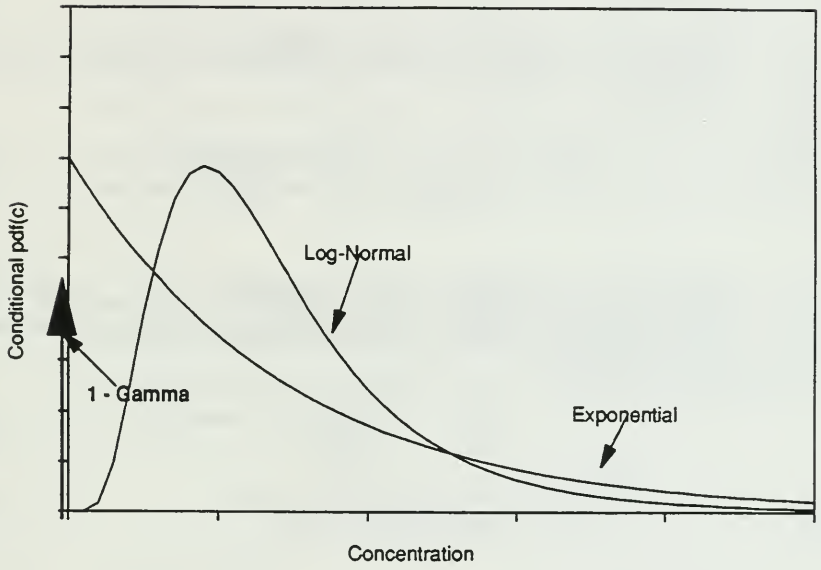

$$\gamma = \frac{2}{I^2 + 1} \quad . \qquad [3.20]$$

Lognormal

Csanady (1973), Gifford (1972), Wilson (1982) support the use of the log-normal distribution,

$$p_p(c) = \frac{1}{\sqrt{2\Pi}\,\sigma_{pL}\,c} \exp\left[- \frac{[\ln(c/\overline{c_{pm}})]^2}{2\sigma_{pL}^2} \right] \qquad [3.21]$$

where $\overline{c}_{pm}$ is the in-plume median concentration and σ_{pL} is the in-plume logarithmic standard deviation. These parameters are related to conventional in-plume statistics via,

$$\overline{c_{pm}} = \frac{\overline{c_p}}{(1 + I_p^2)^{1/2}} \; ; \qquad [3.22a]$$

$$\sigma_{pL} = [\ln(1 + I_p^2)]^{1/2} \qquad [3.22b]$$

Both Csanady and Gifford suggest that a parcel of contaminated air experiences a series of mixing events on dilutions which are statistically independent or random. Sawford (1987) comments that the log-normal is often used to describe the long-term variations from an extended area source, such as an urban area, where the main dilution mechanism is ventilation due to the mean wind which is generally found to be log-normal.

The above discussion suggest that the log-normal distribution is best suited for in-plume fluctuations while the exponential is most appropriate for meandering plumes. It is evident that intermittency is the key in determining whether the concentrations at a receptor displays an exponential or log-normal distribution.

Clipped Normal

Lewellen and Sykes (1986) provide some theoretical support for the clipped normal pdf. They argue that a rational choice of pdf for a given data set is that with the maximum entropy (minimum information) which satisfies the known physical constraints. The constraints they choose for concentration fluctuations are: no negative concentrations, a specified mean and variance, and a finite intermittency. They required γ to be a function of the fluctuation intensity *i* only to avoid any additional independent parameters. Sawford (1987), Dinar et al. (1988), Mylne and Mason (1990) found that the clipped normal fits their data sets better than the exponential.

The clipped normal is a normal Gaussian pdf for $c > 0$ with the integrated probability of negative concentrations being transferred into a dirac function at $c = 0$ to represent the intermittency effect. The function is specified in terms of two parameters u and σ as

$$p_p(c) = \frac{1}{\gamma} \cdot \frac{1}{\sqrt{2\Pi\sigma_o}} \exp\left(\frac{(c - u_o)^2}{2\sigma_o}\right) \qquad [3.23a]$$

and

$$\gamma = 1/2\left[erfc\left(\frac{-u_o}{\sqrt{2}\sigma_o}\right)\right], \qquad [3.23b]$$

where u_o and σ_o are numerically determined from given values of $\bar{c}$ and $\overline{c'^2}$, i.e.,

$$\bar{c} = \frac{\sigma_o}{\sqrt{2\pi}} \exp\frac{-u_o^2}{2\sigma_o} + u_o\gamma \qquad [3.24a]$$

$$\overline{c'^2} = u_o\,\bar{c} + \sigma_o^2\gamma \qquad [3.24b]$$

Lewellen and Sykes (1986) show good agreement with LIDAR observations of power-plant plumes out to 1 km and 2 km that if the conditional pdf is an exponential, it is completely specified by $\bar{c}_p$ but with γ freely chosen, the uncondition pdf becomes a function of two parameters. For both the log-normal and clipped-normal distributions, two parameters fully specify the conditional statistics; in the case of the clipped normal distribution, these two parameters also determine the intermittency.

Sawford (1987) compared the first four central conditional moments of the above distributions to 6 sec average concentrations taken during neutral and unstable conditions. The exponential distribution gives a reasonable upper limit to the measured distribution but overpredicts the 3rd and 4th moments as well as the frequency of the higher concentrations. The log-normal distribution gives an adequate representation of the data over a wide range but appears to have the opposite curvature to the trend in the data at the upper end. This levels to over estimates of the 3rd and 4th moments. The clipped-normal gives reasonable representation of the entire data including the frequency of high concentration but cannot predict the γ adequately. This is in contrast to work carried by Mylne and Mason (1990) and Dinar, et al (1988) who show a good correlation between predicted and observed γ under similar atmospheric and release conditions.

3.3 FURTHER DEVELOPMENT OF THE EMPIRICAL GAUSSIAN MODEL

As presented above, there are several practical models and techniques to calculate the unconditional and conditional fluctuations $\overline{c'^2}$ and subsequently $\overline{c_p'^2}$, $\bar{c}_p$ and γ. All have merit and applicability to various atmospheric and source conditions. For the current study, we are specifically interested in the applicability of the empirical Gaussian model (EGM) as developed by Wilson.

Section 3.1.2 presented the EGM and the requisite equations are,

$$\overline{c^2} = \left(\frac{q}{2\pi U_o \sigma_y \sigma_z}\right)^2 \left(\exp -\frac{1}{2}\left(\frac{y}{\sigma_y}\right)^2\right) \times \left[\left(\exp -\frac{1}{2}\left(\frac{z - h_v}{\sigma_z}\right)^2\right) - \alpha \exp\left(-\frac{1}{2}\left(\frac{z + h_v}{\sigma_z}\right)^2\right)\right] \quad [3.5]$$

$$\left(\frac{h_v}{\sigma_z}\right)^2 = \left(\frac{h}{\sigma_z}\right)^2 + \phi \quad [3.6]$$

$$\frac{q}{Q} = \frac{C_2 \lambda}{(\lambda + \lambda_o^2)^{c_1/2}} \quad [3.7a]$$

$$\lambda_o = \frac{C_3}{\left(C_4 \frac{L_w}{d} + 1\right)} \quad [3.7b]$$

$$\lambda = \frac{\sqrt{\sigma_z \sigma_y}}{H} \quad [3.7c]$$

where:

α = 0.6
ϕ = 0.7064
C_1 = 2.0
C_2 = 0.34
C_3 = 0.12
C_4 = 0.055

In addition, the mean concentration is assumed to be Gaussian as well.

$$\bar{c} = \frac{Q}{2\pi\sigma_y\sigma_z} \exp\left(-1/2\ \frac{y^2}{\sigma_y^2}\right)\left[\exp\left(-1/2\ \frac{(z-h)^2}{\sigma_z^2}\right) + \exp\left(-1/2\ \frac{(z+h)^2}{\sigma_z^2}\right)\right] \quad [3.25]$$

The above constants were determined via fitting the appropriate equation to wind tunnel data. The predicted curves give good representation of the measured data and the parameters have good physical justification (Hanna, 1984).

Equation (3.5) is reasonable approximation, since the production or generation of fluctuations would naturally occur at the point of maximum concentration gradient which is analogous to turbulent kinetic energy production.

The "along-wind" variance source formula (3.7) is based on the semi-empirical balance local advection-dissipation terms (3-2). The use of the parameters λ to specify downwind distance is based on the expectation that most of the effects of varying turbulence scale under different atmospheric stabilities and terrain roughness will be accounted for by specifying downwind position in terms of plume dimensions rather than distance from the source. The virtual origin λ_o in (3.7b) contains all the effects of source size and atmospheric turbulence scale. As the plume from an elevated source moves downwind, it will sample the small turbulence scales near the ground, and large scales above the source height. Wilson states that this equation is valid only for

$$4 < \frac{L_w}{D} < 40 \quad .$$

The wind tunnel data shows that the sampling of small scales is the dominant effect as the plume moves downwind, and that the use of a constant scale $L_w = h$ causes (3.7a) to overpredict the variance source strength q far downwind. Based on the wind tunnel data, Wilson et al. (1985) suggest the following:

$$L_w = 0.6\, h \exp\left(-\left(\frac{\sigma^2}{h}\right)^2\right) \qquad [3.8]$$

It is useful to consider the vertical source displacement (i.e., h_v) and the sink terms (i.e., α) separately. For a source which far above the surface, Wilson (1986) shows

$$i_\infty = \frac{q}{Q} \exp\left[\frac{y^2}{2\sigma_y^2}\right] \exp\left[\frac{2(z-h)^2 - (z-hv)^2}{4\sigma_z^2}\right] \qquad [3.26]$$

where i_∞ is the intensity in the absence of image reflection (as per the mean concentration) and variance image sink terms. The relation between intensity i and i_∞ is given as

$$\frac{i}{i_\infty} = \frac{\left[1 - \alpha \exp\left(-\frac{2h_v z}{\sigma_z^2}\right)\right]^{1/2}}{1 + \exp\left(\frac{-2hz}{\sigma_z^2}\right)} \qquad [3.27]$$

which includes the sink term as per (3.5).

An important approach put forth by Wilson et al. (1985) was to develop a surrogate model for the conditional variance $\overline{c_p'^2}$ to determine γ. This is the opposite to what Hanna (1984b) and Fackrell and Robins (1982), who modelled γ to obtain the conditional statistics.

Wilson et al. states that it is difficult to formulate a γ model because the model must take into account the "dual structure" which considers both meandering and in-plume fluctuations. He argues that his approach works well because the conditional intensity is virtually constant across the vertical and lateral extent of the plume. Experimental evidence by Fackrell (1978) and Dinar et al. (1988) seems to verify this. This suggests that the inhomogeneous mixing of source material

with entrained air has some self-preserving structure that depends on time of travel from the point of release, rather than on a diffusion process across the plume.

Wilson's approach was based on simulating the conditions where $\gamma = 1$ and $i_p = i$ in the current equation set. This theoretical extension allows the prediction of "in-plume" variance, and at the same time assures that the equation for i_p will be physically and mathematically consistent with the existing model for total intensity, i.

Fackrell and Robins (1980) measurements of the effects of source size indicate that $\lambda = 1.0$ will be observed on the plume axis when the integral scale of turbulence (L) is less than source's diameter (d). Wilson's assumption is that this condition can be simulated in the total variance model by setting the scaling height $L_w = 0$ in (3.7b). This simple condition should make the plume appear to be diffusing in a field of small scale turbulence where $\lambda = 1.0$, and for which (2.11) shows the conditional and total variances will be equal. With $L_w = 0$ (3.7a) and (3.7b) are combined to give the conditional variance source strength,

$$\frac{q_p}{Q} = \frac{0.38\,\lambda}{\lambda^2 + (0.12)^2} \qquad [3.28]$$

keeping in mind that all of this applies only on the plume axis for an elevated source with $h >> \sigma_z$. Far above the ground, the plume variance may be computed from the total variance model (3.5) by setting $z = h$ and $y = 0$.

$$\overline{c_{p\infty}^2} = \left(\frac{q_p}{2\pi U_o \sigma_y \sigma_z}\right)^2 \exp\left(-\frac{1}{4}\left(\frac{h - hv}{\sigma_z}\right)^2\right) \qquad [3.29]$$

where the subscript "∞" is used to denote this conditional variance on the plume axis far from the dissipative effects of the ground surface.

Noting that intermittency is unity (γ for this situation, (2.8) shows that $\overline{c}_p = \overline{c}$, which can be computed from the Gaussian plume model to be,

$$\bar{c}_{p\infty} = \frac{Q}{2\pi\, U_o \sigma_y \sigma_z} \qquad [3.30]$$

assuming $h >> \sigma_z$.

Combining (3.29) and (3.30) yields the conditional fluctuation intensity

$$i_{p\infty} = \frac{q_p}{Q} \exp\left(-\frac{(h - hv)^2}{4\sigma_z^2}\right) \qquad [3.31]$$

which is assumed to be constant over the entire plume cross-section at any fixed downwind x (or λ) location.

Wilson subsequently assumes that the dissipation of variance by the small scale turbulence near the ground has the same relative effect on the conditional intensity i_p as it does on the total intensity i. That is,

$$\frac{i_p}{i_{p\infty}} = \frac{i}{i_\infty} \qquad [3.32]$$

where the subscript "∞" refers to the intensity at the same location but with the ground plane removed. In practical terms, the ground plane effect is removed by simply deleting the image source term in the mean concentration equation, and the image sink term in for the variance. This results in

$$i_p = i_{p\infty} \frac{\left[1 - \alpha \exp\left(-2\frac{h_v z}{\sigma_z^2}\right)\right]^{0.5}}{\left[1 + \exp\left(-2\frac{hz}{\sigma_z^2}\right)\right]} \qquad [3.33]$$

This completes the model for i and i_p, via 3.27, 3.33, with 3.6 and 3.7.

The intermittency is subsequently calculated via (2.11b) i.e.,

$$\gamma = \frac{i_p^2 + 1}{i^2 + 1} \qquad [2.11b]$$

The above theory generates instabilities at $y > 2\,\sigma_y$ where it unrealistically predicts increasing c_p with increasing crosswind distance (Wilson, 1982). This instability is caused by underpredictions of γ due to over-predictions of i at the fringes. Wilson (1982) suggest an "additive correction" for the error which is given as

$$\gamma = \gamma' + 0.01\,\gamma_o \qquad [3.34]$$

where γ' is the intermittency calculated via the above equation set at the crosswind distance (y) and γ_o is the intermittency at the centerline.

The EGM model developed above provides the requisite equations to predict the statistics required to describe the concentration fluctuations. An appropriate pdf is required such that the intermittency, mean concentration and total or unconditional variance can be used to predict the probability of peak levels.

The distinctly different shapes of the pdf's for log-normal and exponential distributions are shown schematically in Figure 3-1. The exponential function is physically realistic only for highly intermittent plumes which have a conditional fluctuation intensity of unity. While a log-normal has the capability of dealing with conditional fluctuation intensities different from unity (non-intermittent), it has the physically unrealistic property that the probability of observing a concentration only slightly greater than zero, is very small, while at the same time there is a large probability of observing zero concentration, when intermittency removes the plume from the receptor. In highly intermittent plumes where there is a significant probability of zero concentration, the exponential model realistically predicts a smooth monotonically increasing probability of observing small concentrations. The clipped-normal distribution is a normal distribution displaced by an off-set factor which produces an area from the origin to the left which is equal to the frequency of zero observations (1-γ). A smooth transition from zero to non-zero readings is illustrated. The clipped-normal seems to be most appropriate for low intermittency.

The log-normal distribution seems appropriate for the current modelling equation set because the EGM is an in-plume fluctuation model which has been expanded to predict i_p and γ. It should be noted that the exponential distribution does not require the prediction of i_p since γ is a residual of the distribution. Similarly with the clipped-normal, $\overline{c}$, and $\overline{c'^2}$ are required with γ subsequently part of the equation set. Due to the complexity of solving the equation set and the current conflicting evidence, the clipped-normal is not considered here.

The plume spreads on dispersion coefficients σ_y and σ_z used to estimate concentration fluctuations via the EGM are based on wind tunnel derived values or plume half-widths. Atmospheric, as well as wind tunnel, dispersion coefficients consist of a meandering component (σ_{ym}) and an "instantaneous" component (σ_{yi}) which make up the total spread (Gifford, 1959; Csanady, 1972) via,

$$\sigma_y^2 = \sigma_{yI}^2 + \sigma_{ym}^2 \qquad [3.35]$$

and σ_y is used in the prediction of mean concentrations. In theory, σ_{yi} should be used to calculate the concentration intensities. In practice, σ_{yi} is virtually impossible to predict. Wilson (1982) and Wilson and Simms (1985) suggest that the total spread can be related to a quasi-instantaneous spread via the empirical relation,

$$\frac{\sigma_y(T_s)}{\sigma_y(T_{ref})} = \left(\frac{T_s}{T_{ref}}\right)^p . \qquad [3.36]$$

where T_{ref} is the reference sampling time of the total spread (~ 60 min), T_s is the "quasi-instantaneous" time, σ_y (T_{ref}) is the total spread, and p is a constant (~ 0.3). Wilson suggests that using T_s equate to 3 min. is a reasonable compromise between theory and practice. Thus, all lateral dispersion coefficients used to predict concentration fluctuations are "corrected" to the quasi-instantaneous value with [3.36].

The Wilson EGM incorporates the following significant components:

i) Concentration variance ($\overline{c'^2}$) is dispersed in a similar fashion to mass.

ii) Variance source strength (q) decays with distance and scale of dispersion.

iii) The conditional fluctuation intensity (i_p) is constant over the crosswind section at any fixed downwind distance.

iv) The conditional variance source strength (q_p) decays in a similar fashion as q.

v) The distributions of concentrations over time are log-normal.

vi) The cross-wind spreads (σ_y) are corrected to 3 minutes via [3.36].

4 OME CONCENTRATION FLUCTUATION MODEL FRAMEWORK AND ITS COMPONENTS

The modelling framework employed in the study is presented in Figure 4-1. The modelling package has been named GASFLUC.

The first module consists of the equation used in the new CAP formulations. Meteorological and source data required by these formulations are read into this module. The outputs are the time-averaged concentrations at receptor points of interest. These can be used for regulatory purposes or to field measurements for validating the formulations used in this module.

The second module consists of the EGM equations developed by Wilson, for conditional and unconditional fluctuation intensity and intermittency, as described in Section 3.3. It uses as input the outputs from Module 1, or, optionally, field measurements of these quantities. This option is provided so that Modules 2 and 3 would be tested independent of the formulations in Module 1. The outputs from Module 2, which are plume intermittency and time-averaged fluctuation intensity at receptor points of interest, can also be compared directly with field measurements of these parameters for model validation purposes.

Module 3 consists of the equations describing the frequency distribution of concentration fluctuations (3.21 and 3.22 or 3.19 and 3.20). It uses as input the outputs from Modules 1 and 2 or, optionally, field measurements of these quantities for testing Module 3 independent of formulations in Modules 1 and 2. The predicted output frequency distribution can be used for regulatory purposes, or compared to field measurements for validating this module.

FIGURE 4-1

OME Concentration Fluctuation Model Framework and Its Components

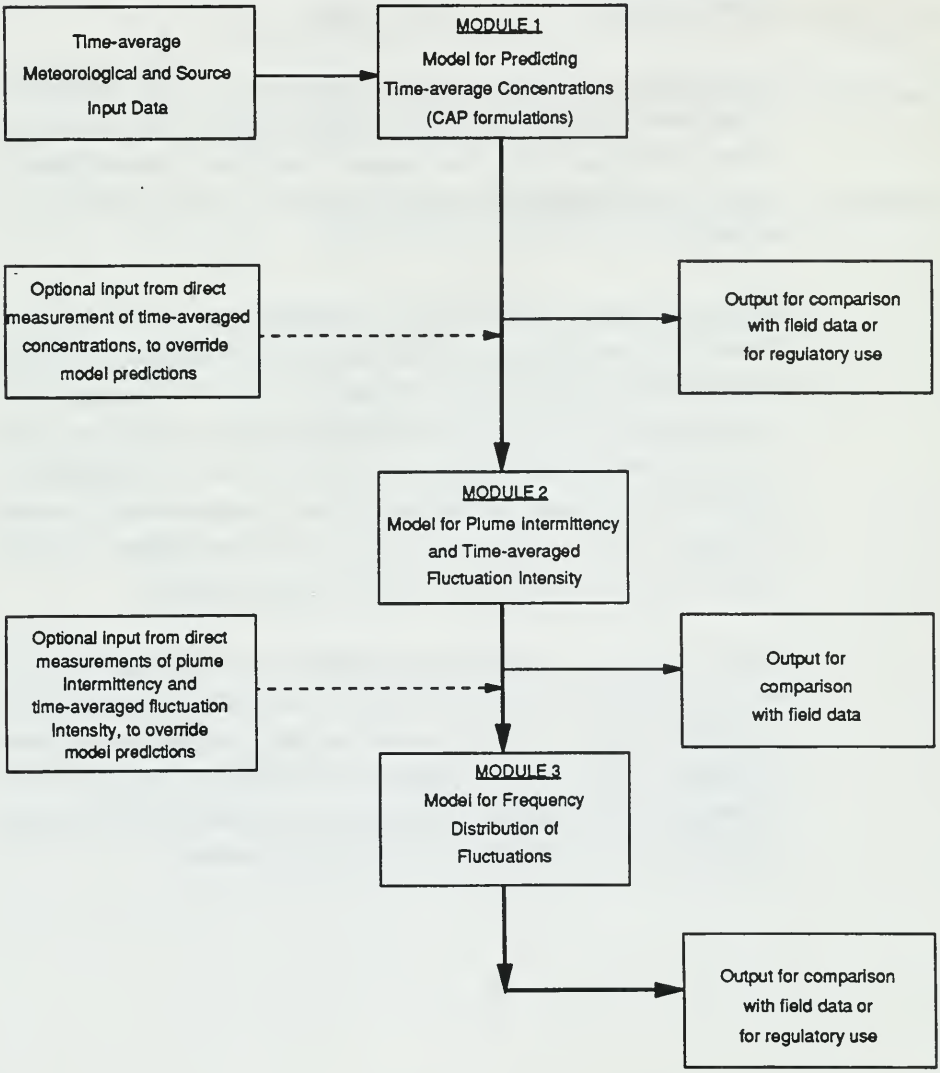

4.1 INTERFACING OME CAP MODEL WITH EGM CONCENTRATION FLUCTUATION MODEL

Compatibility between models will always be a contention issue requiring further debate and analysis. For example, it is likely that the EGM is not appropriate to couple with the CAP convective condition model since the CAP model is based on Venkatram (1985) "touch-down model". The PDF model (3.14) is likely a more suitable model. For the current study, it is assumed that there is complete compatibility between CAP and EGM.

Section 3-3 presented a closed set of equations for generating unconditional and conditional plume concentration intensities and intermittency (3.5, 3.6, 3.7, 3.26, 3.29, 3.31 and 3.36). These equations require the following input parameters from the CAP module:

- plume centerline elevation (h);
- mixing layer depth (H);
- stack diameter (d) or initial wake induced spread (σ_o);
- receptor cross-wind and elevation (y, z); and
- plume dispersion parameters (σ_y and σ_z).

The above parameters are generally readily available from the CAP model with certain exceptions. In these exceptions, assumptions have been made to complete the input parameter set.

For near surface releases, under convective, neutral and stable atmospheric conditions, σ_z is not calculated but the mean height of dispersion ($\bar{z}$) is provided. Under these conditions, the plume centerline height is equated to $\bar{z}$ and σ_z is set equal to 1.1 $\bar{z}$.

The EGM generate conditional and unconditional concentration intensities and intermittency which are used as input to the frequency distribution module. The exponential distribution (3.28) requires only the mean concentration ($\bar{c}$), and either γ or i since there is a unique relationship between the two (3.29). The log-normal distribution (3.30) requires $\bar{c}$, γ and i in its formulations.

The output of the distribution module is a cumulative frequency distribution showing the concentration at various percentile levels (i.e., 50-th, 75-th, 90-th, 95-th and 99-th) for each receptor and meteorological condition.

The cdf will have a particular form when measured with a certain averaging time (T_A) and it is important to know how P(c, T_A) as well as all other fluctuation statistics vary with T_A.

The amount of change in the cdf due to smoothing the time series depends on the averaging time relative to the time scales of the dominant fluctuations. It is therefore closely related to the velocity fluctuation spectrum and varies with distance in a similar way (Mylene and Mason, 1990). Field studies at several hundred meter range, the measured cdf was virtually unchanged by smoothing with averaging periods between 0.1s and 10s. In shorter range experiments (Mylene and Mason, 1990), averaging times larger than 1s generated significant variation in the 90-th percentile and greater. Intuitively, the longer the averaging time, the closer to unity γ approaches and thus $\bar{c}_p \rightarrow \bar{c}$. Basically, the number of non-zero measurements are reduced.

As the EGM model is based on Fackrell and Robins (1982a,b) wind tunnel data using a fast response flame ionization detector, it is assumed that the concentration cdf represents the concentrations over an averaging time of the order of seconds. This is generally the length of time for a breath.

5 ERCB FIELD MEASUREMENT PROGRAM

The Field Measurement Program (ERCB, 1990) consisted of tracer and meteorological components. The study site was located on reasonably flat terrain about 20 km to the east of Calgary, Alberta. The tracer release and sampling occurred during October, November and December, 1988. The meteorological station started collecting data in October 1988 and continued to operate until a 12-month data set was collected.

5.1 TRACER STUDY

On 33 evenings in October, November and December, 1988 when suitable dispersion conditions prevailed, SF_6 was released with the aid of a fan to simulate a continuous release of gas escaping from a well or a ruptured pipeline. A large fan was used for elevated releases and a smaller fan was used for ground level releases. The large fan was oriented vertically and had a nominal flow rate of 700 m^3/min) was mounted in the centre of an octagonal enclosure 40 cm in height and 220 cm in diameter. The flow for the ground release was oriented downwards. The SF_6 flow rates for both types of releases were measured using a linear mass flow meter. During the 33 field tests, the average SF_6 flow rate was 2.1 g/s.

In-plume SF_6 concentrations were then measured by continuous SF_6 analysers (Scientech Inc., Pullman, Washington) mounted in trucks. The SF_6 analysers are based on an electron capture detector (ECD) and have an SF_6 detection limit of 10 ppt and a response time of 0.4 seconds. SF_6 concentrations were recorded on portable MS-DOS based personal computers equipped with 12 bit A-D cards. Multipoint analyser calibrations before and after each test were conducted using several standard SF_6 concentration gases ranging from 0 to 5000 ppt. Single point span checks were performed at regular intervals in the field.

A combination of mobile and stationary monitoring was conducted to obtain plume concentration profiles 700, 1400 and 2100 m downwind of the release point. Mobile monitoring provided nearly instantaneous plume profiles, while the stationary monitoring provided plume intermittency information. A number of sampling arcs were pre-surveyed for the field tests. Five alternate source locations were selected to account for different wind directions (Figure 5-1). Plume locations were established using survey stakes located on each sampling arc. These stakes were located at 20 m (for the 700 m distance), 30 m (for the 1400 m distance) and 40 m (for the 2100 m distance) intervals. The stationary analyser was located at a fixed position on one of these arcs for a minimum period of 30 minutes before a decision was made regarding its relocation.

The data reduction consisted of converting the concentration data which were stored in A-D units ppt (parts per trillion by volume) accounting for baseline drift and using a power law relationship. A total of 846 SF_6 traverse concentration profiles were obtained. In addition, a total of 439 stationary one-half hourly and 5271 stationary three-minute average SF_6 concentration data were collected.

5.2 METEOROLOGICAL STUDY

A 25 m tower adjacent to the tracer release site served as a platform for the meteorological sensors (Figure 5-2). Three-axis sonic anemometers at four levels (4, 10, 16 and 25 m) were used to measure mean winds, their variance and fluxes of heat and momentum. Three Applied Technologies Inc. SWS/3 Three Axis Wind Systems were used at the 4, 16 and 25 m levels and a single Kaijo-Denki Co. Ltd. Model DAT 310 with the TR61A probe was mounted at the 10 m level. Means, variances and co-variance terms were recorded as three-minute averages on an MS-DOS 80386 personal computer. The resolutions of the sonic anemometer are typically given as 0.01 m/s. During each tracer test, high frequency sonic anemometer data from the 10 and 25 m levels were collected and archived at a nominal 10 Hz rate. About 300 hours of high frequency data at 2.14 Mb per hour were collected on a streaming tape drive.

FIGURE 5-1

Schematic of ERCB Field Measurement Locations

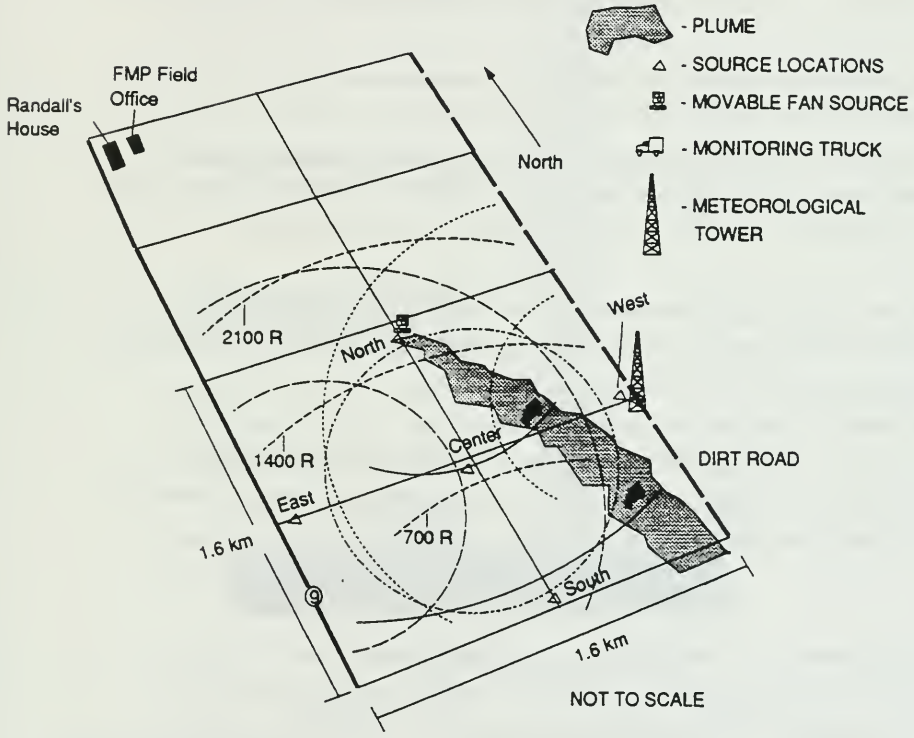

FIGURE 5-2

Schematic of Relative Locations of Sensors on Meteorological Tower

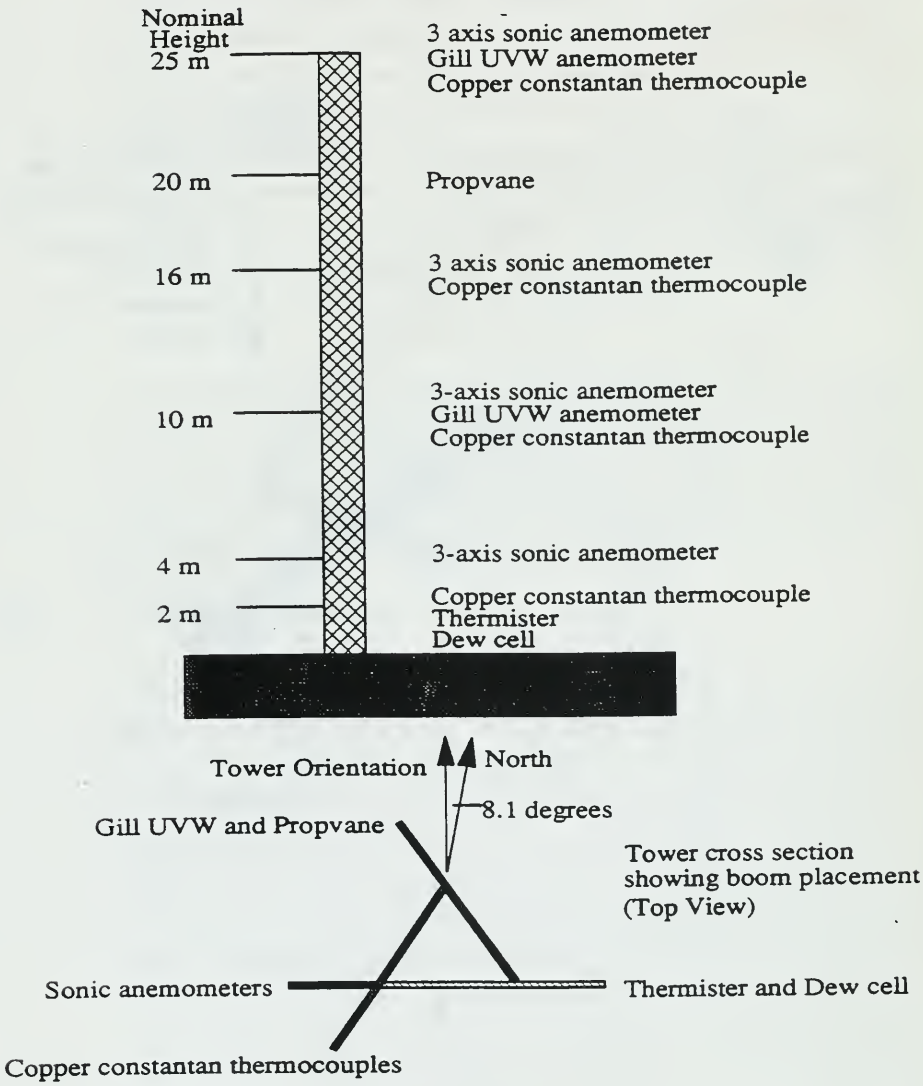

For high wind speeds, the horizontal wind can contaminate the sonic temperature. A semi-empirical factor was used to correct the high frequency sonic temperature which was used to estimate the heat flux. This produced some uncertainty in the estimation of the heat flux term, especially under very low turbulence conditions.

Additional sensors on the tower included back-up Gill UVW propeller anemometers (10 and 25 m) and aspirated temperature sensors (2, 10, 16 and 25 m). The back-up anemometers allowed for comparison to the more sophisticated sonic systems. In addition, measurements of net radiation, relative humidity, barometric pressure and soil heat flux were made. All conventional meteorological sensors were sampled at 1 Hz. Three-minute averages from these sensors were archived on a continuous basis using Campbell Scientific 21X and CR-21 data loggers.

All 3-minute average data (both sonic and conventional) were quality controlled and stored. The data included means, variances and co-variance terms in addition to calculated values of boundary layer terms such as: heat flux, friction velocity, Monin-Obukhov length, flux Richardson number, bulk Richardson number and Gradient Richardson number. A second data set comprised of the same parameters for a 30-minute averaging time was also prepared. The 30-minute data file also included the estimation of Pasquill-Gifford stability class based on on-site data and on nearby Calgary International Airport data.

During the winter, the data recovery for the sonic anemometer systems ranged from 75 to 85%. For the other sensors, the data recovery was typically in the 85 to 90% range during the period October 1988 to March 1989. During the summer period (April to October 1989), the highest data recovery was for the 10 m level sonic anemometer (90%) and for the temperature, soil heat flux, solar radiation and pressure sensors (~95%).

5.3 FIELD MEASUREMENT PROGRAM RESULTS

The stationary tracer study results were merged with the meteorological data sets to generate a single database which would be manipulated for subsequent EGM model comparison. Of the 439 half-hour stationary SF_6 measurements, 310 cases had valid 30-minute meteorological data associated with them.

Table 5-1 summarizes the field measurement program. The distribution shows that 75.8% of the measurements were taken during stable atmospheric while 24.2% during neutral. A majority of the measurements were taken during ground level releases under stable conditions.

The atmospheric stability condition was determined as per the methodology defined in CAP (OME, 1990). Table 5-1 presents the average of the parameters, namely:

- u_* - friction velocity (cm/s)
- u - mean wind speed (m/s)
- H_o - heat flux (w/m^2)
- L - Monin-Obukov length (m)
- z_i - mixing depth (m)

The mixing depth was calculated as per CAP while the other parameters were provided in the data set. Data obtained at the 10 m level was used to define the boundary layer. In cases where the parameter was not available at the 10 m level, the same parameter at 4 m was used. If neither was available, the parameter was calculated from other measured values such as the strear stress ($\overline{u' w'}$) for friction velocity or the temperature-vertical velocity fluctuation co-variance ($\overline{w' T'}$) for the heat flux at first the 10 m and then 4 m elevation. If the parameter set could not be completed, the case was considered invalid and deleted from the database. A complete description of the boundary layer characteristics and measurements is provided in ERCB (1990).

TABLE 5-1

Summary of ERCB Field Condition

RELEASE SCENARIO	ATMOSPHERIC STABILITY	DISTANCE (m)	NO. OF CASES	%	AVERAGE METEOROLOGICAL CONDITIONS				
					u_* (cm/s)	$\bar{u}$ (m/s)	H_o (w/m^2)	L (m)	z_i[1] (m)
Elevated	Stable	700	1	0.3	13.9	3.3	-9.4	23	175
		1400	9	2.9	9.3	3.3	-10.0	7.9	105
	Neutral	700	0	0	-	-	-	-	-
		1400	20	6.4	10.1	2.7	-2.6	65	181
Surface	Stable	700	224	72.3	20.6	5.1	-28	4.6	120
		1400	1	0.3	6.8	1.0	-12	0.9	120
	Neutral	700	52	16.8	12.1	3.2	-0.8	112	205
		1400	3	1.0	6.6	2.0	-1.9	3.9	55
			310	100%					

[1]Calculated as per CAP pre-processor.

CONCORD ENVIRONMENTAL

The stationary SF_6 tracer data were collected to provide a measure of the time varying concentrations at a fixed point in-line with the wind. The data were saved for one-half hour average periods only when the analyzer recorded non-zero SF_6 concentrations during that period. The stationary monitors frequently recorded zero readings due to plume meander and wind shifts. Most of the stationary data were collected at 700 m, with a ground level release under stable atmospheric conditions (Table 5-1). Figure 5-3 presents a sample of the data. Information provided includes:

- unconditional and conditional mean concentration ($\bar{c}$ and $\bar{c}_p$),
- unconditional and conditional concentration intensity (i and i_p),
- intermittency (γ), and
- cumulative distribution (cdf).

Figure 5-4 presents the frequency of instantaneous peak-to-30-minute mean for all valid data. Approximately 47% of the peak-to-mean ratios are between 3-9 while 15% are greater than 23. The large portion in excess of 23 indicates a high degree of intermittency likely due to plume meander.

FIGURE 5-3

Sample of SF_6 Tracer Gas Results

STATIONARY STATISTICS (T33B15)
Scans : 100 to 9875
Date : 12-23-1988 Start Time : 04:59:37
Location: U9 on 700 m C Source : C Ground
Abs. Coordinates: (North 2424.1 m, East 731.7 m)
Transport from 160.52 deg
Power Law Cal. : ppt = 497.45 *(voltage)^ 1.0582

PERIOD # 1
Time : 5 : 1 : 9 to 5 : 31 : 8 (1800 s)
Maximum Concentration (ppt) : 2641
Peak (99 perc) to mean ratio : 3.632988
Plume intermittency : .8577778

	Total	Conditional
Mean Concentration (ppt)	691.5428	806.2027
Concentration fluc. intensity (%)	100.3129	84.90773
Skewness	.7993599	.6336346
Kurtosis	2.579021	2.404772

Percentile: 50 99 (Interpolated)
Conc. (ppt) : 500 2512

Percentile:	14.22	15.06	25.78	40.33	51.78	74.61	92.28	95.89	98.44
Conc. (ppt):	2	11	51	248	546	1201	1781	2085	2441

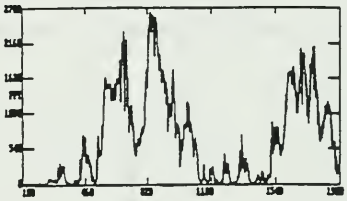

PERIOD # 2
Time : 5 : 31 : 9 to 6 : 1 : 8 (1800 s)
Maximum Concentration (ppt) : 2144
Peak (99 perc) to mean ratio : 8.970975
Plume intermittency : .2961111

	Total	Conditional
Mean Concentration (ppt)	217.4117	734.2233
Concentration fluc. intensity (%)	214.4807	81.13446
Skewness	2.330832	.6354301
Kurtosis	7.565648	2.263143

Percentile: 50 99 (Interpolated)
Conc. (ppt) : 0 1950

Percentile:	70.39	70.56	73.22	77.78	82.39	91.17	95.22	97.06	99.28
Conc. (ppt):	2	10	46	215	462	996	1461	1703	1986

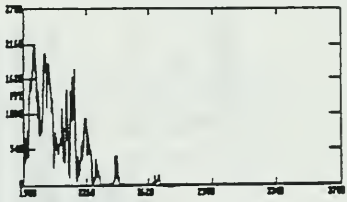

PERIOD # 3
Time : 6 : 1 : 9 to 6 : 31 : 8 (1800 s)
Maximum Concentration (ppt) : 1182
Peak (99 perc) to mean ratio : 10.36592
Plume intermittency : .2966667

	Total	Conditional
Mean Concentration (ppt)	90.00889	303.4008
Concentration fluc. intensity (%)	227.7878	91.43247
Skewness	2.718115	1.017165
Kurtosis	10.15387	3.156486

Percentile: 50 99 (Interpolated)
Conc. (ppt) : 0 933

Percentile:	70.33	70.44	72.72	82.89	88.28	94.83	98.00	99.22	99.67
Conc. (ppt):	2	8	34	142	287	583	830	956	1101

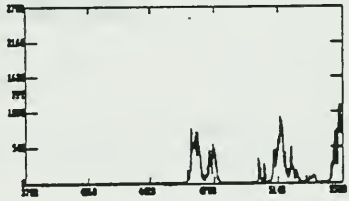

PERIOD # 4
Time : 6 : 31 : 9 to 7 : 1 : 8 (1800 s)
Maximum Concentration (ppt) : 1951
Peak (99 perc) to mean ratio : 8.927212
Plume intermittency : .2661111

	Total	Conditional
Mean Concentration (ppt)	186.6478	701.3904
Concentration fluc. intensity (%)	223.9907	77.53965
Skewness	2.245777	.257856
Kurtosis	6.795547	1.726516

Percentile: 50 99 (Interpolated)
Conc. (ppt) : 0 1666

Percentile:	73.39	73.72	76.11	81.22	84.33	89.28	95.94	98.39	99.78
Conc. (ppt):	2	10	44	201	429	915	1336	1554	1809

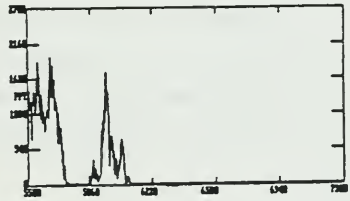

FIGURE 5-4

Frequency Distribution of the Instantaneous Peak SF_6 Concentration to the 30 Minute Mean SF_6 Concentration

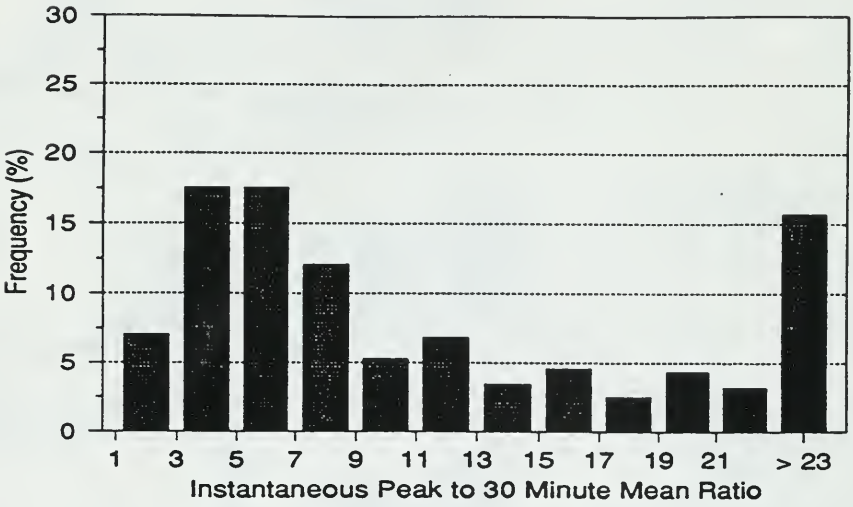

6 SENSITIVITY ANALYSIS OF EGM

As shown in Section 3.3, the EGM concentration fluctuation model uses six constants in its formulations which were derived by Wilson via systematically fitting the wind tunnel data of Fackrell and Robins (1982a, b) to this equations. To evaluate whether these constants are robust or global such that they can be employed in atmospheric flows under various conditions a sensitivity analysis is required. From the previous chapter, four conditions were considered in the field testing program.

i) Surface releases under neutral stability
ii) Surface releases under stable stability
iii) Elevated releases under neutral stability
iv) Elevated releases under stable stability

The following section deals with the sensitivity of i, i_p and γ with each of the six constants independently of each other under the above four atmospheric/emission scenarios. The methodology was to vary the six constants by $\pm$ 50% and evaluate the change in i, i_p and γ with cross-wind distance at ground level. Table 6-1 presents the six constants and the upper and lower limits.

6.1 SENSITIVITY OF α

Alpha (α) is the fraction of the image sink strength term in (3.5) which accounts for surface dissipation. Figures 6-1 to 6-3 present the variation in i_p, γ and i with α and cross-wind location.

The conditional intensity i_p is invariant with respect to cross-wind distance as expected. Typically, an increase in α will result in a decrease in i_p, since we are increasing the dissipation source strength in 3.5 and conversely by decreasing α, i_p increases. An increase in α shows a greater change in i_p than a decrease in α.

TABLE 6-1

Variation of EGM Constants

PARAMETER	LOWER LIMIT - 50%	BASE	UPPER LIMIT + 50%
α	0.3	0.6	0.9
ϕ	0.3532	0.7064	1.0594
C_1	1.0	2.0	3.0
C_2	0.17	0.34	0.51
C_3	0.06	0.12	0.18
C_4	0.0275	0.055	0.0825

FIGURE 6-1

Sensitivity Analysis: α on Conditional Concentration Intensity

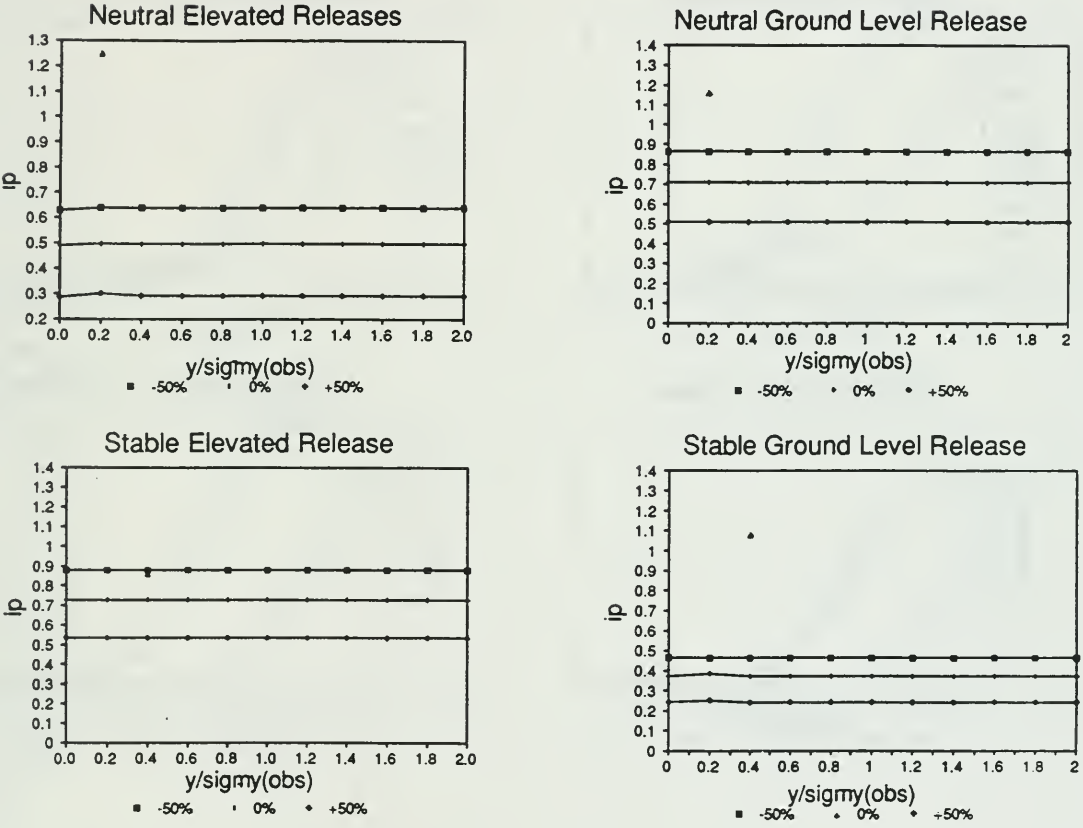

FIGURE 6-2

Sensitivity Analysis: α on Intermittency

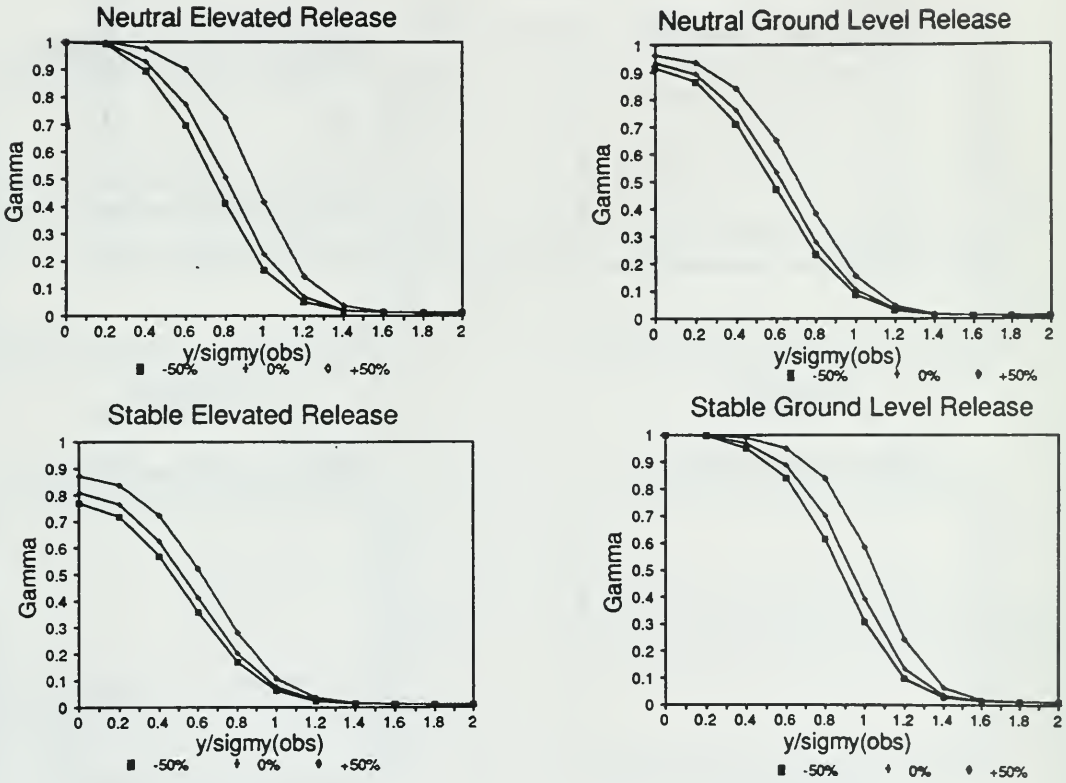

FIGURE 6-3

Sensitivity Analysis: α on Unconditional Concentration Intensity

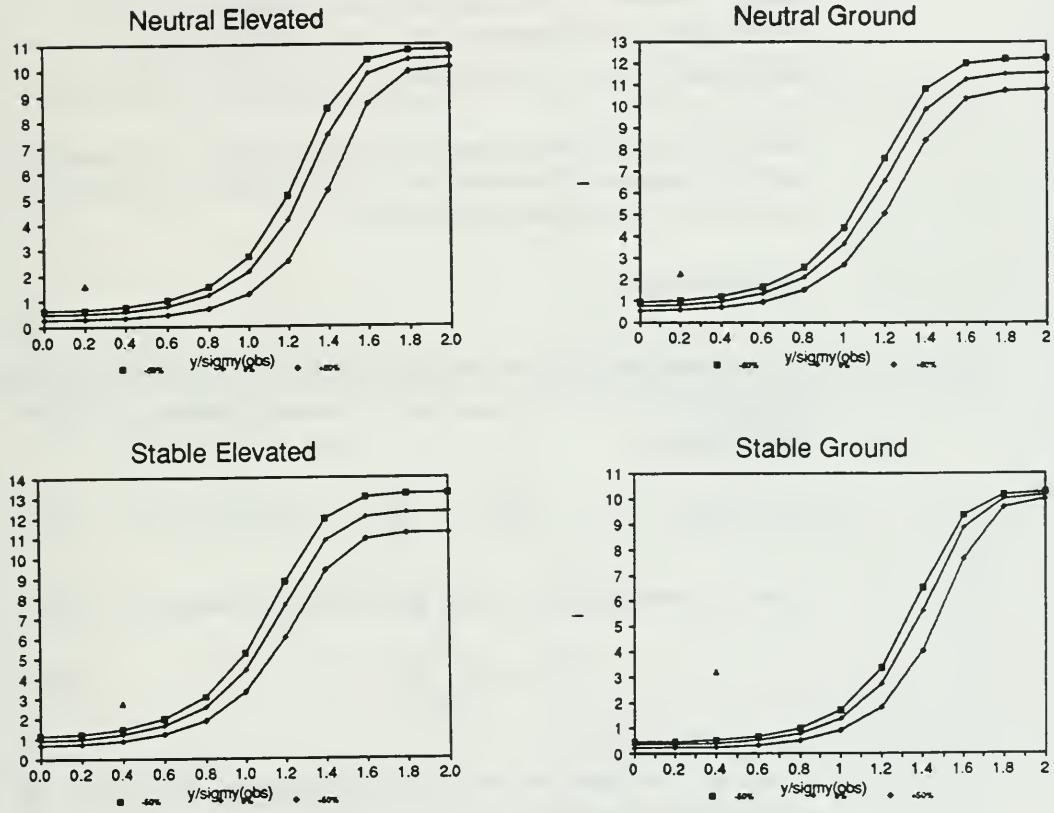

The effect of α on intermittency (γ) is shown in Figure 6-2. The increase in α shows an increase in γ which suggests the contaminant plume is present more often than not (i.e., less meandering or greater homogeneous mixing within the plume). The effect of α on γ varies with cross-wind distance and scenario. The largest variations occur between 0.6 and 1.0 σ_y's from the centreline with largest occurring under neutral elevated releases.

Similar trends to the above are observed in Figure 6-3 with α on the unconditional intensity i. Generally, i is insensitive to α near the centreline but becomes much more sensitive as the edges are approached.

6.2 SENSITIVITY OF C_1

C_1 is the power term in the "along wind" source dissipation formulation (3.7a). The term was developed from the local advection dissipation balance (see Chapter 3.1.1 and 3.1.2):

$$u \frac{\partial \overline{c^2}}{\partial x} = - \frac{\overline{c^2}}{T_d} \qquad [6.1]$$

where T_d is the dissipation time scale assuming the form (Wilson et al., 1982a)

$$T_d = \frac{(x + x_o)}{C_1 u} \quad . \qquad [6.2]$$

Figures 6-4 to 6-6 present the effect of a ± 50% change in C_1 on i_p, γ and i. the results show significant sensitivity on C_1.

The conditional intensity can be shown to be functionally dependent on C_1, assuming $\lambda \propto x$, as

$$i_p \propto \frac{1}{x^{C_1 - 1}} \qquad [6.3]$$

FIGURE 6-4

Sensitivity Analysis: C_1 on Conditional Concentration Intensity

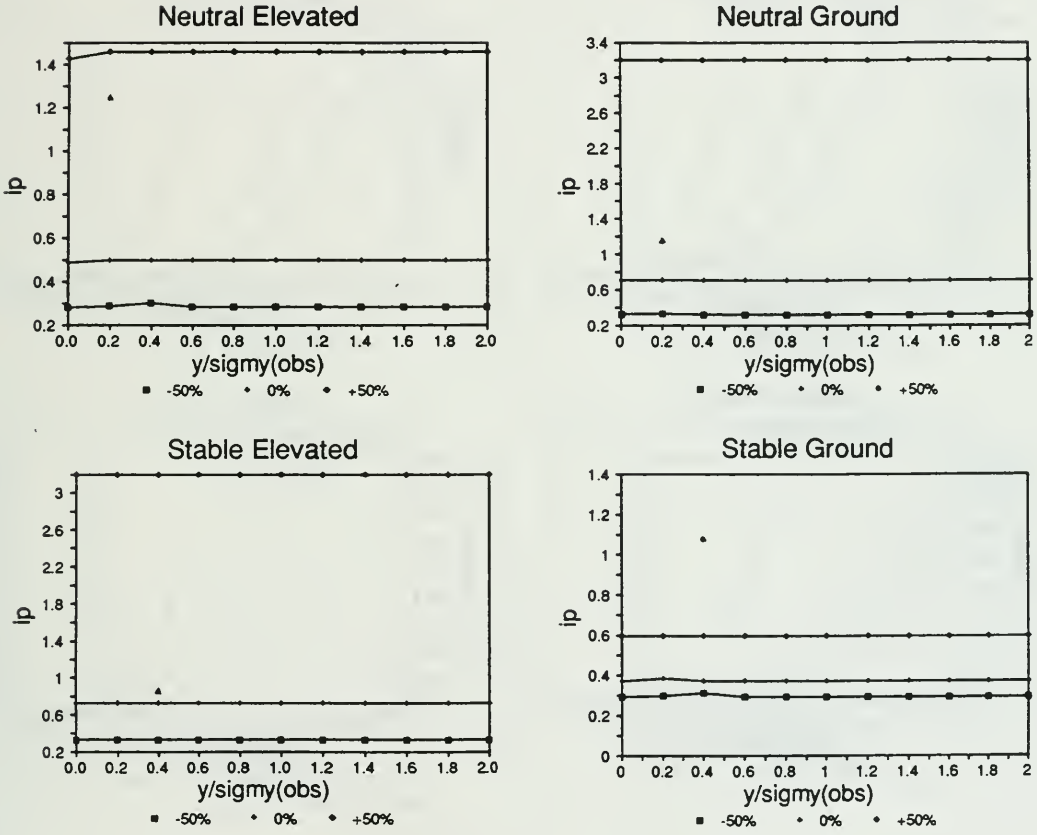

FIGURE 6-5

Sensitivity Analysis: C_1 on Intermittency

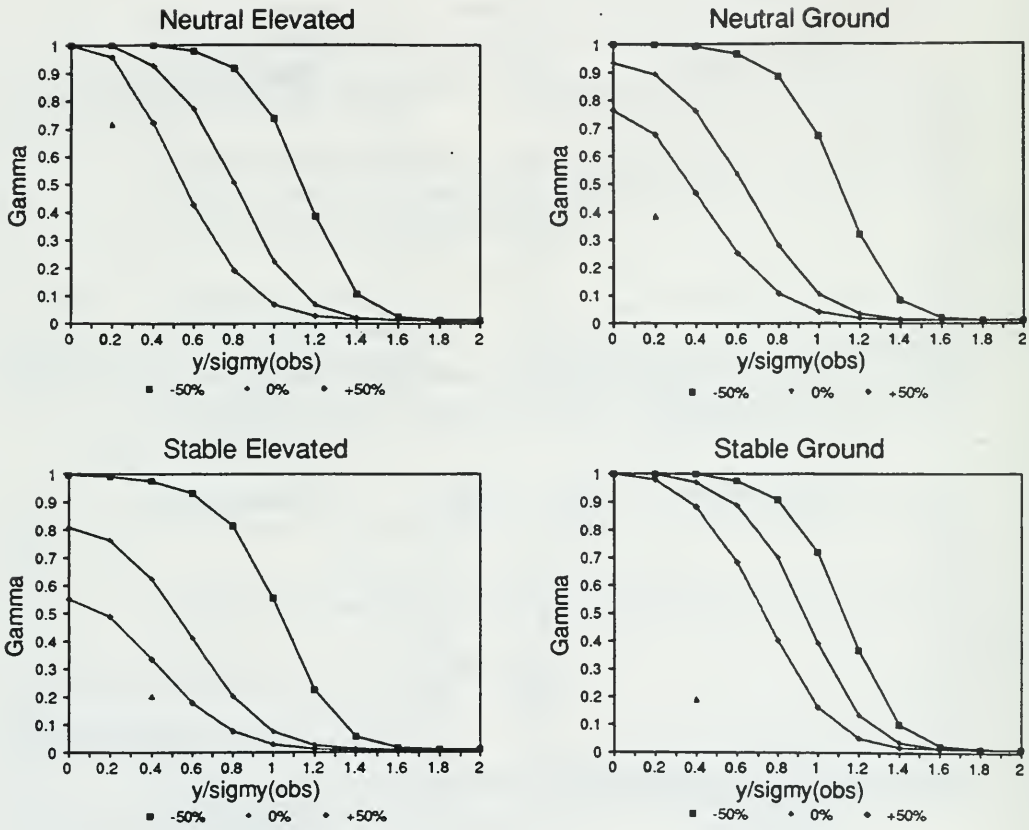

FIGURE 6-6

Sensitivity Analysis: C_1 on Unconditional Concentration Intensity

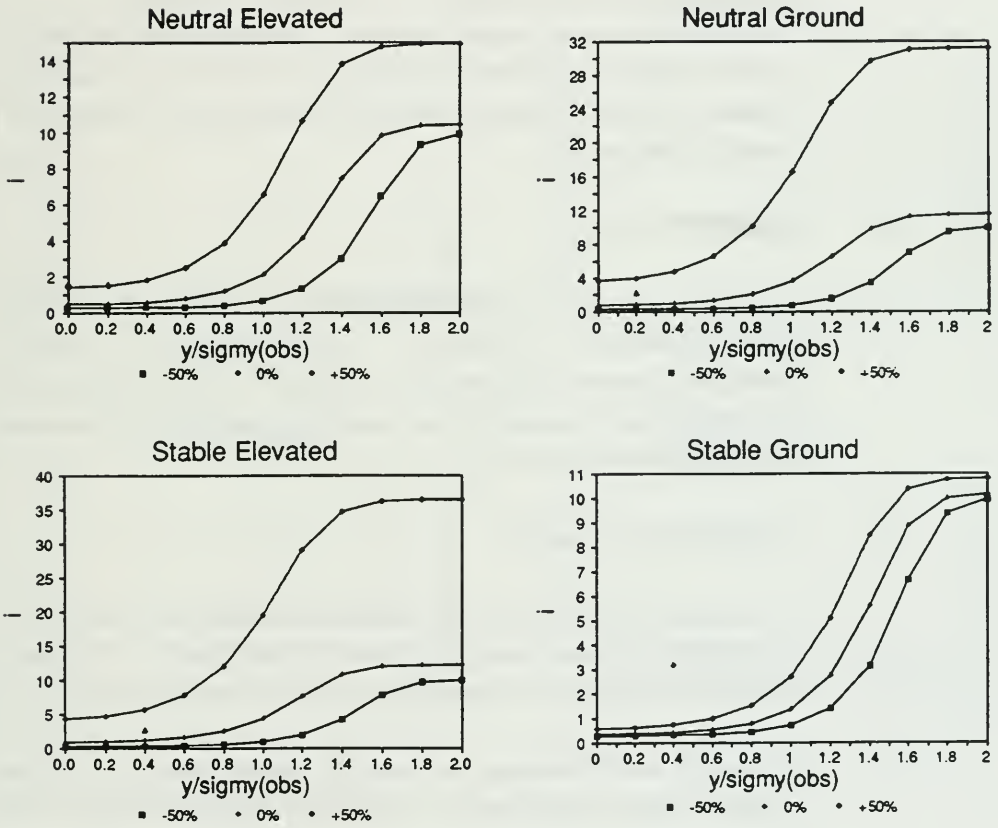

Thus as C_1 becomes larger, the term on the right hand side becomes significantly smaller. This is reflected in Figure 6-4 for all scenarios except with stable ground level releases.

The high sensitivity is also reflected in α and i as shown in Figures 6-5 and 6-6. C_1 is the most sensitive of all the parameters. The above figures also show a measured result for each scenario. In most cases, the measured value falls within the actual value and the upper limit except for intermittency where it seems to be below the +50% curve.

6.3 SENSITIVITY OF C_2

As with C_1, C_2 is used in the along wind source dissipation term (3.7a) but is directly proportional to i_p (Figure 6-7). A ±50% increase in C_2 shows a proportional increase in i_p for all scenarios. Similarly, for γ and i (Figures 6-8 and 6-9), the increase or decrease in C_2 is reflected both terms but the increases are not directly proportional as with i_p.

6.4 SENSITIVITY OF C_3 AND C_4

The constants C_3 and C_4 are used in determining the virtual source term (λ_o) in 3.7b which is also used in along wind source dissipation equation. Conditional intensity can be shown to be inversely proportional to C_3 and proportional to C_4.

Figures 6-10 and 6-13 illustrate the invariance of i_p with C_3 and C_4. There is virtually no effect on i_p by changing C_4 by ±50% for any of the four scenarios while some change is shown for 3 of the scenarios with respect to C_3. Similarly for γ and i with respect to C_3 and C_4 (Figures 6-11 to 6-12 and 6-14 to 6-15).

FIGURE 6-7

Sensitivity Analysis: C_2 on Conditional Concentration Intensity

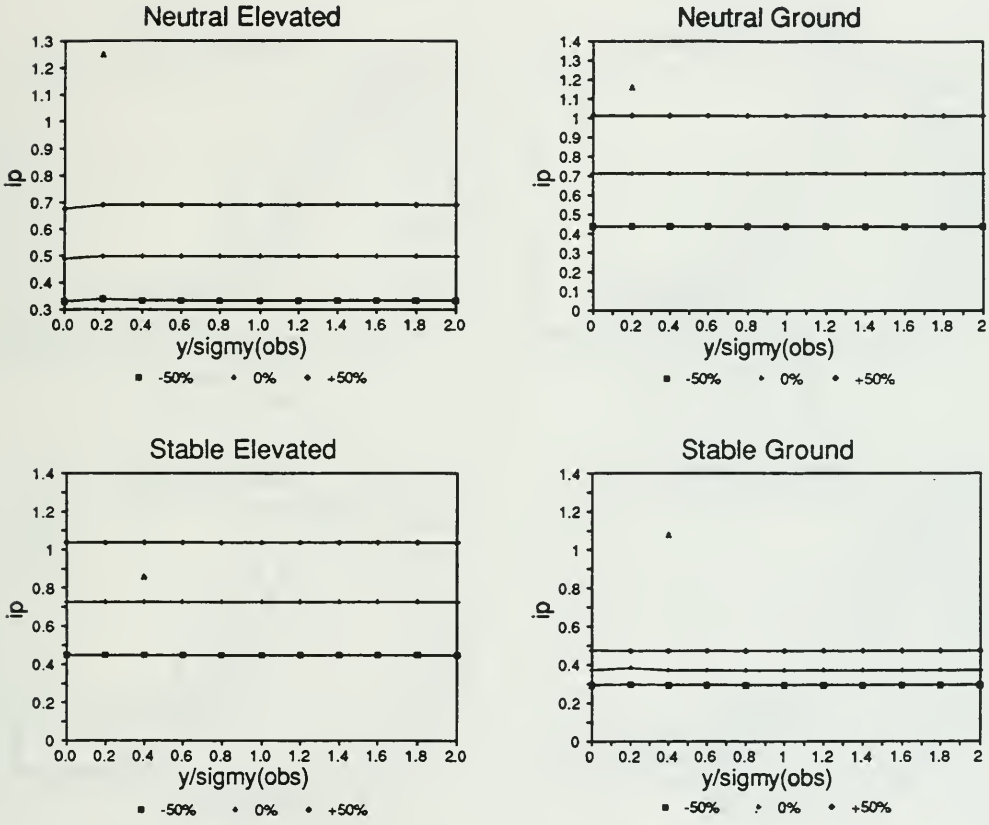

FIGURE 6-8

Sensitivity Analysis: C_2 on Intermittency

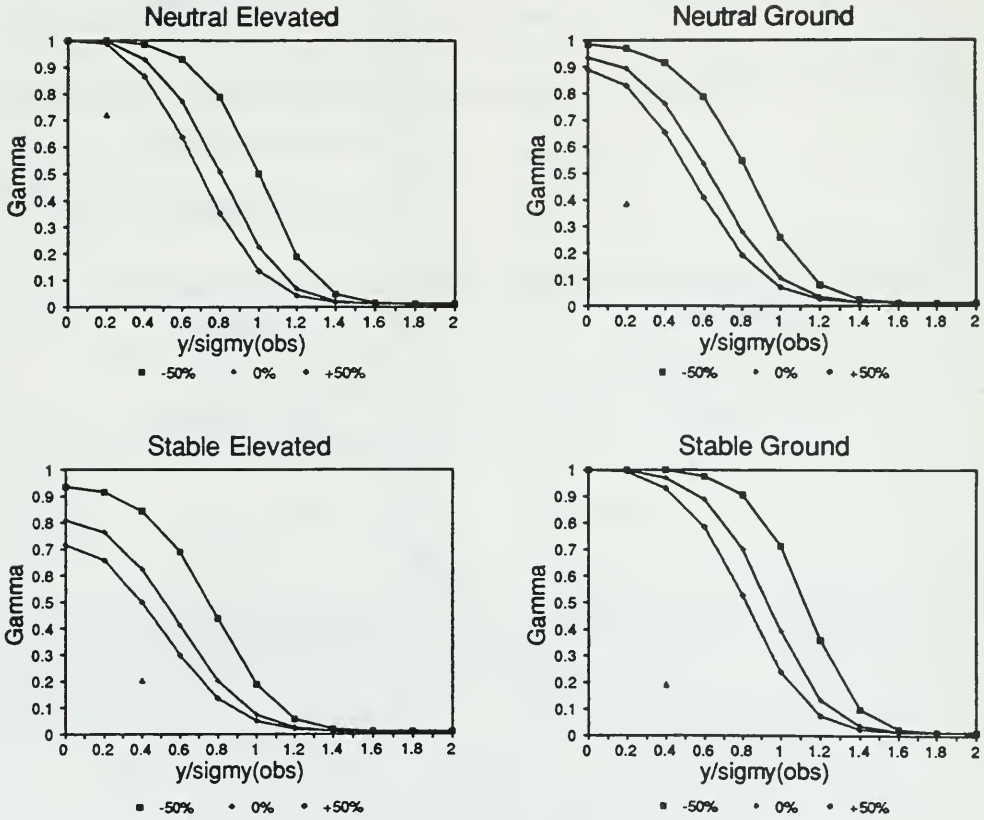

FIGURE 6-9

Sensitivity Analysis: C_2 on Unconditional Concentration Intensity

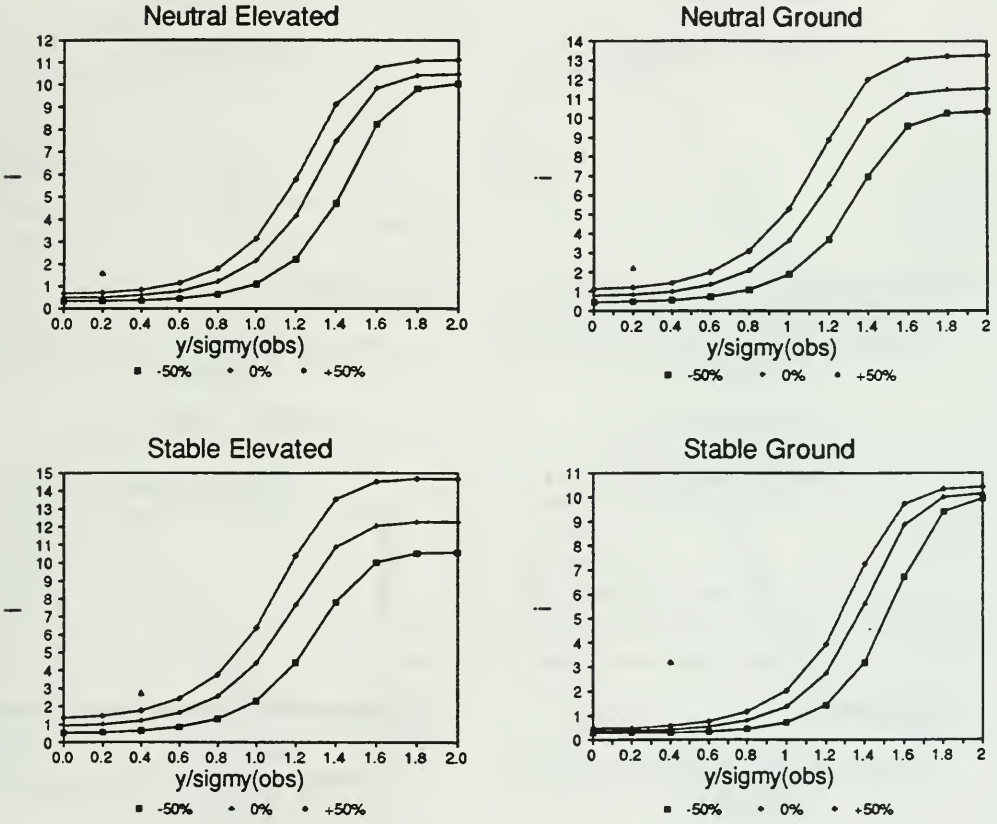

FIGURE 6-10

Sensitivity Analysis: C_3 on Conditional Concentration Intensity

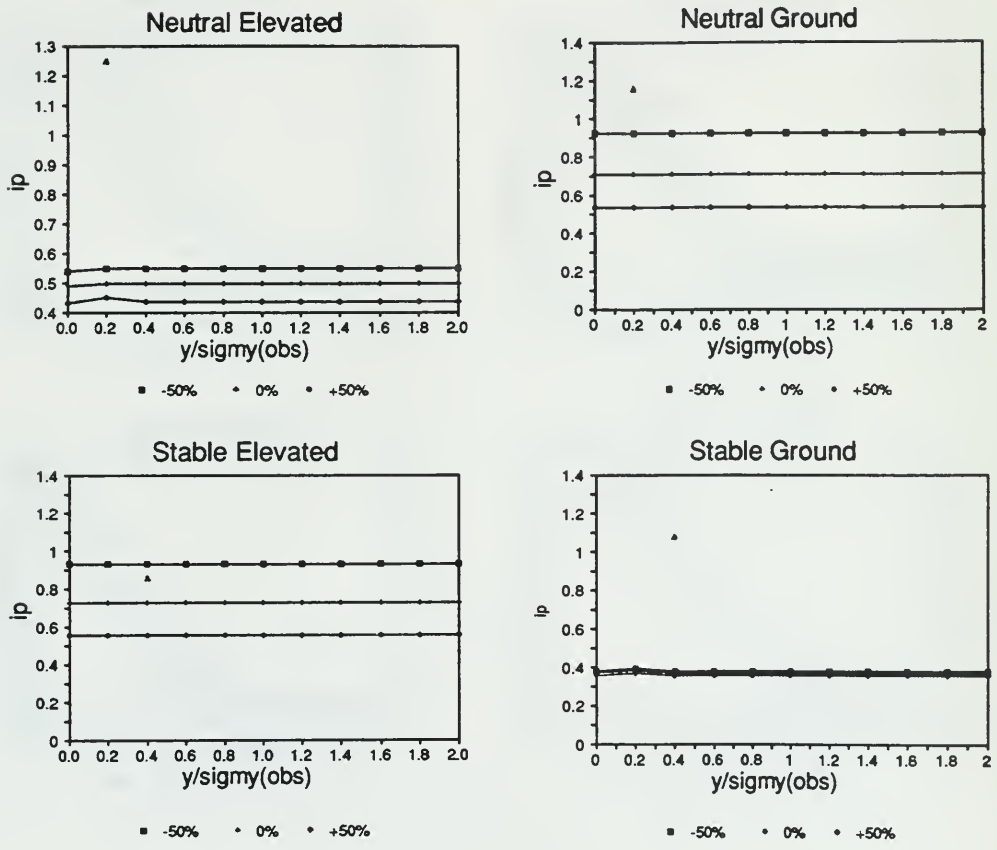

FIGURE 6-11

Sensitivity Analysis: C_3 on Intermittency

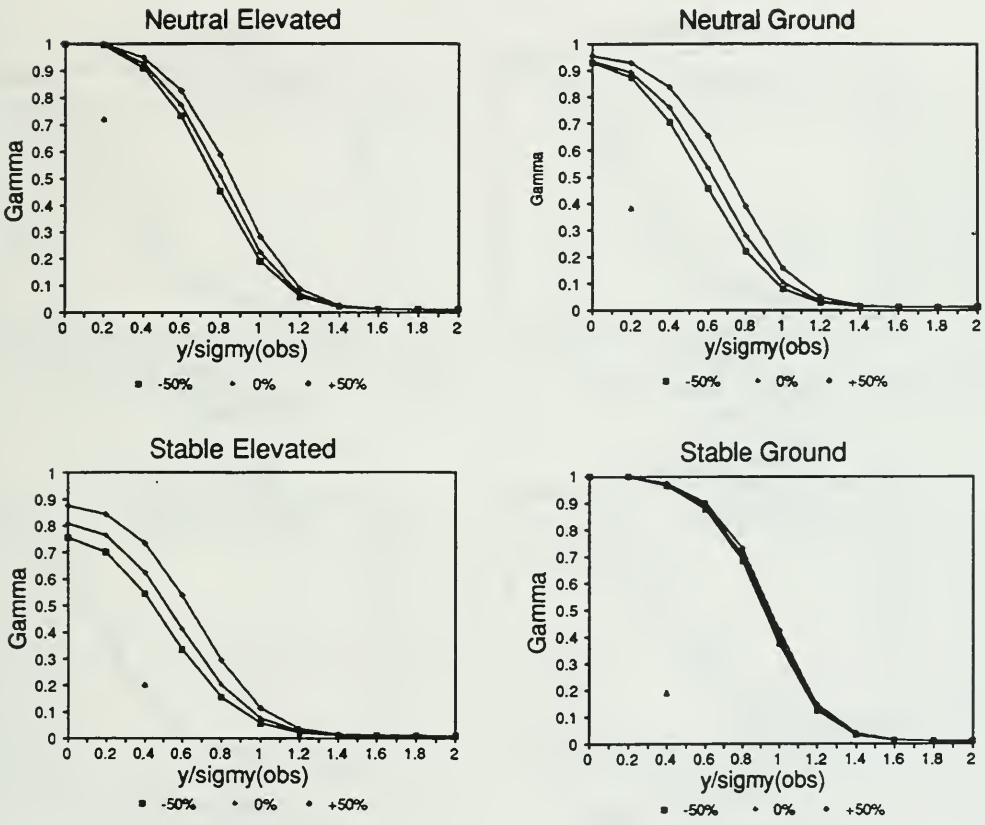

FIGURE 6-12

Sensitivity Analysis: C_3 on Unconditional Concentration Intensity

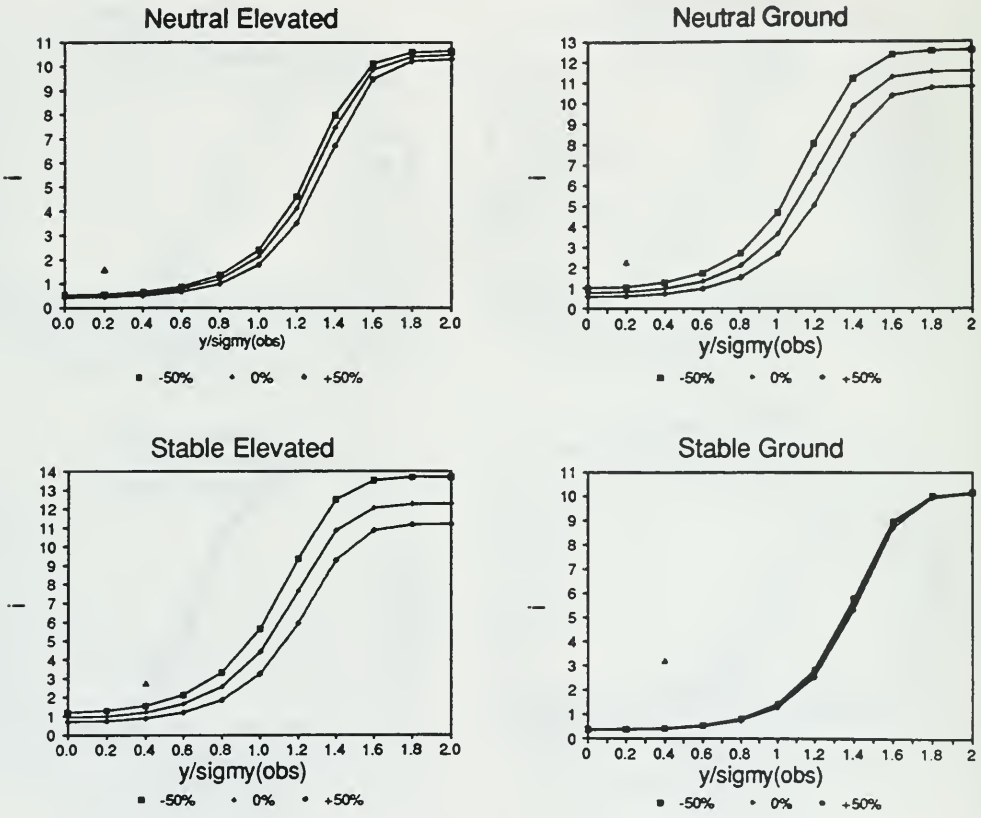

FIGURE 6-13

Sensitivity Analysis: C_4 on Conditional Concentration Intensity

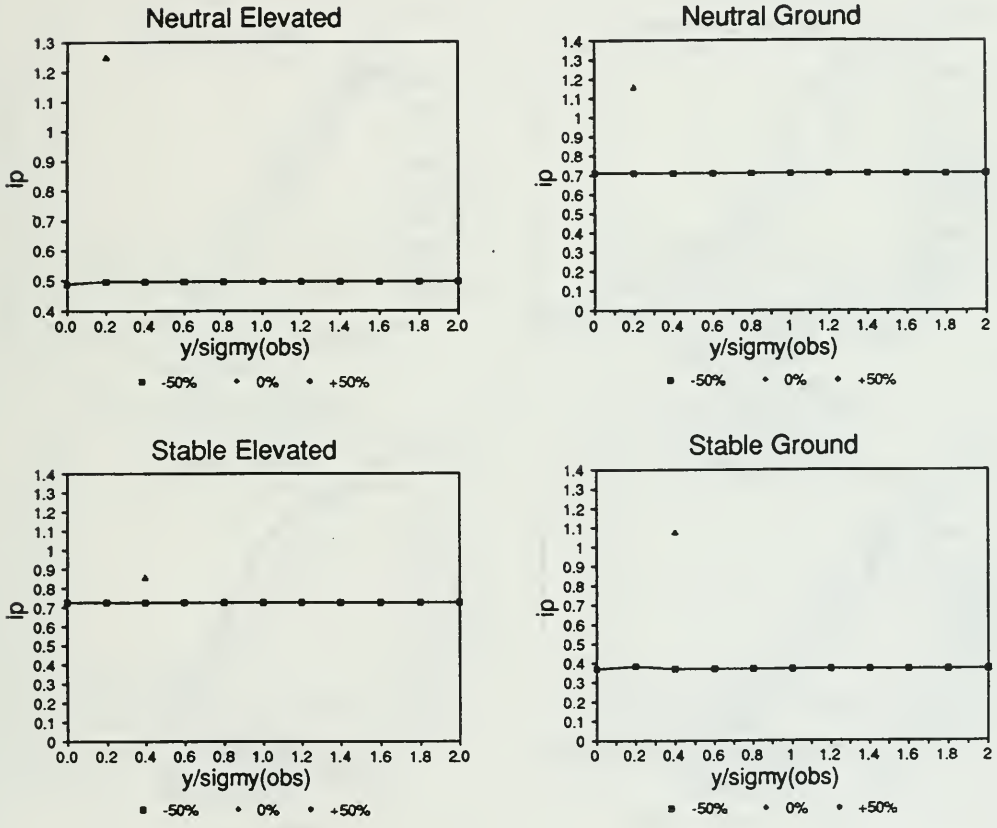

FIGURE 6-14

Sensitivity Analysis: C_4 on Intermittency

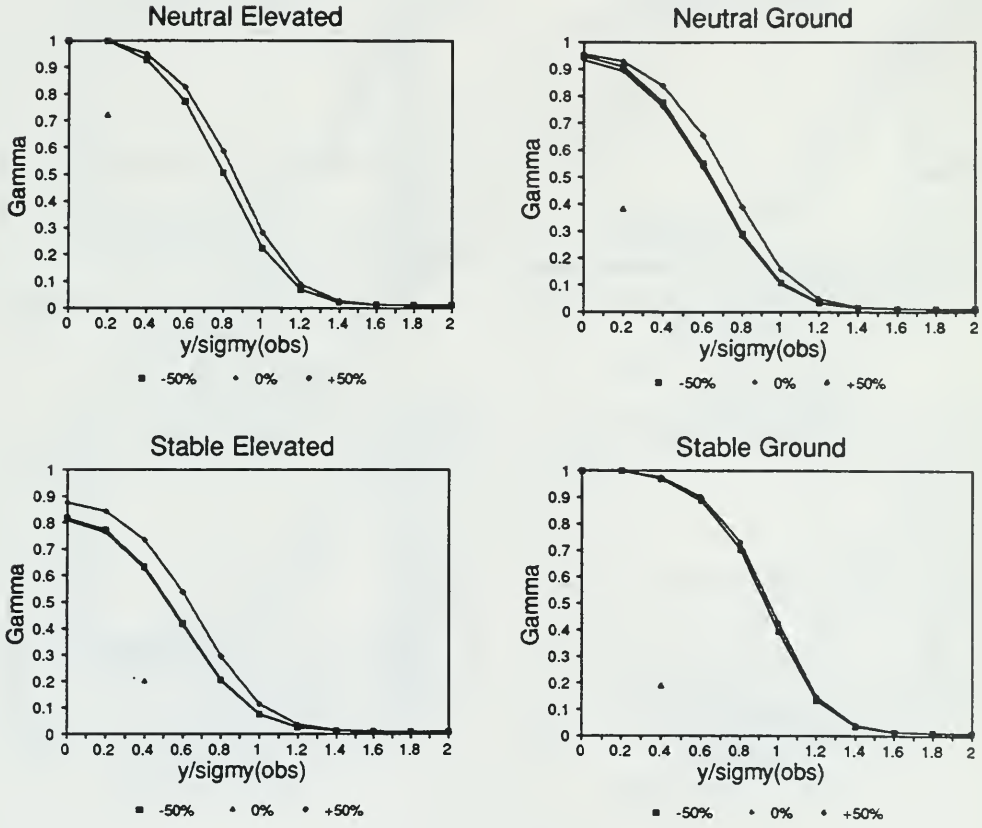

FIGURE 6-15

Sensitivity Analysis: C_4 on Unconditional Concentration Intensity

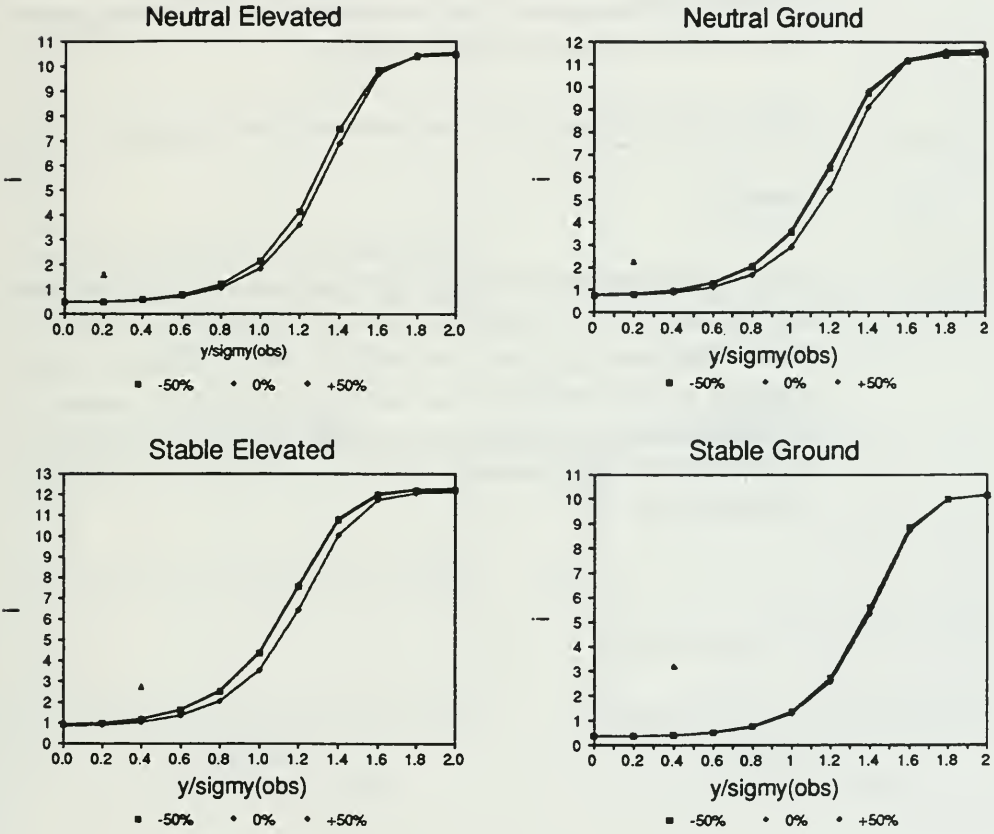

6.5 SENSITIVITY OF ϕ

The parameter ϕ is employed in 3.6 and represents the relative vertical displacement of the variance source term above the plume centreline. This will generally place the source term near the largest vertical concentration gradient which is the zone of maximum variance production.

Figures 6-16 to 6-18 show that i_p, γ and i are invariant with respect to ϕ.

6.6 SUMMARY

The sensitivity analysis indicates that i_p, γ and i are most sensitive to C_1 which is a scaling constant used in the dissipation time scale equation. The variables are virtually insensitive to C_3, C_4 and ϕ. The conditional intensity seems to be linearly dependent on the constants and, as expected, is constant with respect to crosswind distance. The graphical data indicates that i and γ are sensitive to crosswind location. Strong changes in five of the six constants did not cause the i_p to exceed unity.

FIGURE 6-16

Sensitivity Analysis: ϕ on Conditional Concentration Intensity

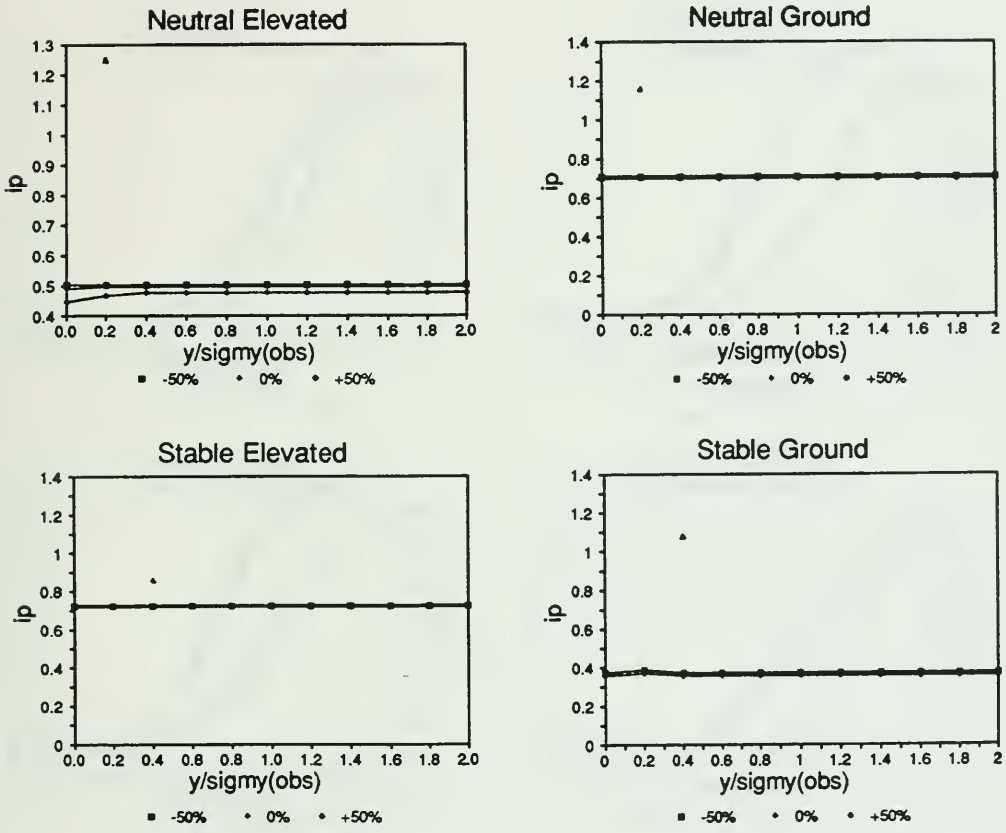

FIGURE 6-17

Sensitivity Analysis: ϕ on Intermittency

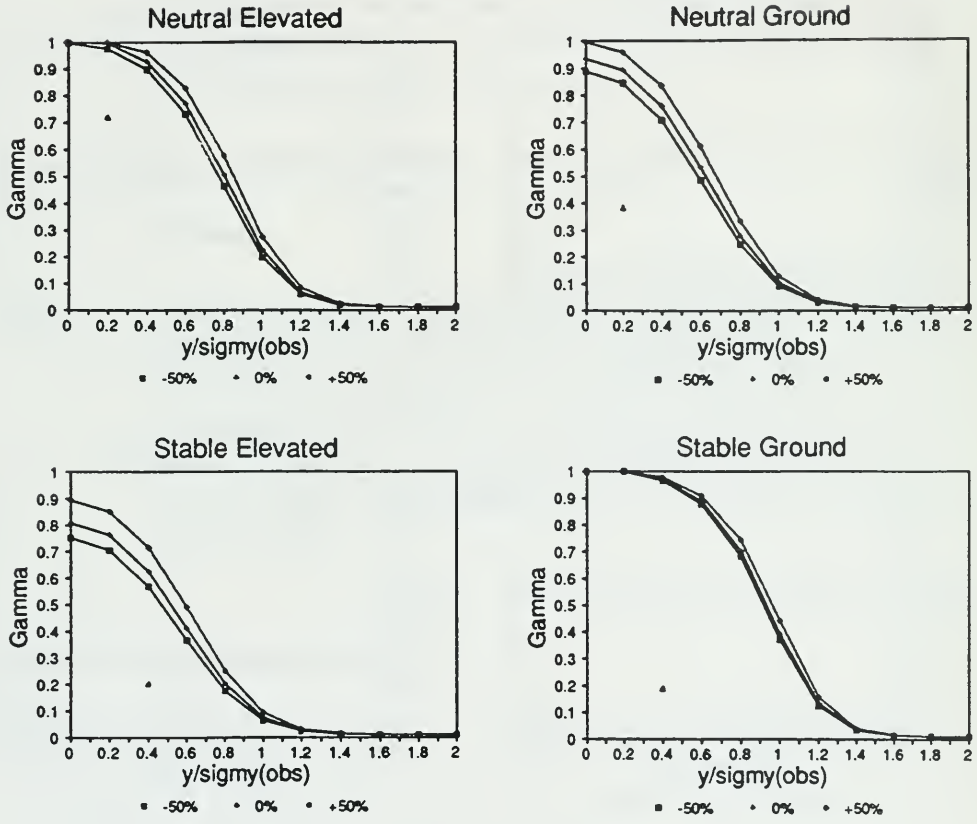

FIGURE 6-18

Sensitivity Analysis: ϕ on Unconditional Concentration Intensity

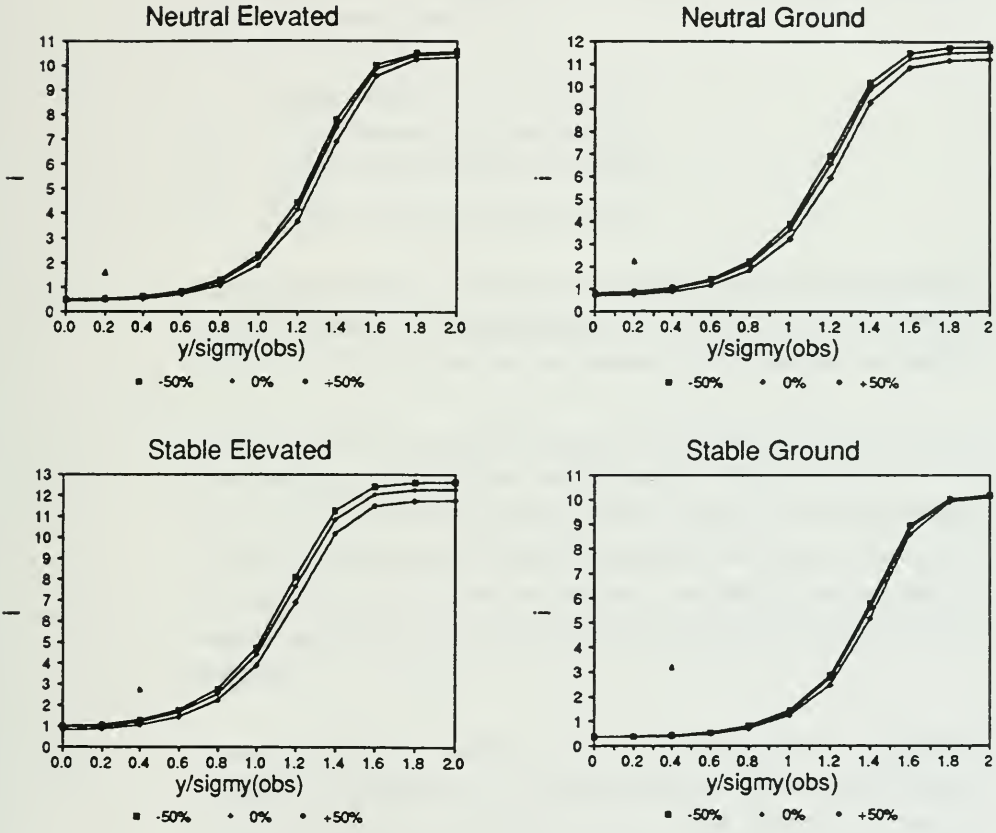

7 EVALUATION OF GAS/EGM PREDICTIONS WITH FIELD DATA

The results of the GASFLUC model are compared with the SF_6 stationary field measurements. As in Section 6, the field tests were categorized under four atmospheric release scenarios, i.e.

i) Surface release under neutral stability
ii) Surface release under stable stability
iii) Elevated release under neutral stability
iv) Elevated release under stable stability

for comparison purposes. As there was insufficient measurement data to compare the model predictions with observations as a function of downwind distance, the 700 m and 1400 m data were merged together to form one data set per scenario.

The primary objective of these comparisons, is to evaluate the performance of the EGM module when coupled with the OME Clean Air Program GAS model. The GAS model calculates mixing height, plume rise, dispersion coefficients and mean 30-minute concentrations. (It has been assumed that the 30-minute concentrations are equivalent to the 60-minute concentration.) The EGM module calculated i, i_p and γ as per Sections 3 and 4 as well as the percentile values via the log-normal distribution.

The performance of the above is evaluated via standard statistical and graphical procedures. Considerable effort has been made to determine the appropriate performance measures for dispersion models (Hanna, 1988). A wide variety of indices have been suggested since it is difficult to arrive at a single quantitative index of accuracy. The statistical techniques applied to present investigation are presented in Section 7.1.

Predicted mean concentrations and dispersion coefficients from the GAS model are compared to measured values under the emission/meteorological scenarios mentioned above (Section 7.2). Comparison between mixing height and plume rise were not carried out at this time. Table 7-1 presents the typical source characteristics used in the model. Measured emission rates for each case was used in predicting the downwind concentration. The exit temperature was taken as the ambient air temperature resulting in momentum generated plume rise.

The EGM parameters (i, i_p and γ) are compared against measured values in Section 7.3 while the log-normal distribution and the exponential distributions are compared in Section 7.4.

7.1 STATISTICS OF MODEL PERFORMANCE EVALUATION

Statistical analysis of the predictions and the observations is central to the model performance evaluation. The methods discussed by Fox (1981), Pendergrass and Rao (1984) and Rao et al. (1985) are used for the model evaluation and comparison with GAS & EGM.

In the discussion that follows, O_i refers to observed concentration and P_i refers to the corresponding calculated concentration at the same location during the same time period; N is the total number of observations. Means are computed as,

$$\bar{O} = (1/N)\sum_{i=1}^{N} O_i \qquad [7.1a]$$

$$\bar{P} = (1/N)\sum_{i=1}^{N} P_i \qquad [7.1b]$$

TABLE 7-1

Source Characteristics Used in Model Elevation

SOURCE CHARACTERISTICS		ELEVATED	GROUND
Height	(m)	2.3	0.3
Radius	(m)	0.3725	1.1
Exit Velocity	(m/s)	26.7	0.17
Exit Temperature	(°C)	Ambient	Ambient

Residuals are defined as the differences between observed and predicted concentrations such that,

$$D_l = O_l - P_l \quad . \qquad [7.2]$$

The predicted and the corresponding observed concentrations are treated as pairs in this analysis. The specific analysis procedures employed are given below.

1. Means and standard deviations of observed and predicted concentrations are compared.

2. Least-square linear regression is performed between predicted (on the ordinate) and observed (on the abscissa), to determine a slope, intercept, as well as the correlation coefficient, R.

3. Mean and standard deviation of the ratios between predicted and observed values are computed.

4. The following measures of differences between model predictions and observations were specifically recommended at the Woods Hole EPA/AMS workshop (Fox, 1981) for assessing the model performance.

   i) Mean difference between predicted and observed values is given by:

$$\overline{D} = \overline{O} - \overline{P} = (1/N)\sum_{l=1}^{N} D_l \qquad [7.3]$$

   ii) Mean relative bias is computed as:

$$\frac{\overline{P - O}}{\overline{O}} = \frac{1}{N}\sum_{l=1}^{N}\frac{D_l}{O_l} \qquad [7.4]$$

iii) The root mean square error (RMSE) of the relative bias is given by

$$RMSE = \left[((N - 1)/N)\ S^2_{\frac{D}{O}} + \left(\frac{\overline{D}^2}{\overline{O}}\right)\right]^{1/2} \qquad [7.5]$$

iv) Average absolute gross error of the concentration difference is given by

$$|\overline{D}| = (1/N) \sum_{i=1}^{N} |D_i| \ . \qquad [7.6]$$

v) Unsystematic and systematic mean square errors (MSE) are computed as

$$MSE_U = (1/N) \sum_{i=1}^{N} (P_i - \hat{P}_i)^2 \qquad [7.7]$$

$$MSE_S = (1/N) \sum_{i=1}^{N} (\hat{P}_i - O_i)^2 \qquad [7.8]$$

where $\hat{P}_i$ is derived from the relation $\hat{P}_i = a + b\ O_i$; a is the intercept and b is the slope of the linear regression line.

Rao et al (1985) found that the MSE measures can illuminate the sources or types of errors, which may be of considerable help in refining a model. If MSE is entirely, or largely, composed of MSE_U, perhaps the model is as good as possible and may not require major modification.

6. Another descriptive statistic is the index of agreement (see Wilimott, 1982) which is a measure of the degree to which the observed variate is accurately estimated by the simulated variate. The index of agreement (I) is expressed as,

$$I = 1 - \frac{\sum_{i=1}^{N} (P'_i - O'_i)^2}{\sum_{i=1}^{N} (|P'_i| + |O'_i|)^2} \qquad [7.8]$$

where $P_i' = P_i - \bar{O}$, and $O_i' = O_i - \bar{O}$.

The variable I specifies the degree to which the observed deviations about $\bar{O}$ correspond, both in magnitude and sign, to the predicted deviations from $\bar{O}$ (see Rao et al., 1985a).

7. Mean fractional error is computed as

$$MFE = (1/N) \sum_{i=1}^{N} \left[(O_i - P_i)/[(O_i + P_i)/2]^{1/2}\right] \qquad [7.9]$$

The algebraic mean error defined as (O - P), emphasizes the largest observations and predictions and slights the smaller ones. The relative error, defined in a symmetric form as (O - P)/[O + P)/2], tends to emphasize the smallest observations and predictions and slights the larger observations and predictions. Thus, the residual or mean fractional error as defined in Equation (7.9) achieves a reasonable compromise between the algebraic error and the relative error.

In many cases, the SF_6 samplers were located well off the 30-minute average wind vector direction which defines the centreline of the plume. This was primarily due to the wind changing direction during the measurement period. Figure 7-1 presents the frequency of measurements as function of normalized crosswind distance for the four stability/release scenarios. A significant portion of the data were taken at $y \geq 3\ \sigma_y$ where σ_y is predicted via the CAP model.

FIGURE 7-1a

Normalized Cross-Wind Distance Distribution
Neutral/Surface

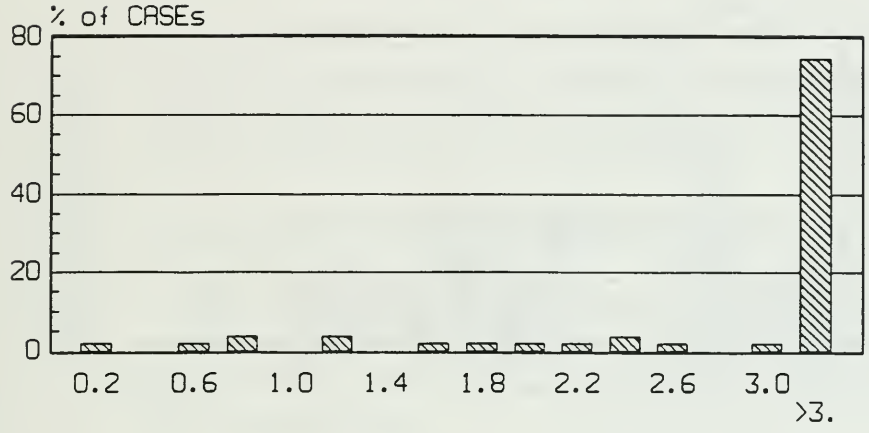

FIGURE 7-1b

Normalized Cross-Wind Distance Distribution
Stable/Surface

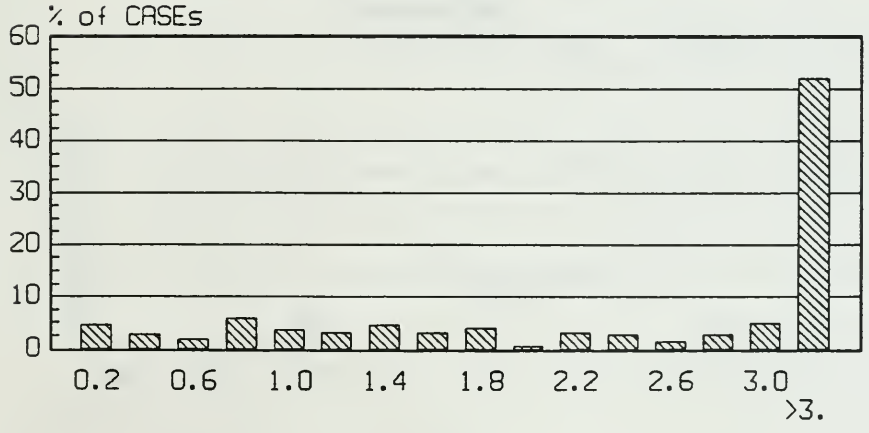

FIGURE 7-1c

Normalized Cross-Wind Distance Distribution
Neutral/Elevated

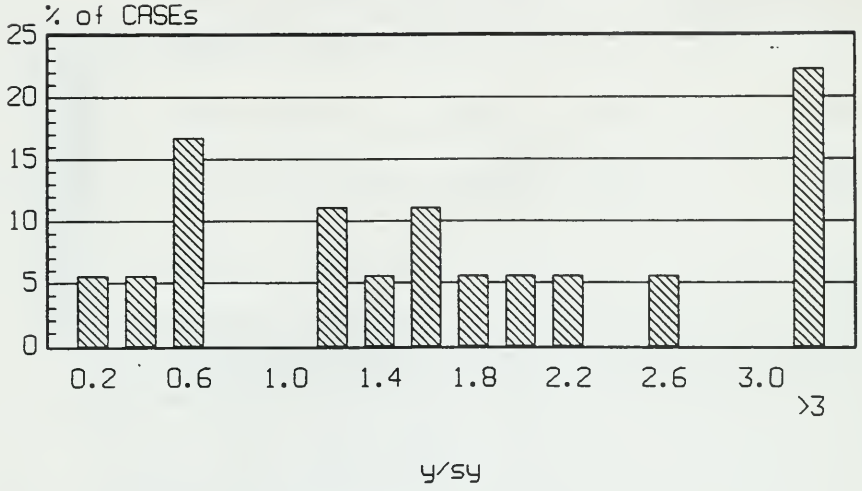

FIGURE 7-1d

Normalized Cross-Wind Distance Distribution
Stable/Elevated

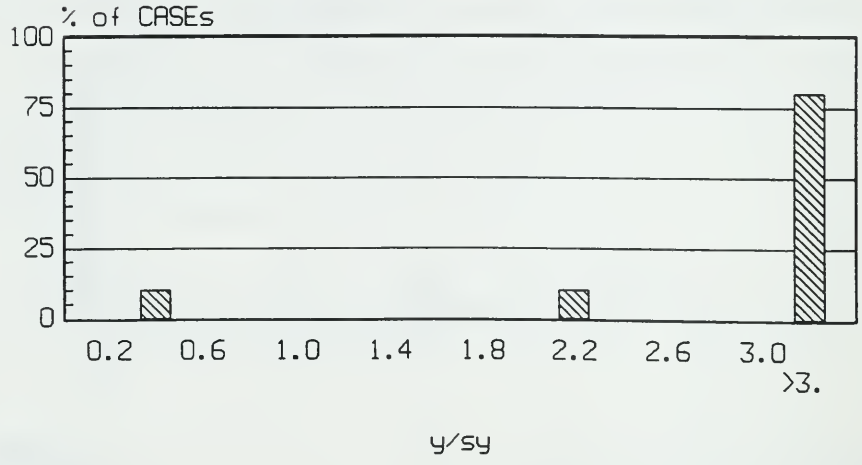

To provide a fair model evaluation data set, only measurement taken within ± 2.2 σ_y were considered. This significantly reduced the number of available cases for evaluation. Table 7-2 presents a summary of the final valid data set used in the evaluation.

Table 7-3 summarizes the statistical performance measures for mean concentration ($\overline{c}$), crosswind dispersion coefficient (σ_y), unconditional intensity (i), conditional intensity (i_p) and intermittency (γ) for the four scenarios. Insufficient data were available for assessing stable/elevated releases.

7.2 MEAN CONCENTRATION AND DISPERSION COEFFICIENTS

Mean concentrations and dispersion coefficients were predicted via the GAS model for comparison with the field data using meteorological information described above. Of significant interest is the comparison of crosswind coefficients with "pseudo" measured values.

The meteorological data sets included measurements of the crosswind turbulent velocity fluctuations ($\overline{v'^2}$) which can be related to the wind direction variance (σ_θ^2) via,

$$\sigma_\theta = \tan^{-1}\left[\frac{\sqrt{\overline{v'^2}}}{\overline{u}}\right] \quad (rad) \quad . \qquad [7.10]$$

An estimate of the crosswind dispersion coefficient (σ_y) can be obtained via,

$$\sigma_y = \frac{\sigma_\theta \cdot x}{(1 + x/2500)^{1/2}} \quad (m) \quad . \qquad [7.11]$$

TABLE 7-2

Summary of Evaluation Data Set

RELEASE SCENARIO	ATMOSPHERIC STABILITY	DOWNWIND (m)	CROSSWIND (y/σ_y)	NO. OF CASES	%	AVERAGE METEOROLOGICAL				
						u_* (cm/s)	$\bar{u}$ (m/s)	H_{o_2} (w/m^2)	L (m)	z_i[1] (m)
Elevated	Stable	1345	1.2	1	2	9	3.1	-6.8	18	270
	Neutral	1393	1.1	13	12	10.1	2.8	-2.5	95	215
Surface	Stable	700	1.0	82	77	21	5.9	-33	74	128
	Neutral	698	1.2	10	9	18.6	5.0	-1.0	381	366
				107	100%					

[1] Calculated as per CAP pre-processor.

TABLE 7-3

Summary of Statistical Indices for EGM Evaluation

	Neutral/Surface		Stable/Surface		Neutral/Elevated		Stable/Elevated	
Sigma-Y	O	P	O	P	O	P	O	P
Count	10.00	10.00	82.00	82.00	13.00	13.00	1.00	1.00
Avg	83.22	26.02	64.02	26.30	150.89	104.78	188.10	35.30
STD	32.45	10.19	31.24	7.53	54.07	0.47	n/a	n/a
Gross Error	57.20		37.72		60.00		152.80	
P/O	0.37		0.45		0.86		0.19	
(P-O)/O	-0.63		-0.55		-0.14		-0.81	
RMSE	0.65		0.56		0.52		n/a	
Intercept	38.32		19.32		104.44		n/a	
Slope	-0.15		0.11		0.00		n/a	
R	0.47		0.45		0.26		n/a	
MSEu	2%		2%		0%		n/a	
MSEs	98%		98%		100%		n/a	
I	0.39		0.40		0.46		n/a	
MFE	0.98		0.78		0.27		n/a	

	Neutral/Surface		Stable/Surface		Neutral/Elevated		Stable/Elevated	
Concentration	O	P	O	P	O	P	O	P
Count	10.00	10.00	82.00	82.00	13.00	13.00	1.00	1.00
Avg	112.50	369.90	284.11	465.99	142.62	95.56	36.00	36.40
STD	83.17	428.65	292.99	531.39	153.54	59.64	n/a	n/a
Gross Error	277.82		329.27		94.17		-0.40	
P/O	3.53		4.57		3.29		1.01	
(P-O)/O	2.53		3.57		2.29		0.01	
RMSE	4.12		9.19		7.76		n/a	
Intercept	153.68		275.74		86.74		n/a	
Slope	1.92		0.67		0.06		n/a	
R	0.37		0.37		0.16		n/a	
MSEu	69%		85%		13%		n/a	
MSEs	31%		15%		87%		n/a	
I	0.22		0.53		0.42		n/a	
MFE	-0.72		-0.47		0.04		n/a	

TABLE 7-3 (Cont'd)

Summary of Statistical Indices for EGM Evaluation

Unconditional	Neutral/Surface		Stable/Surface		Neutral/Elevated		Stable/Elevated	
Intensity (i)	O	P	O	P	O	P	O	P
Count	10.00	10.00	82.00	82.00	13.00	13.00	1.00	1.00
Avg	1.79	214.19	1.59	109.09	2.10	54.83	2.75	1308.00
STD	1.10	578.33	1.09	301.66	1.90	107.28	n/a	n/a
Gross Error	212.63		107.65		53.51		-1305.25	
P/O	78.77		73.82		23.69		475.64	
(P-O)/O	77.77		72.82		22.69		474.64	
RMSE	164.37		243.42		52.63		n/a	
Intercept	-428.54		109.59		-5.87		n/a	
Slope	358.07		-0.32		28.93		n/a	
R	0.68		0.00		0.51		n/a	
MSEu	47%		89%		60%		n/a	
MSEs	53%		11%		40%		n/a	
I	0.00		0.00		0.03		n/a	
MFE	-0.83		-0.96		-0.67		n/a	

Conditional	Neutral/Surface		Stable/Surface		Neutral/Elevated		Stable/Elevated	
Intensity (ip)	O	P	O	P	O	P	O	P
Count	10.00	10.00	82.00	82.00	13.00	13.00	1.00	1.00
Avg	0.94	0.57	0.83	0.82	0.95	0.52	0.86	0.72
STD	0.41	0.15	0.33	0.13	0.39	0.05	n/a	n/a
Gross Error	0.45		0.23		0.47		0.14	
P/O	0.58		1.10		0.66		0.84	
(P-O)/O	-0.42		0.10		-0.34		-0.16	
RMSE	0.43		0.43		0.45		n/a	
Intercept	0.32		0.73		0.58		n/a	
Slope	0.27		0.10		-0.06		n/a	
R	0.75		0.26		0.45		n/a	
MSEu	4%		16%		1%		n/a	
MSEs	96%		84%		99%		n/a	
I	0.60		0.44		0.42		n/a	
MFE	0.29		-0.05		0.49		n/a	

TABLE 7-3 (Cont'd)

Summary of Statistical Indices for EGM Evaluation

Intermittency (Gamma)	Neutral/Surface		Stable/Surface		Neutral/Elevated		Stable/Elevated	
	O	P	O	P	O	P	O	P
Count	10.00	10.00	82.00	82.00	13.00	13.00	1.00	1.00
Avg	0.48	0.26	0.61	0.30	0.53	0.37	0.20	0.01
STD	0.30	0.33	0.27	0.34	0.24	0.43	n/a	n/a
Gross Error	0.30		0.38		0.40		0.19	
P/O	0.50		0.48		0.70		0.05	
(P–O)/O	–0.50		–0.52		–0.30		–0.95	
RMSE	0.69		0.74		0.92		n/a	
Intercept	0.02		0.02		0.13		n/a	
Slope	0.49		0.45		0.45		n/a	
R	0.46		0.35		0.25		n/a	
MSEu	54%		46%		79%		n/a	
MSEs	46%		54%		21%		n/a	
I	0.64		0.54		0.53		n/a	
MFE	0.64		0.96		0.90		n/a	

CONCORD
ENVIRONMENTAL

Figures 7-2a to 7-2c present predicted versus observed crosswind dispersion coefficients. Typically, the σ_y's are underpredicted by the GAS model. All scenarios show the same relative RMSE which is virtually all systematic (Table 7-2). The sources for systematic errors include improper emission data, meteorological data and model formulation. The surface releases show a higher correlation coefficient than the elevated release but the elevated release has a slightly higher index of agreement (I).

Figures 7-3a to 7-3c present the paired comparison of predicted and observed mean concentrations. The comparison shows a bias of overprediction by a factor 3.5 to 4.5. The overpredictions are not unexpected because σ_y's are generally underpredicted. Table 7-2 shows that stable surface release scenarios has a better index of agreement than the others but has a higher RMSE. The surface release scenarios have a larger unsystematic error (MSEu) than the elevated release. This suggests that improvements or refinements to the GAS surface release model may be required.

To further examine the relative error of the GAS model, Figures 7-4 to 7-6 present the relative error as a function of wind speed (u) and normalized crosswind distance (y/σ_y). With respect to wind speed, the relative error is typically smaller at the higher winds. It is of interest, that the greatest error occurs under low winds stable conditions, where the predicted concentration is about an order of magnitude greater than the observed. The model gives reasonable results as a function of crosswind distance (Figures 7-4b to 7-6b). The model predicts within a factor of 5 of the observed values, with the exception of one point under the neutral/elevated scenario, within 2.2 σ_y of the centreline.

FIGURE 7-2a

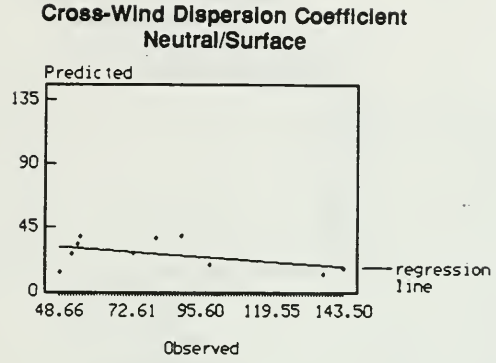

FIGURE 7-2b

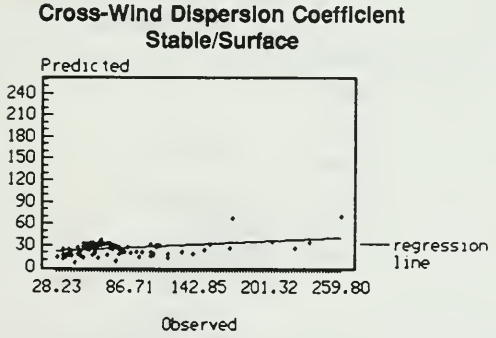

FIGURE 7-2c

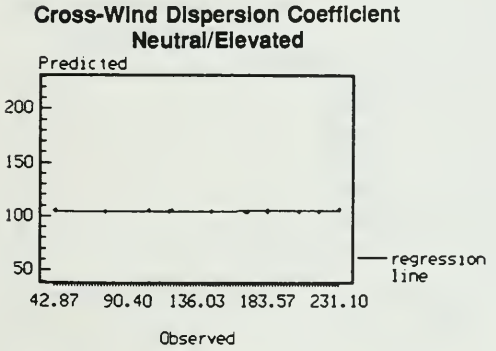

FIGURE 7-3a

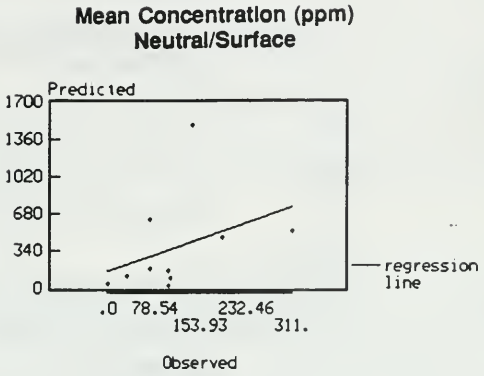

FIGURE 7-3b

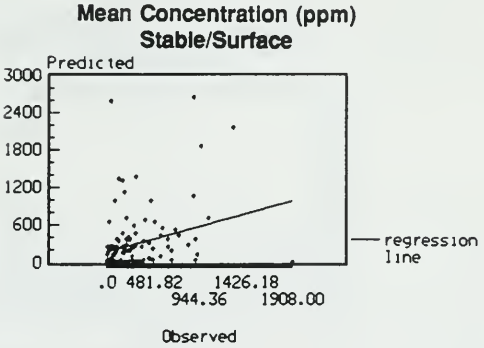

FIGURE 7-3c

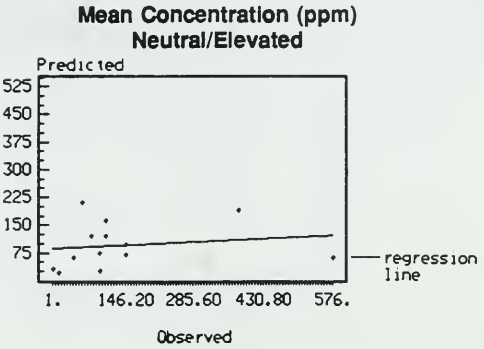

FIGURE 7-4a

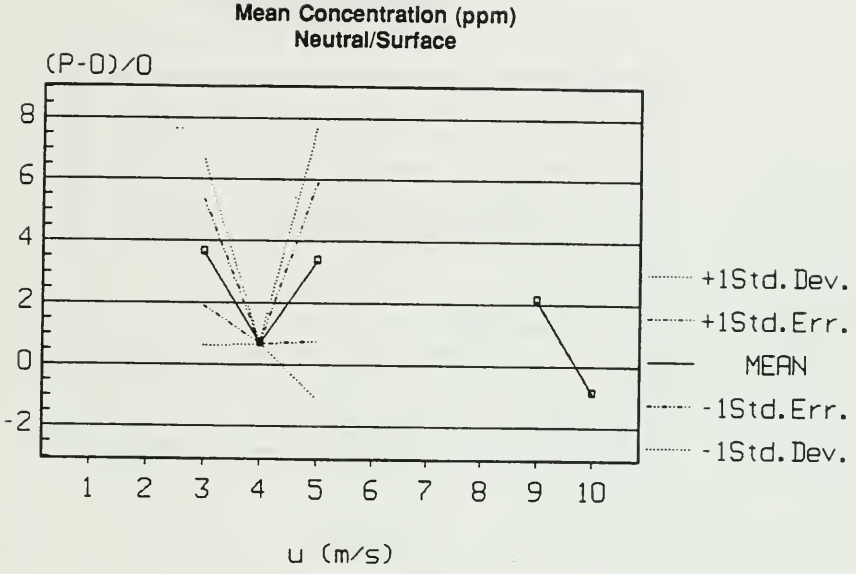

FIGURE 7-4b

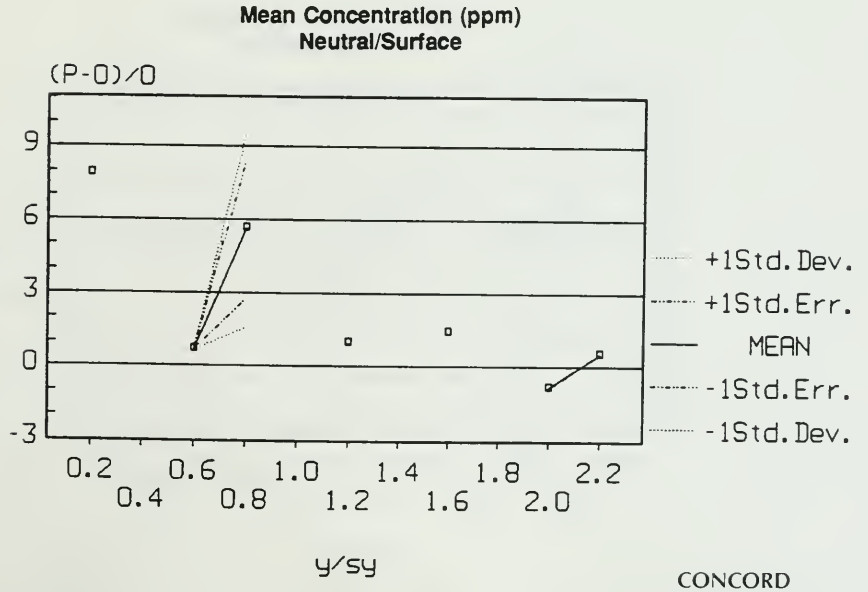

FIGURE 7-5a

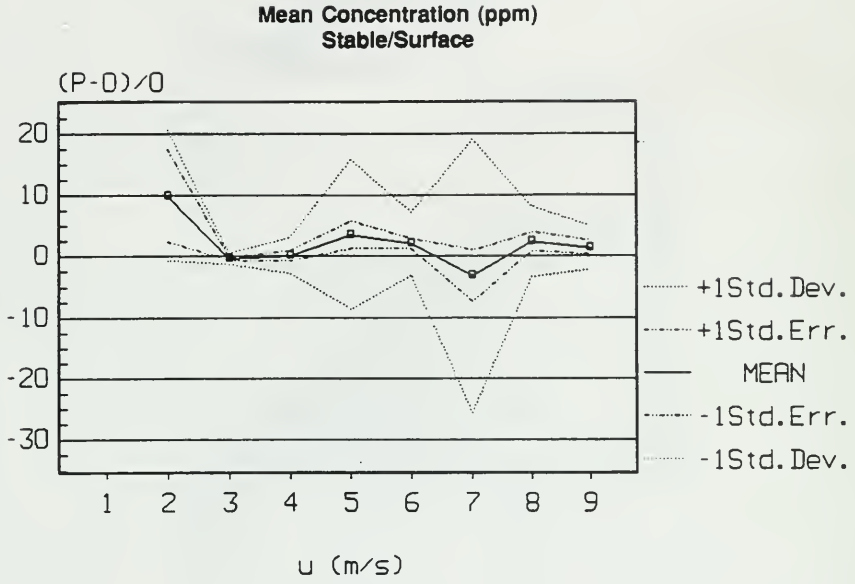

FIGURE 7-5b

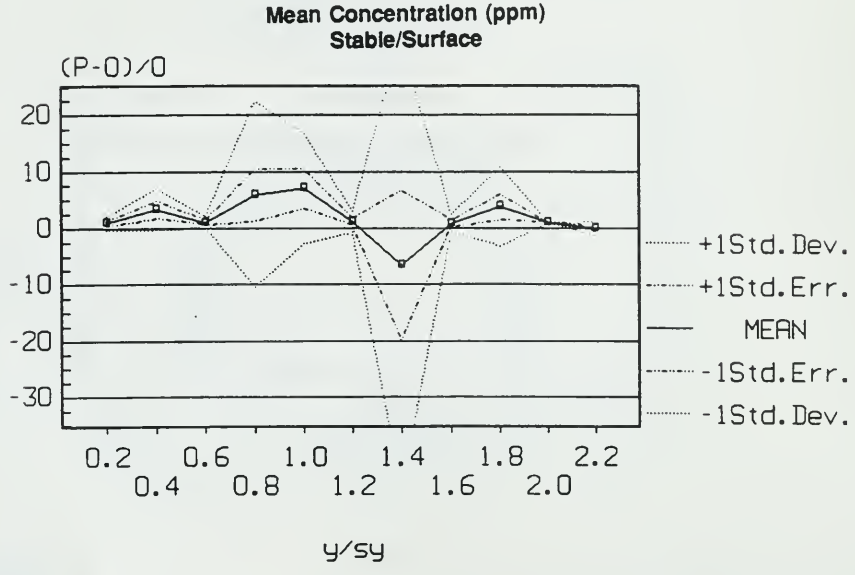

FIGURE 7-6a

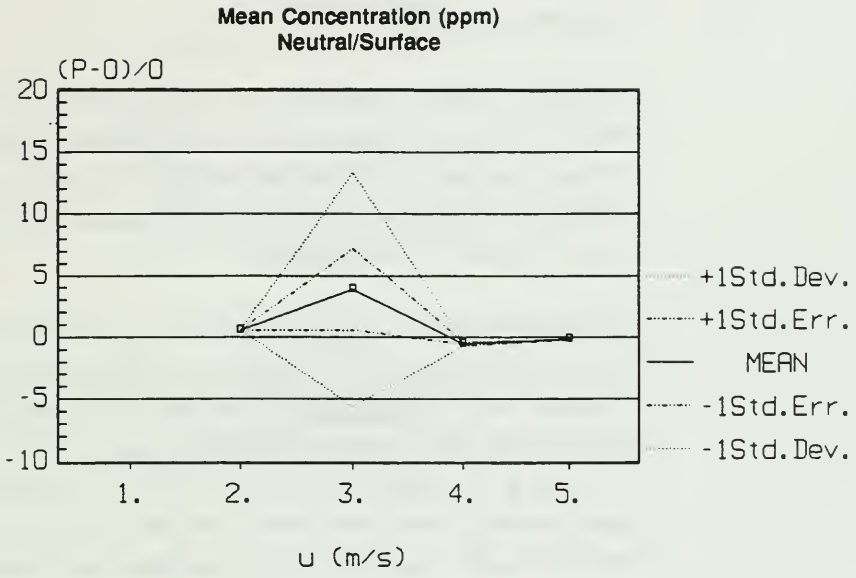

FIGURE 7-6b

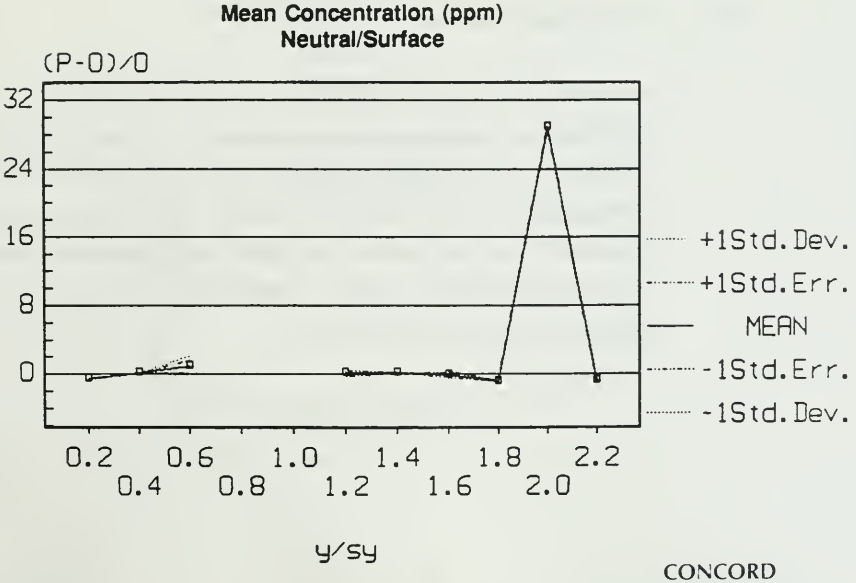

7.3 EGM MODEL EVALUATION

7.3.1 Unconditional Intensity

Unconditional intensity is calculated via the EGM module as described earlier. Figure 7-7 present the predicted and observed unconditional intensities. The EGM significantly overpredicts and has virtual zero index of agreement (I), for all cases (Table 7-2). The stable/surface scenario has the highest unsystematic error while the other two have virtual equal diversion.

The relative bias as a function of wind speed and y/σ_y is presented in Figures 7-8 to 7-10. There is insufficient information with respect to wind speed to evaluate any trends. There is a significant trend with respect to crosswind distances. As discussed earlier, the unconditional intensity is unstable at the fringes (i.e., $y > 2\sigma_y$). This is very apparent from Figures 7-8b to 7-10b where the predicted intensity is almost 3 orders of magnitude greater than the observed. The relative bias is significantly reduced at $y < 1.5\sigma_y$ for all cases which should be, therefore, the limit of applicability.

7.3.2 Conditional Intensity

In-plume or conditional intensity as predicted via the EGM is presented. The predicted and observed pairs are presented in Figures 7-11a to 7-11c and the statistical indices are given in Table 7-2. The model seems to provide adequate representation of the conditional intensity. The conditional intensity is under predicted for neutral conditions and slightly overpredicted for stable conditions as well as having a better correlation under neutral. The errors for all scenarios are systematic as shown in Table 7-2.

FIGURE 7-7a

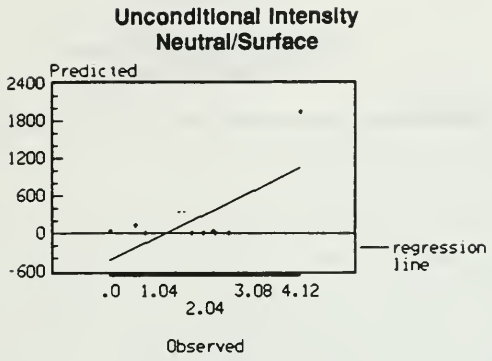

FIGURE 7-7b

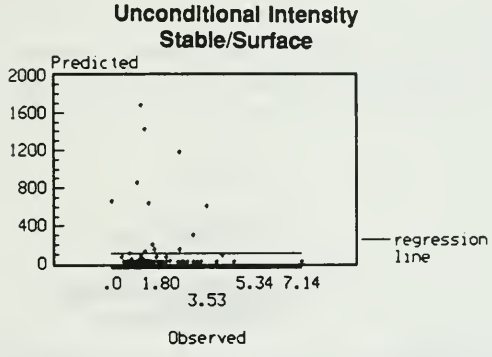

FIGURE 7-7c

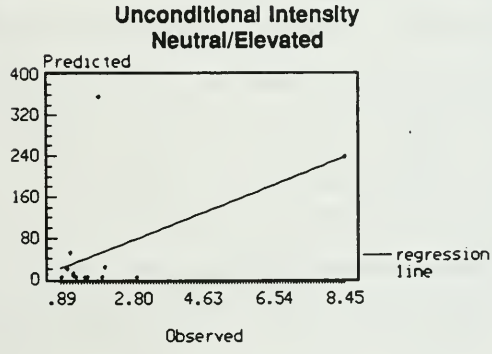

FIGURE 7-8a

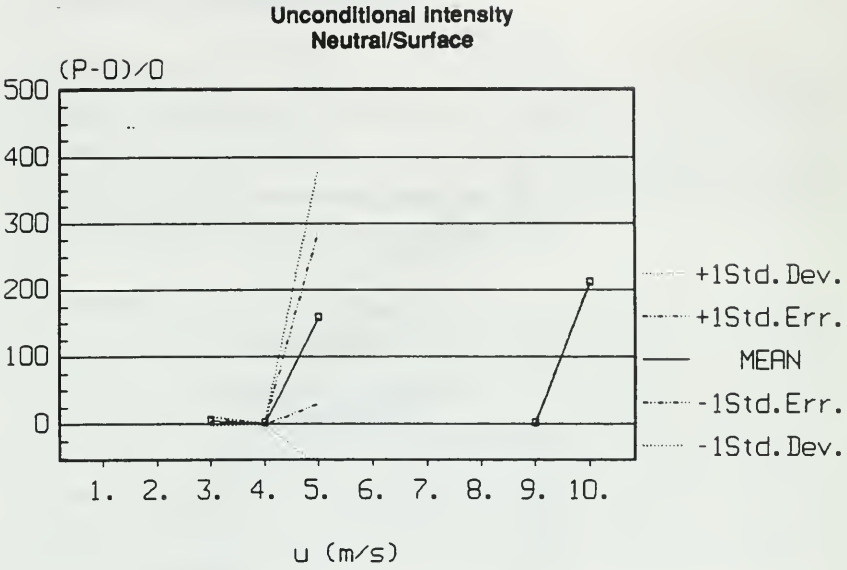

FIGURE 7-8b

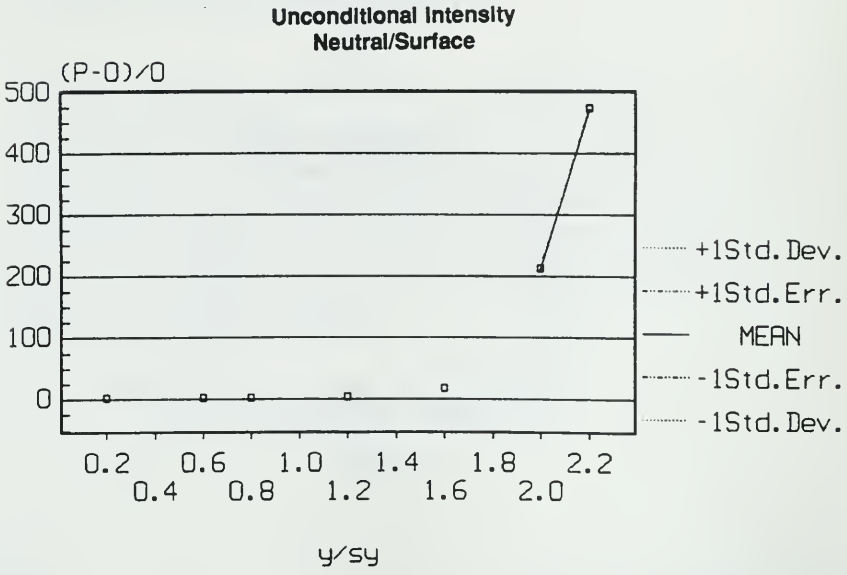

FIGURE 7-9a

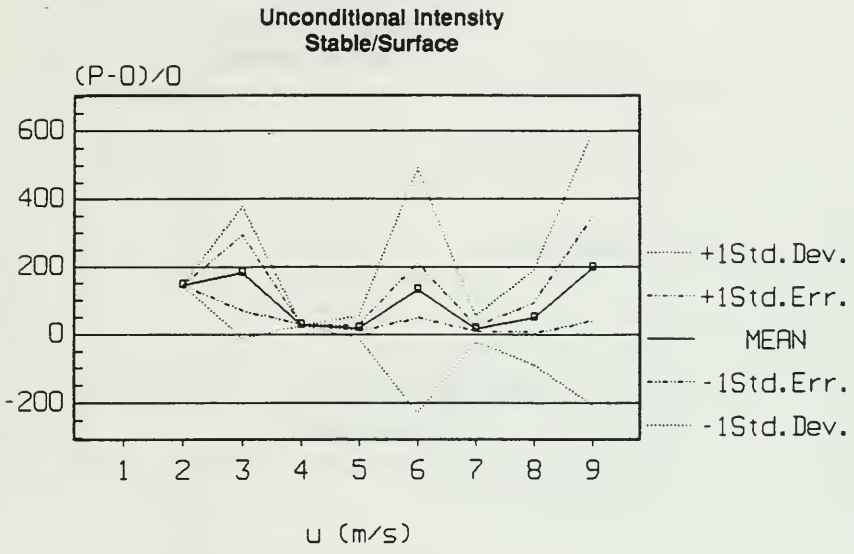

FIGURE 7-9b

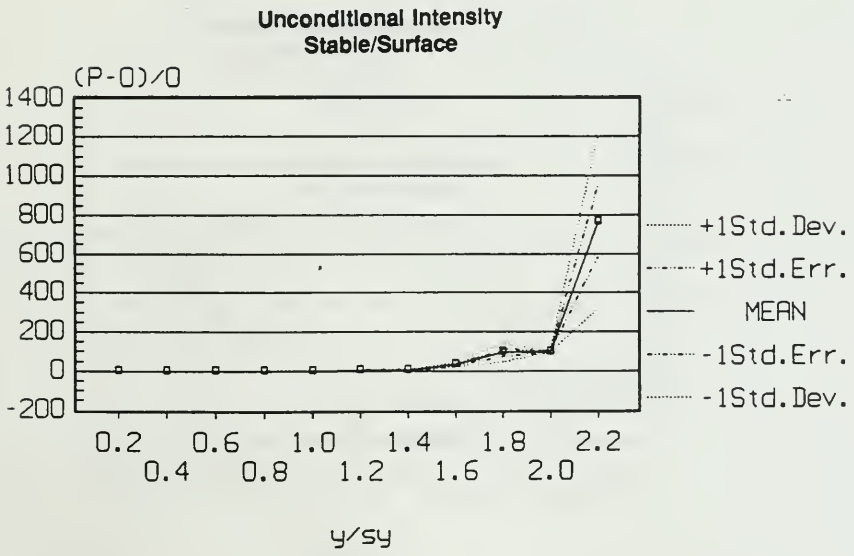

FIGURE 7-10a

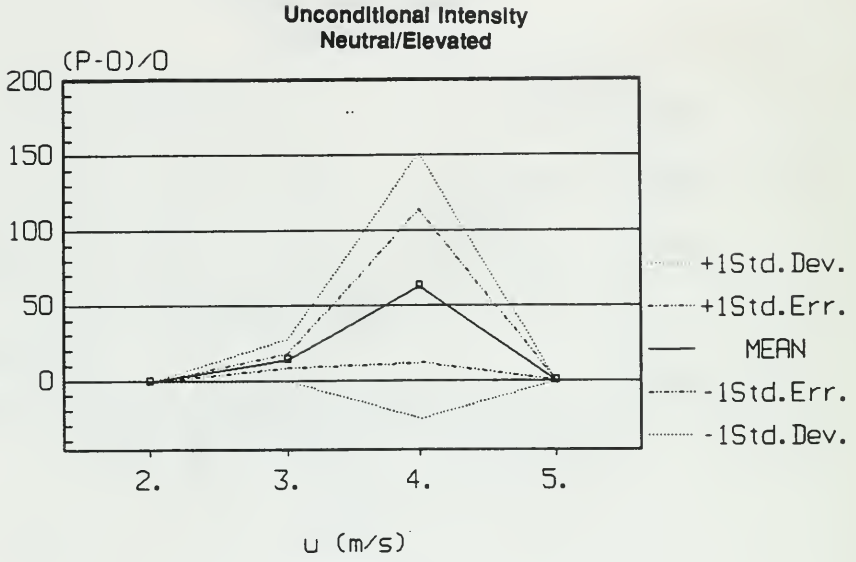

FIGURE 7-10b

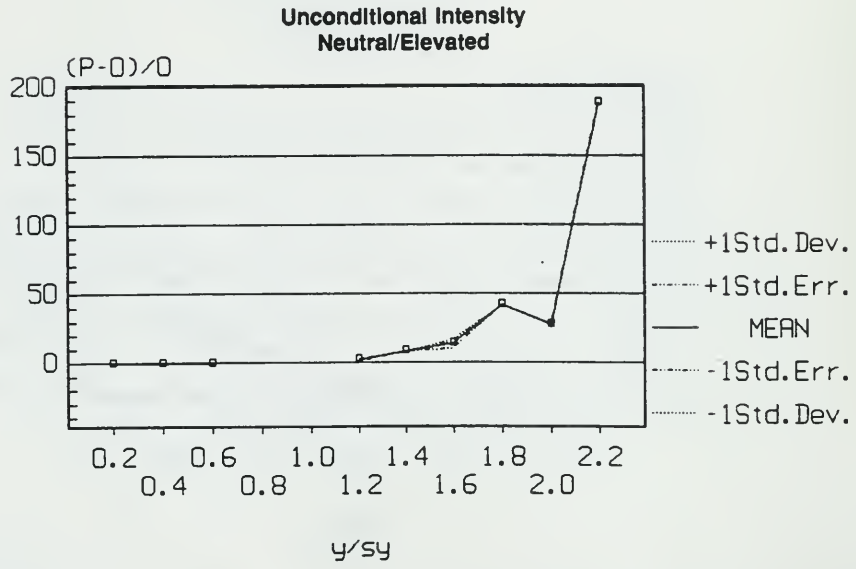

FIGURE 7-11a

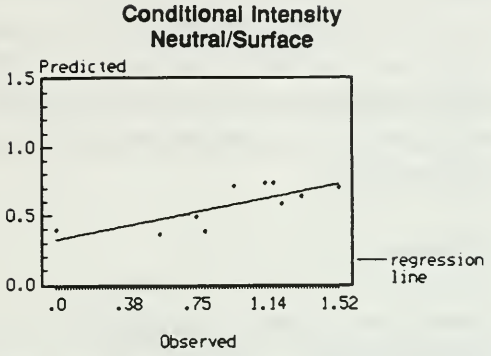

FIGURE 7-11b

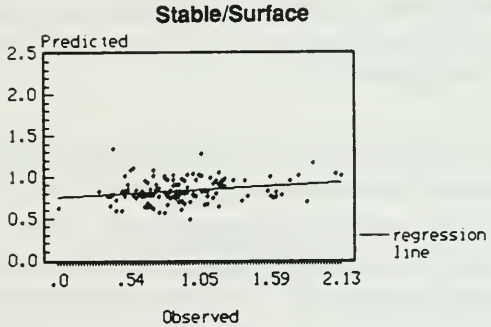

FIGURE 7-11c

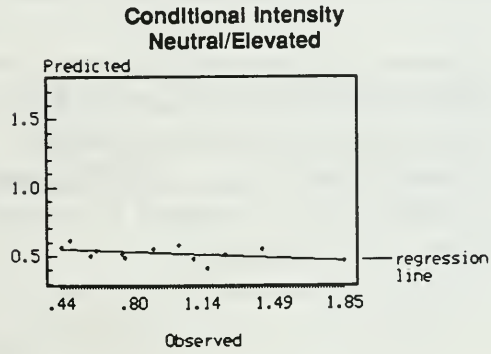

Figures 7-12 to 7-14 present the relative error versus wind speed and y/σ_y. Generally, the error falls within a fairly small range for wind speeds greater than 3 m/s. Substantial error is shown for low winds stable conditions (Figure 7-13a). The errors as a function of y/σ_y are shown in Figures 7-12b to 7-14b. The errors generally range between -0.75 to +0.25 for all scenarios, with the largest errors occurring for $y > 1.4\ \sigma_y$. The small deviations are due to i_p not being a function of y/σ_y (Equ. 3.37).

7.3.3 Intermittency

The intermittency predictions and observed pairs are presented in Figure 7-15 for the various scenarios. There is significant scatter in the data shown little correlation. The error seem to be divided evenly between systematic and unsystematic for surface release scenarios but the error is mostly unsystematic for the elevated release (Table 7-2). In all scenarios considered, γ is underpredicted by approximately 50%.

The relative errors seem to occur at the higher winds for neutral conditions and at the lower wind speeds for stable (Figures 7-16a to 7-18a). All three scenarios show the same trend with respect to y/σ_y (Figures 7-16b to 7-18b). The model tends to overpredict γ near the centreline and significantly underpredicts γ is the fringes are approached. This trend is expected since $\gamma \alpha\ 1/i^2$.

7.4 EVALUATION OF LOG-NORMAL AND EXPONENTIAL DISTRIBUTIONS

An evaluation of the log-normal and exponential distributions is presented. The log-normal is recommended by Wilson for the EGM. The evaluation compares the CDF's of both distributions against observed values. The predicted distributions use measured values of i_p, γ and the percentile to generate normalized concentrations which are compared to normalized (i.e., normalized by the measured mean) observed values.

FIGURE 7-12a

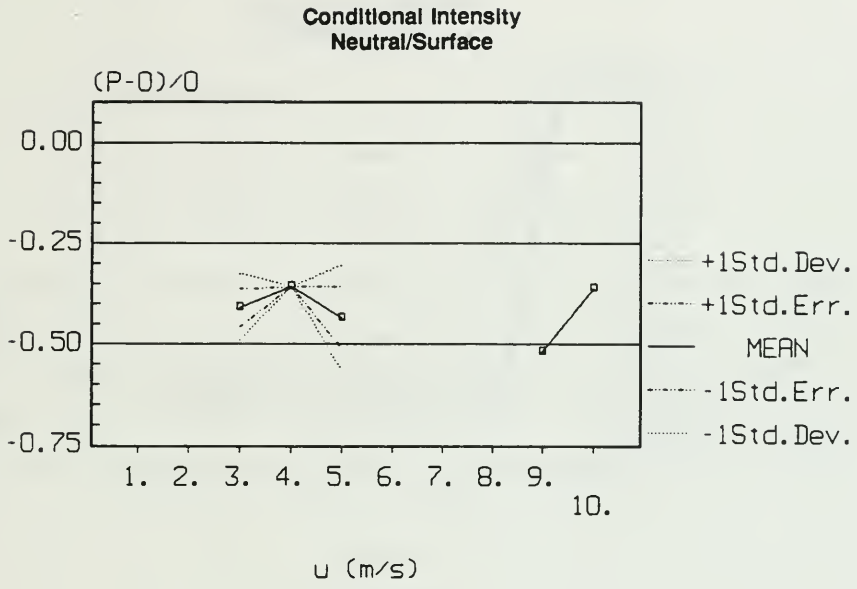

FIGURE 7-12b

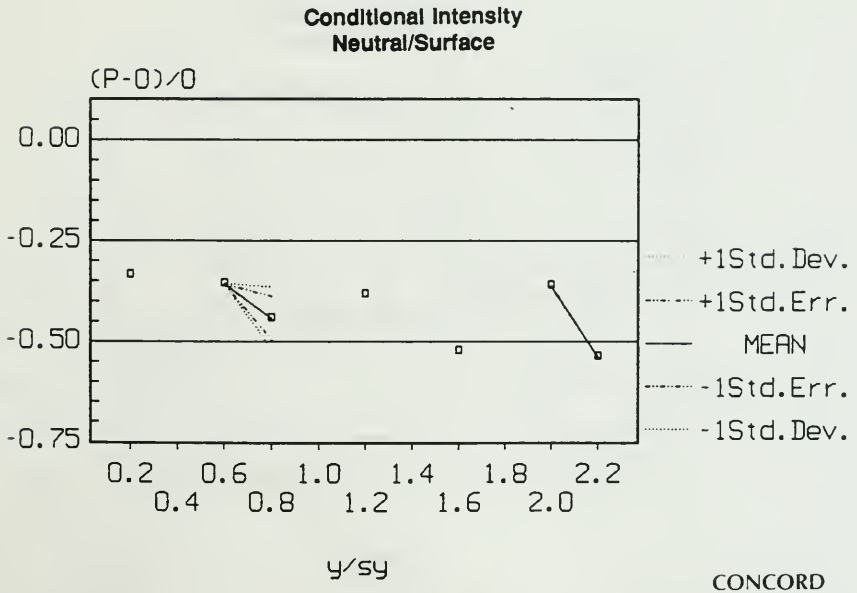

FIGURE 7-13a

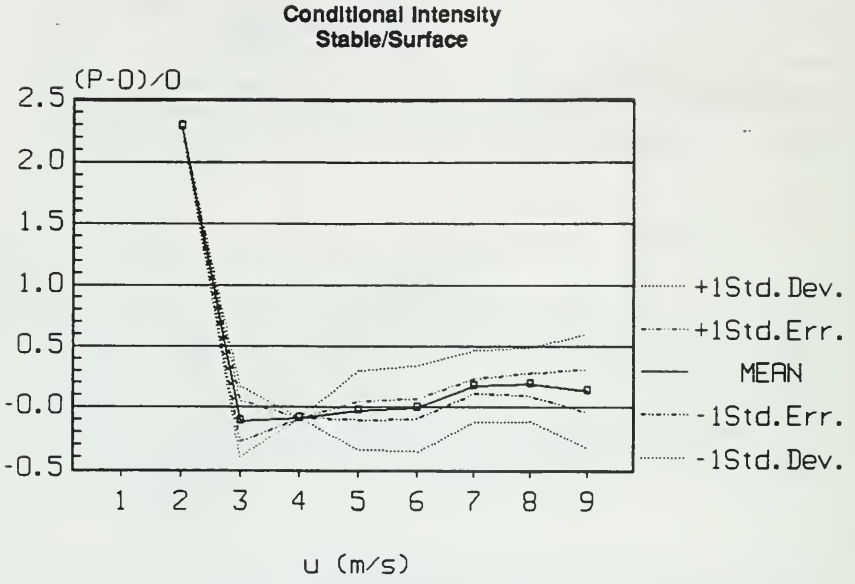

FIGURE 7-13b

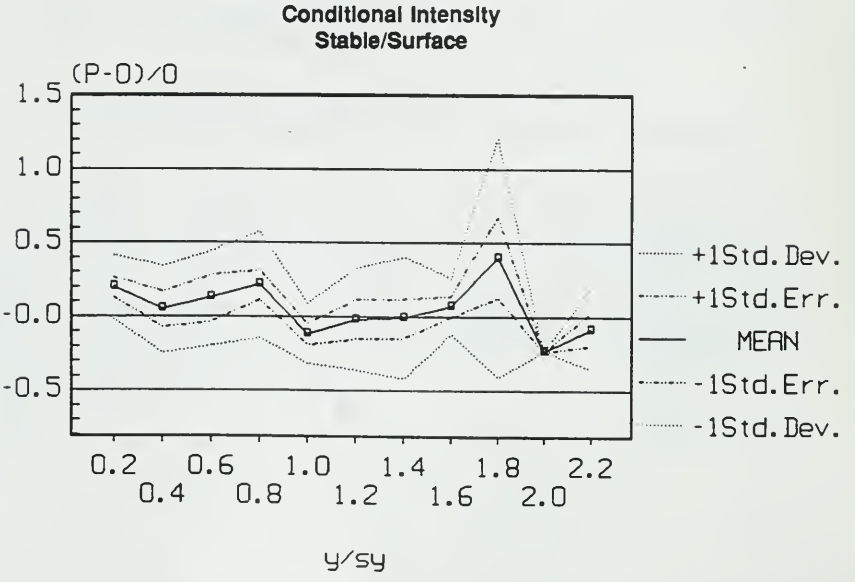

FIGURE 7-14a

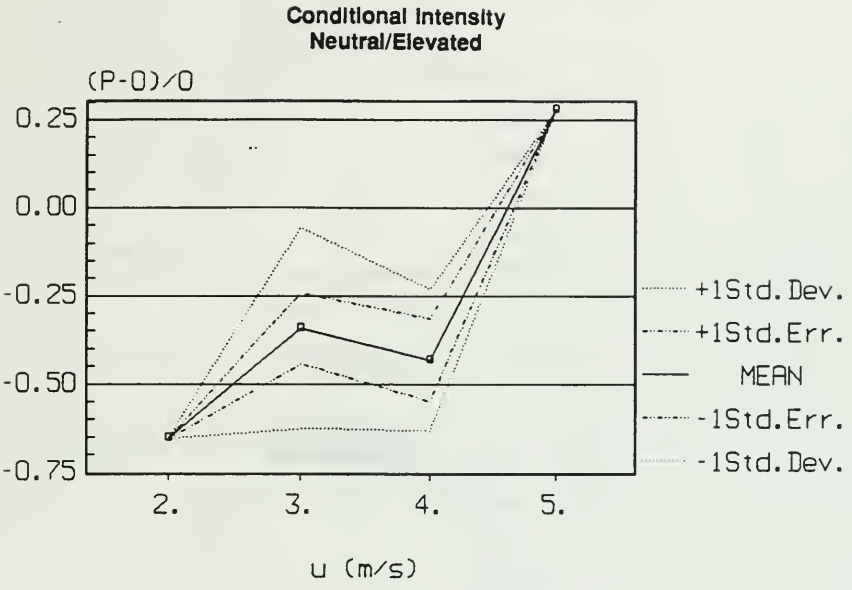

FIGURE 7-14b

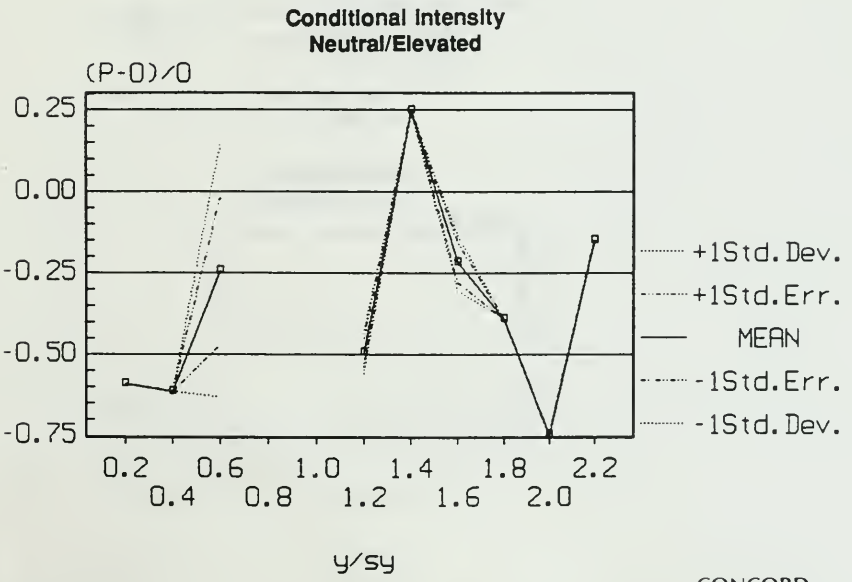

FIGURE 7-15a

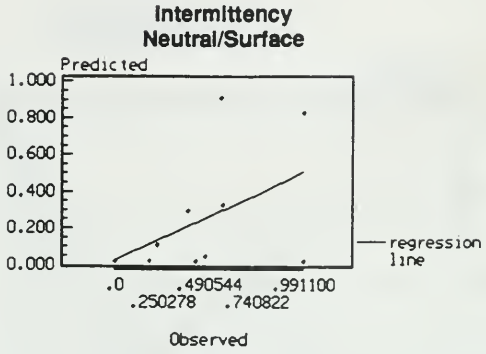

FIGURE 7-15b

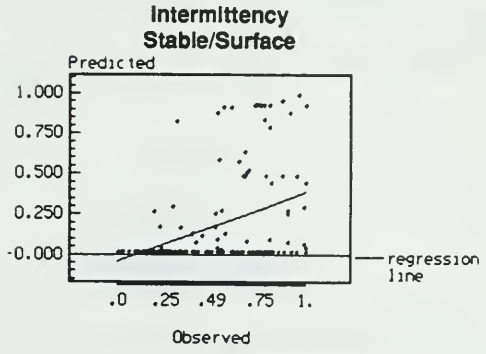

FIGURE 7-15c

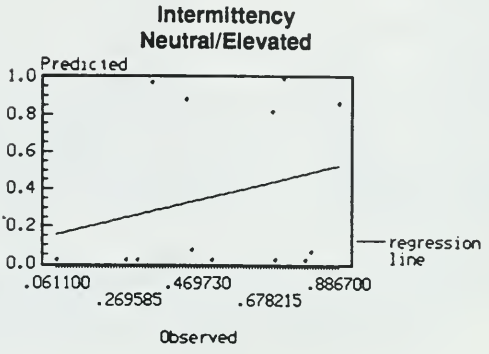

FIGURE 7-16a

Intermittency
Neutral/Surface

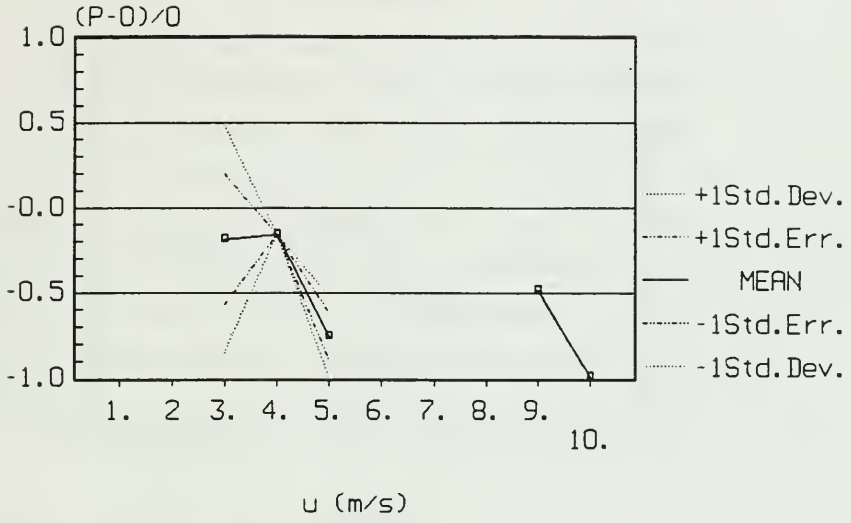

FIGURE 7-16b

Intermittency
Neutral/Surface

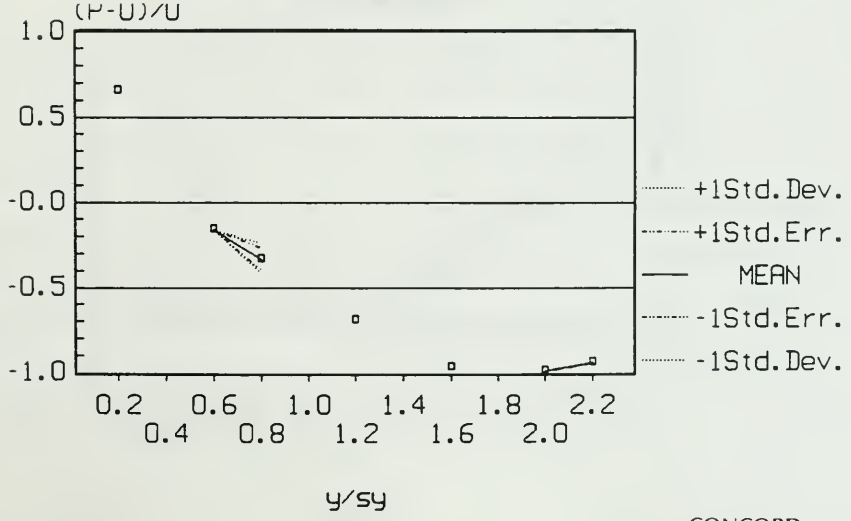

FIGURE 7-17a

Intermittency
Stable/Surface

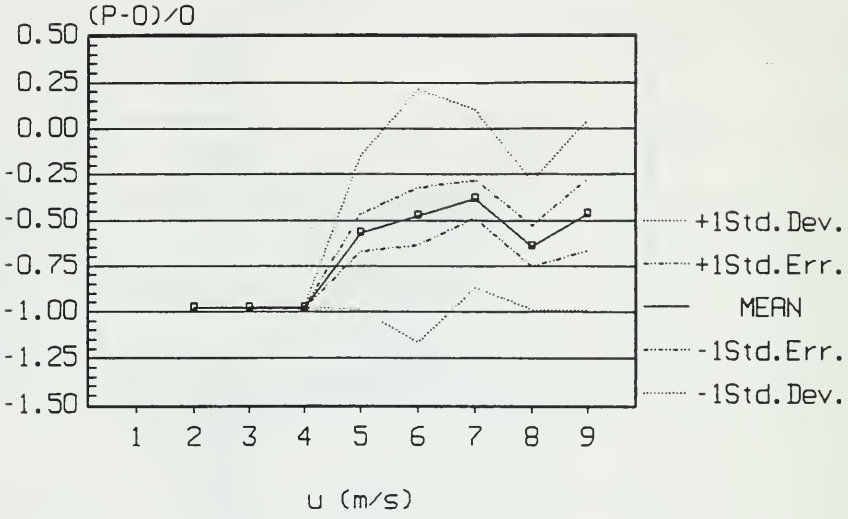

FIGURE 7-17b

Intermittency
Stable/Surface

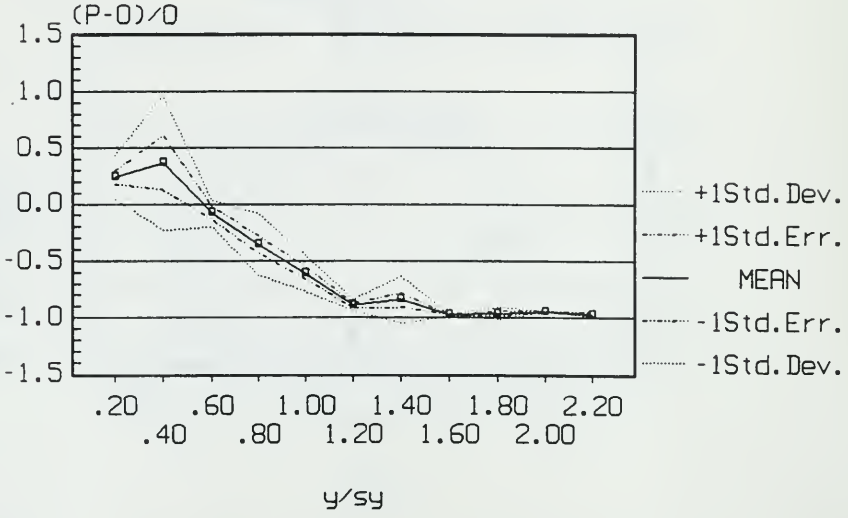

FIGURE 7-18a

Intermittency
Neutral/Elevated

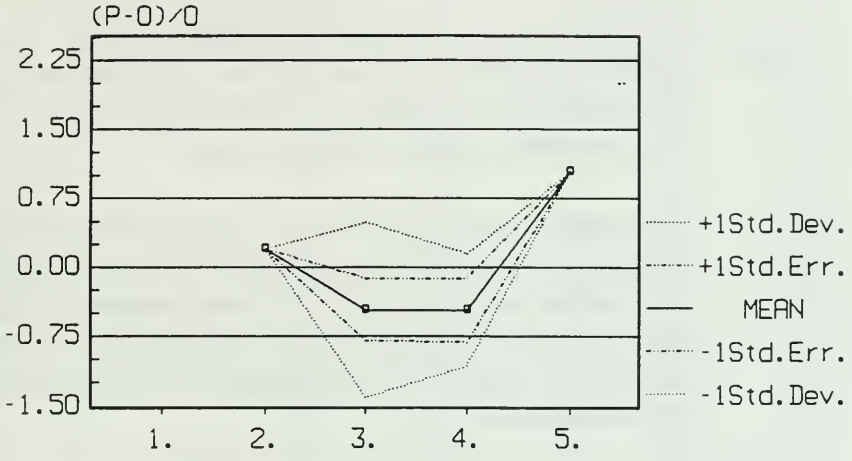

FIGURE 7-18b

Intermittency
Neutral/Elevated

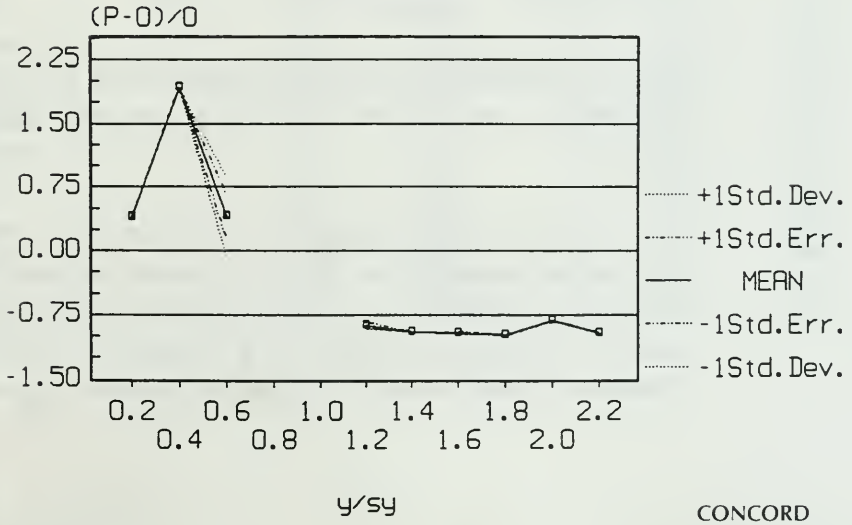

The above comparison can be made independent of the EGM since the distribution of concentrations are invariant to crosswind location and EGM results. The CDF's are effectively isolated from previous calculations.

Table 7-4 summarizes the results of the statistical analysis. The exponential model is better performer for all scenarios. The scattergrams for predicted normalized concentrations against observed is presented in Figures 7-19 to 7-22. The graphical data verifies the statistical summary.

The exponential model predicts similar averages and standard deviations vs the observed distributions for the various scenarios. The log-normal model predicts lower averages and standard deviations. The exponential has a much better index of agreement (I) than the log-normal as well as having a significantly better correlation coefficient (R). The exponential generates a slope close to one in three of the four scenarios.

Both distributions tend to overpredict concentrations (i.e., P-O/O, P/O) with the exception of stable/elevated which shows an underprediction for both models. the errors between models are within the same range. The error analysis shows that the log-normal errors are largely systematic while the exponential errors are largely unsystematic.

The primary objective of the concentration fluctuation model is to calculate peak concentrations, thus the errors associated with percentile levels becomes significant.

Figures 7-23 to 7-26 present the relative error (P-O/O) as a function of percentile, for percentiles greater than 75%-ile. For all scenarios, the log-normal model, underpredicts concentrations for percentiles greater than 85%-ile by less than a factor of 2. The exponential model tends to overpredict at the higher end and underpredict at lower percentiles. The curves are similar for both models. Both

TABLE 7-4

Summary of Statistical Indices for Log-Normal and Exponential Distributions

	Neutral/Surface			Stable/Surface		
	Observed	Log-Normal Predicted	Exponential Predicted	Observed	Log-Normal Predicted	Exponential Predicted
Count	477	477	477	1944	1944	1944
Avg	5.15	1.68	4.91	6.07	1.47	6.19
STD	7.61	1.97	7.15	11.56	1.63	11.96
Gross Error		3.65	1.50		4.74	2.06
P/O		3.33	3.41		2.03	1.96
(P-O)/O		2.33	2.41		1.03	0.96
RMSE		19.71	19.61		8.65	5.60
Intercept		0.96	0.50		1.07	0.68
Slope		0.14	0.86		0.07	0.91
R		0.54	0.91		0.46	0.88
MSEu		5%	87%		1%	97%
MSEs		95%	13%		99%	3%
I		0.48	0.95		0.34	0.93
MFE		0.46	0.01		0.58	0.09

	Neutral/Elevated			Stable/Elevated		
	Observed	Log-Normal Predicted	Exponential Predicted	Observed	Log-Normal Predicted	Exponential Predicted
Count	180	180	180	81	81	81
Avg	5.35	1.62	5.59	3.85	1.48	5.13
STD	11.99	1.95	10.63	3.98	1.55	6.68
Gross Error		3.87	2.06		2.43	1.86
P/O		1.15	1.14		0.58	0.96
(P-O)/O		0.15	0.14		-0.42	-0.04
RMSE		4.72	1.69		0.70	0.64
Intercept		1.15	1.13		0.47	-0.83
Slope		0.09	0.83		0.26	1.55
R		0.54	0.94		0.68	0.93
MSEu		2%	77%		8%	50%
MSEs		98%	23%		92%	50%
I		0.32	0.96		0.61	0.88
MFE		0.68	0.31		0.77	0.31

FIGURE 7-19a

Normalized Concentrations Percentiles
Log-Normal Vs. Observed
Neutral/Surface

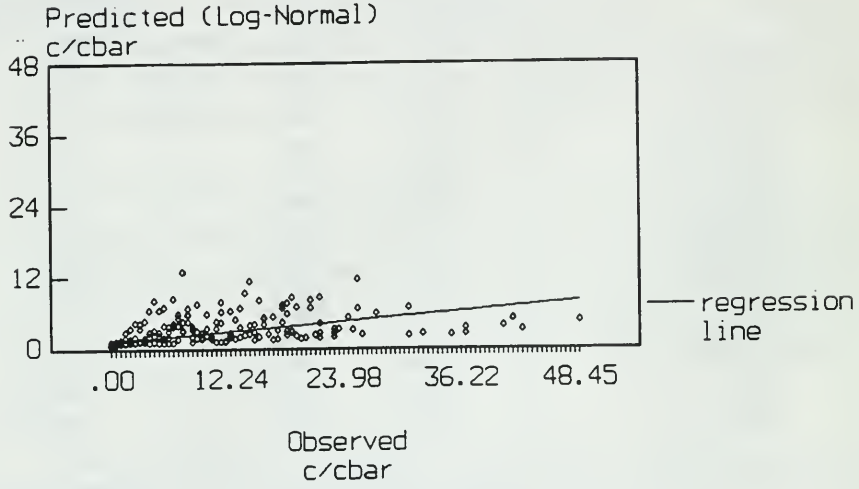

FIGURE 7-19b

Normalized Concentrations Percentiles
Exponential Vs. Observed
Neutral/Surface

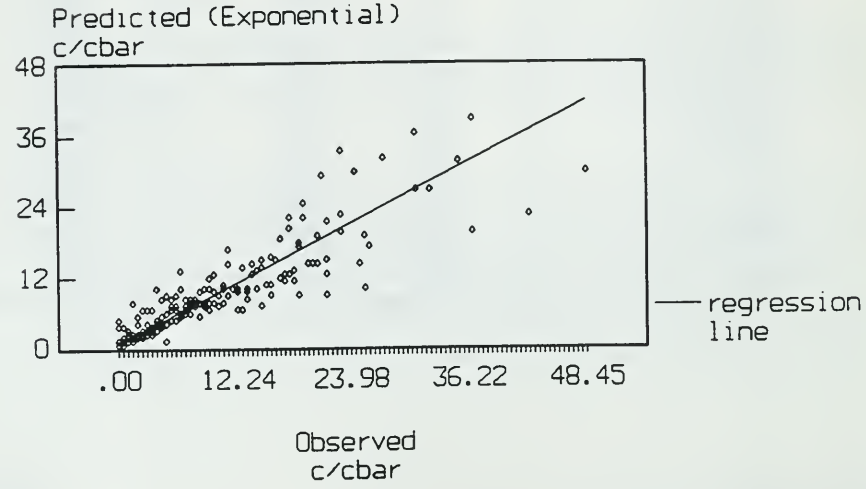

FIGURE 7-20a

Normalized Concentrations Percentiles
Log-Normal Vs. Observed
Stable/Surface

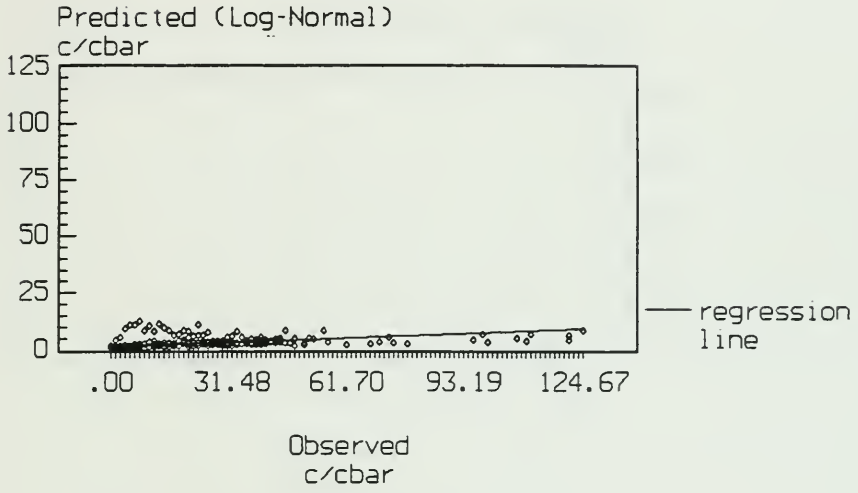

FIGURE 7-20b

Normalized Concentrations Percentiles
Exponential Vs. Observed
Stable/Surface

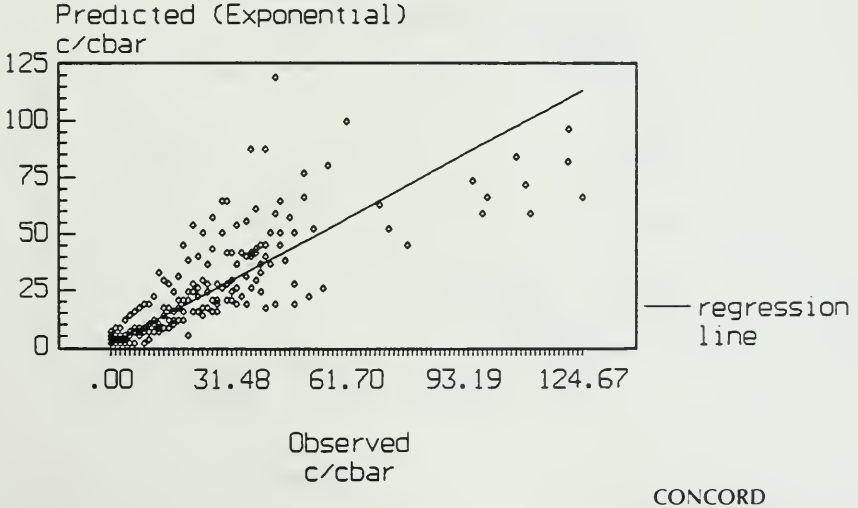

FIGURE 7-21a

Normalized Concentrations Percentiles
Log-Normal Vs. Observed
Neutral/Elevated

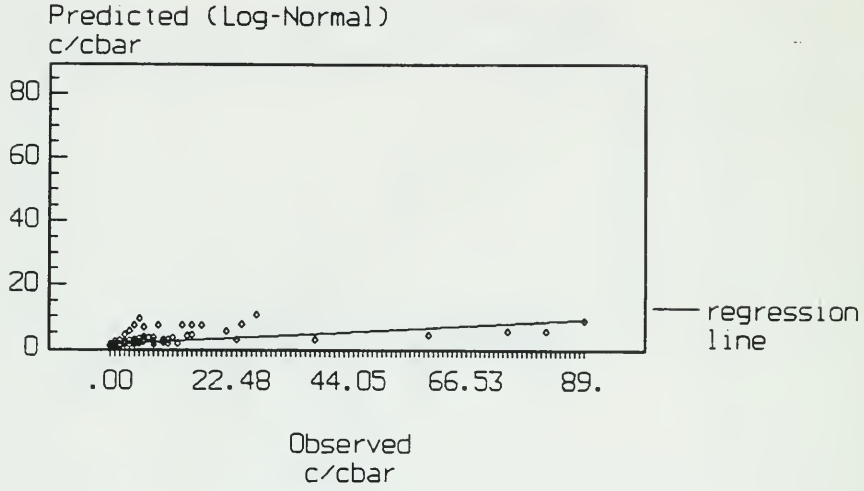

FIGURE 7-21b

Normalized Concentrations Percentiles
Exponential Vs. Observed
Neutral/Elevated

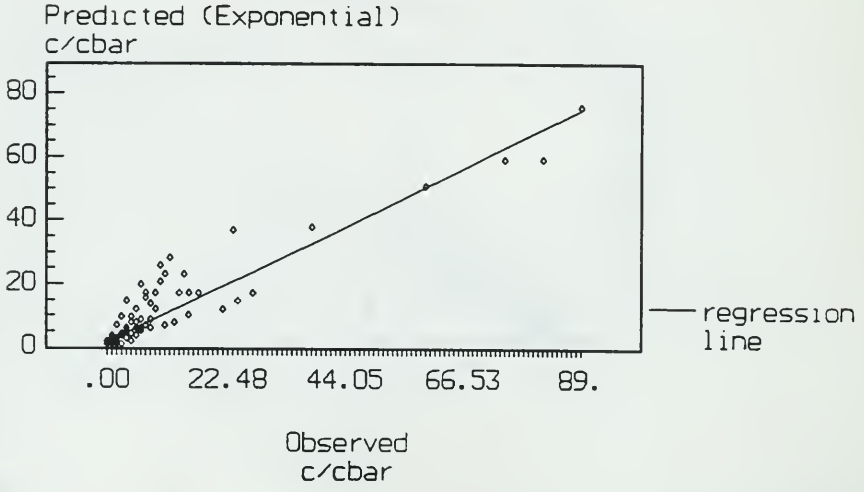

FIGURE 7-22a

Normalized Concentrations Percentiles
Log-Normal Vs. Observed
Stable/Elevated

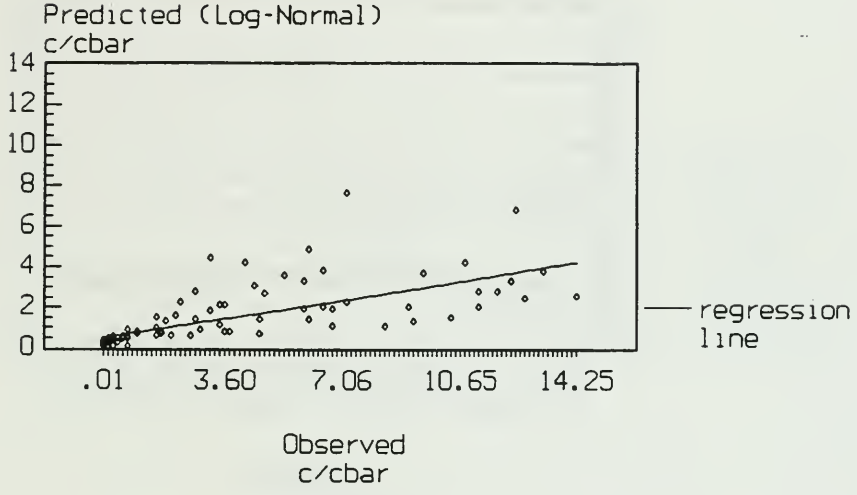

FIGURE 7-22b

Normalized Concentrations Percentiles
Exponential Vs. Observed
Stable/Elevated

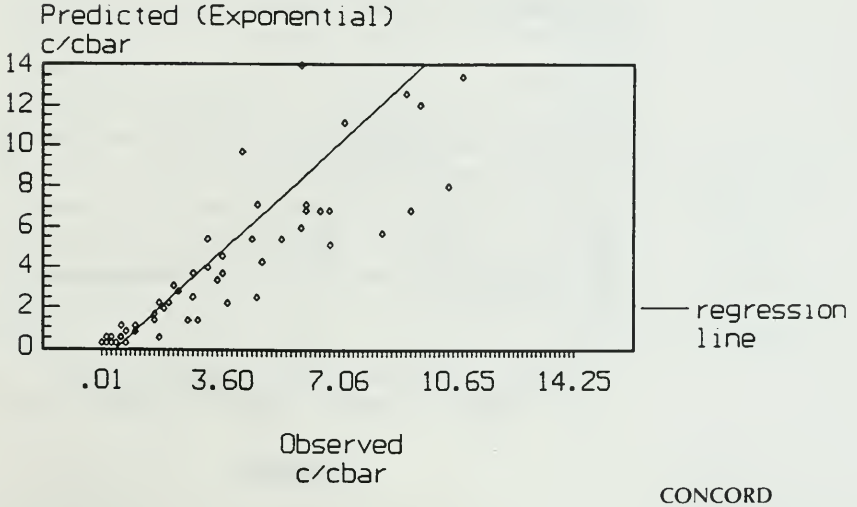

FIGURE 7-23a

Normalized Log-Normal Percentiles
Neutral/Surface

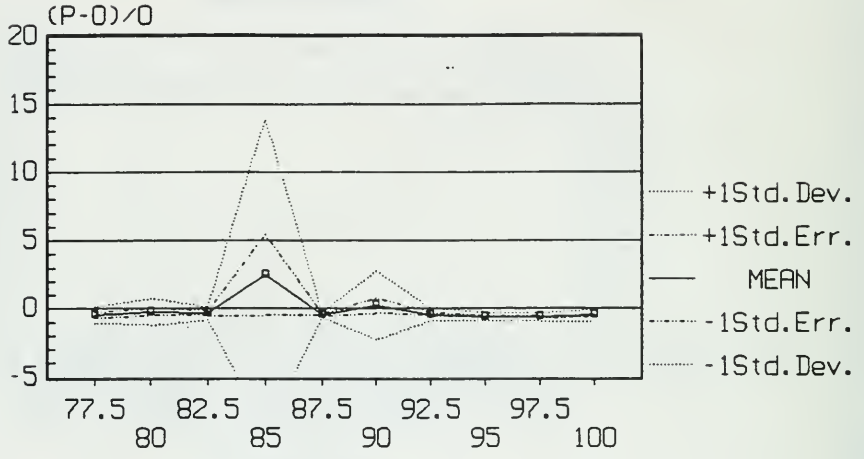

FIGURE 7-23b

Normalized Exponential Percentiles
Neutral/Surface

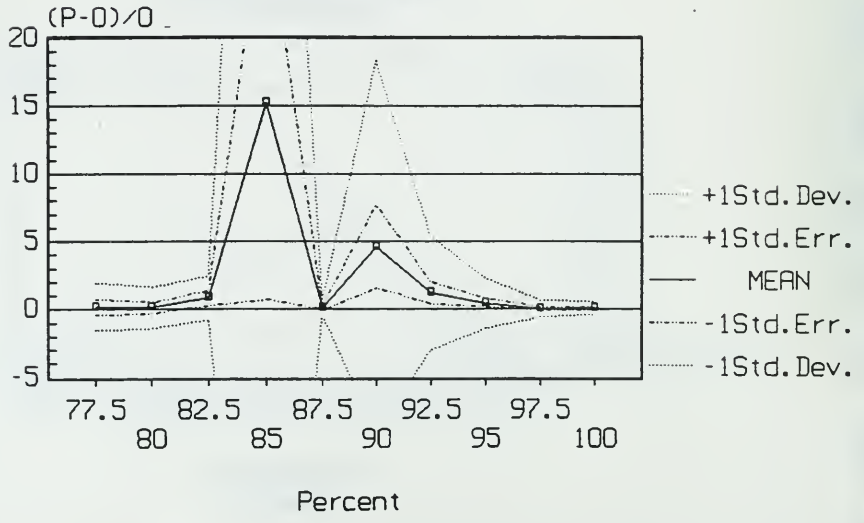

FIGURE 7-24a

Normalized Log-Normal Percentiles
Stable/Surface

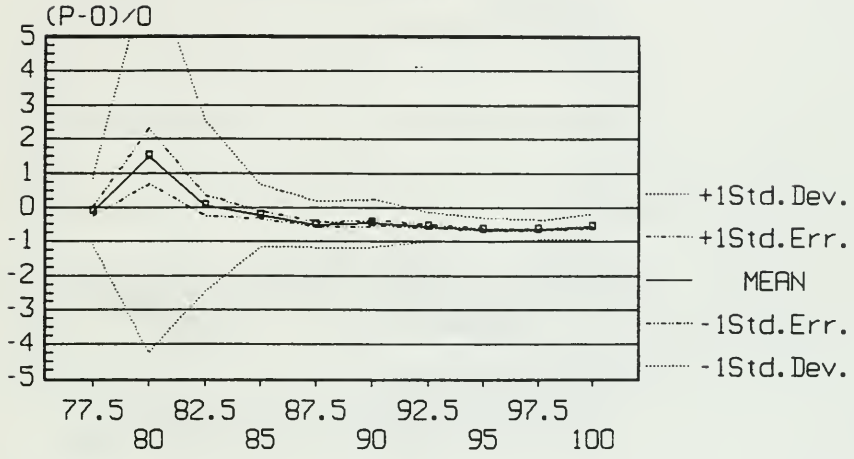

FIGURE 7-24b

Normalized Exponential Percentiles
Stable/Surface

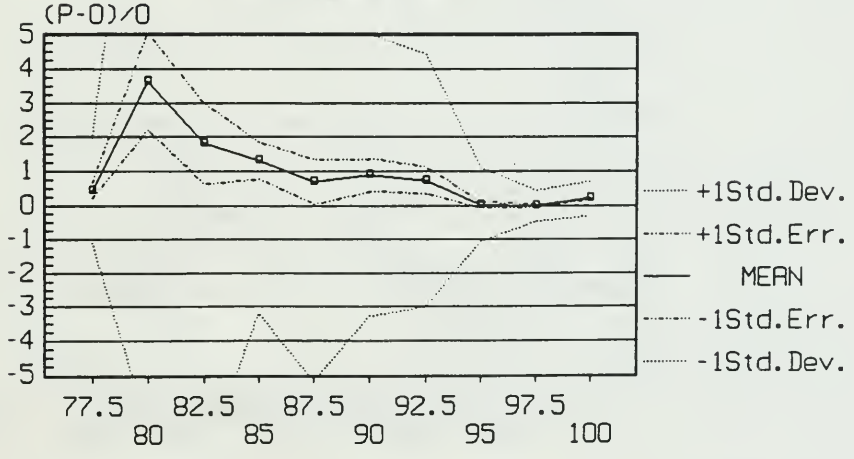

FIGURE 7-25a

Normalized Log-Normal Percentiles
Neutral/Elevated

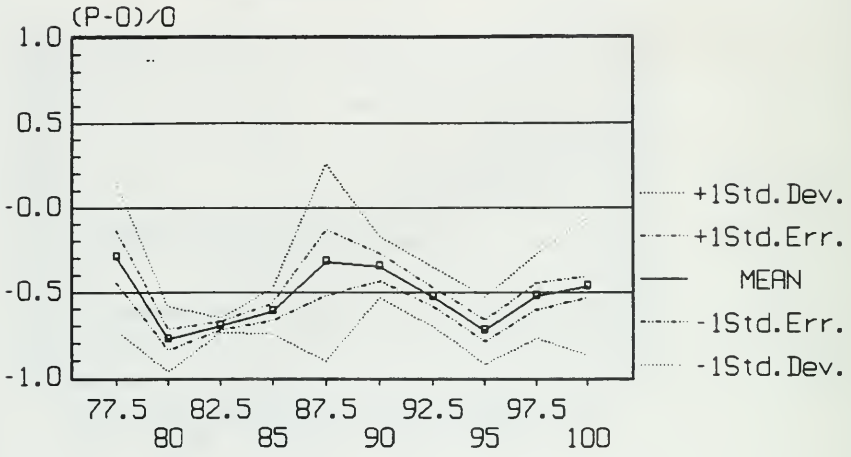

FIGURE 7-25b

Normalized Exponential Percentiles
Neutral/Elevated

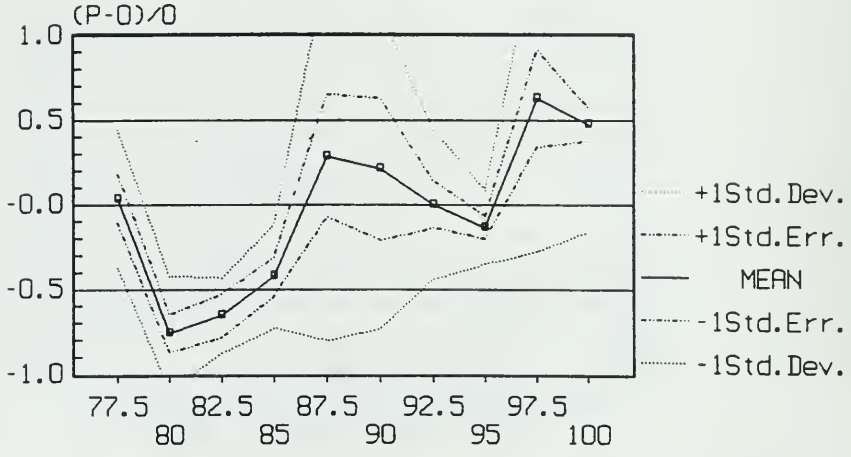

FIGURE 7-26a

Normalized Log-Normal Percentiles
Stable/Elevated

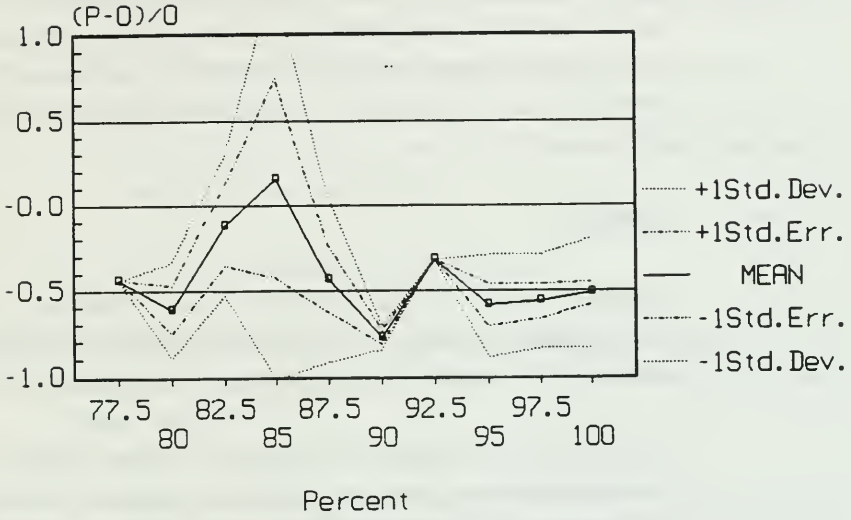

FIGURE 7-26b

Normalized Exponential Percentiles
Stable/Elevated

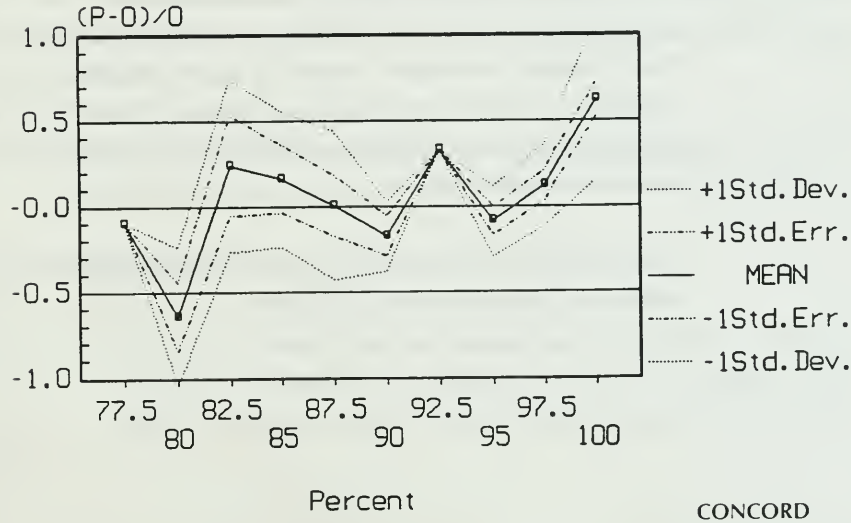

models seems to be a better performers for the ground level release than elevated release at the higher end.

Both models show a bias towards under prediction for the entire data sets, but only the exponential shows a tendency to overprediction at the higher end. This would indicate that log-normal tends to overpredict concentrations at the lower end which is not unexpected since the log-normal shows a discontinuity near the origin (Figure 3.1).

7.5 SUMMARY

The model evaluation shows that the GAS model overpredicts concentrations because of underpredictions of σ_y. The model does provide reasonable levels as a function of crosswind distance and wind speeds, especially at the higher speeds.

The EGM is a poor predictor of i for crosswind distance greater than 1.2 σ_y. These poor predictions lead to poor predictions of γ as well. The model provides good estimates of i_p but generally underpredicts i_p. The largest errors associated with i_p occur under low wind situations when meandering is likely too dominant.

The log-normal distribution was not an adequate model for predicting peak concentrations. It tended to underpredict concentrations at a higher percentiles. The exponential distribution provided a better estimate of the probability distribution. The exponential model is most applicable to highly intermittent plumes and a review of the conditional intensity shows that i_p is very close to unity and γ is approximately 0.5.

The applicability of the exponential model will likely be a function of atmospheric length scale, source diameter and elevation.

8 CONCLUSIONS AND RECOMMENDATIONS

The primary objective of the study was to develop a mathematical model to estimate the magnitude and frequency of concentration fluctuations based on the:

- current CAP model (GAS) to predict time averaged concentrations;
- Wilson's Empirical Gaussian Model (EGM) to estimate plume intermittency and concentration intensity; and
- a log-normal distribution of concentration.

The resultant modelling package provides a distribution of potential "quasi" instantaneous concentrations which make-up the more familiar mean time-averaged concentration.

The focus of the study was to evaluate the applicability of the EGM models (which was developed from wind tunnel observations) and the log-normal distribution against field measurements which were generally taken during stable atmospheric conditions. The EGM module was developed from physical principals but includes six constants which were derived via systematically fitting the developed physical equations to the wind tunnel data. A sensitivity analysis of these constants was also carried.

The conclusions and recommendations are based on the compatibility of the EGM with the GAS model and the results of the sensitivity and field data evaluation.

8.1 CONCLUSION

1. The EGM has its origin from the Gaussian plume model used for predicting mean concentrations in standard dispersion modelling packages. The module is compatible with the GAS model's treatment of elevated point

source releases in neutral and stable conditions which assume a Gaussian distribution of material in the crosswind and downwind directions. The EGM is not compatible with GAS's convective scaling "touch-down" model although the convective model assumes a Gaussian crosswind distribution. Similarly, for near surface releases, the crosswind distribution is Gaussian, but the vertical is exponential. It is likely that the EGM is more compatible with near surface releases than the convective scaling model. It should be noted that the EGM does not include plume meandering.

2. A sensitivity analysis was carried out on the six wind tunnel derived constants and their effect on the unconditional, and conditional intensities and the intermittency as a function of crosswind distance. The analysis shows that stable atmospheric conditions/surface releases are generally the least sensitive to changes in the constants.

   The graphical data shows that the conditional intensity is constant as a function of crosswind distance while the unconditional intensity is most sensitive to changes in the constant, at $y > \sigma_y$ and intermittency is most sensitive at $y < \sigma_y$.

   The sensitivity analysis concludes that the three variables are insensitive to three of the six constants (C_3, C_4 and ϕ) and extremely sensitive to one (C_1). Graphical data indicates that the conditional intensity is linearly dependent on the constants while unconditional intensity and intermittency seem non-linear. Strong changes in five of the six constants did not force conditional intensity over unity.

3. The comparison with field data showed that the GAS model underpredicted σ_y and correspondingly overpredicted concentrations. The GAS model showed fairly good agreement with crosswind predicted concentrations as well as with wind speeds.

The results of EGM comparison shows that the model is a good predictor of conditional intensity but a poor predictor of unconditional intensity and intermittency. The model tended to substantially overpredict unconditional intensity while underpredicting conditional intensity and intermittency. The errors associated with conditional intensity occurred at low speeds when plume meandering is likely to occur. The largest errors associated with intermittency and unconditional intermittency occur at $y > 1.2\ \sigma_y$. The instability occurs much closer to the plume centreline than previously indicated. The correction for intermittency instability as suggested by Wilson tends to reduce its error and thus improve the agreement between observed and predicted intermittency.

4. The comparison between the log-normal and exponential distributions with measured data indicates that the exponential is by far the superior model. The log-normal model tends to underpredict the frequency of high concentrations while the exponential tends to overpredict.

The exponential model is most applicable for highly intermittent plumes (i.e., the intermittency very much less than unity) where the conditional intensity is unity. A review of the observed data confirms that the conditional intensity is close to unity and that the intermittency is approximately 50%.

It is of interest to note that the exponential out performs the log-normal for both surface and elevated scenarios. The relative distance between source and receptor is generally shorter for the surface releases (~ 700 m) than the elevated (~ 1400 m). This indicates that the relative distance and source extent to turbulent length scale are important parameters in determining when the exponential is no longer applicable.

8.2 RECOMMENDATIONS

From the work carried out, a number of recommendation are suggested for the current modelling system and future work.

1. The EGM module can be used with certain restrictions. The model is theoretically compatible and acceptable for use with the GAS neutral and stable elevated release models and incompatible with the convective scaling model. The EGM model is acceptable for use with the near surface releases. The model is very unstable at the plume fringes and should be used at crosswind distances of $y \leq \sigma_y$.

2. From the available literature survey, Venkatram's conditional intensity model should be used for elevated releases in convective conditions.

3. From recent literature, Chatwin and Sullivan (1990) show that the unconditional concentration variance can be predicted via,

$$\overline{c'^2} = B\,\bar{c}\,(A\,\bar{c}_o - \bar{c}) \qquad [8.1]$$

where $\bar{c}_o$ and $\bar{c}$ are the concentrations at the centreline and receptor and A and B are constants derived from fitting to a variety of experiments including Fackrell and Robins (1982) data. The fit to the data is much better than Wilson's equations. The above simple and universal function suggests further examination against full-scale experiments is required.

Further, the other models presented in Section 3 should also be evaluated against full-scale experiments if they are compatible with the GAS model. This also includes Wilson's new modelling set which includes plume meandering (Wilson and Zelt, 1990).

4. The range of applicability of the exponential distribution must be determined. The exponential model is suitable for highly intermittent conditions such as low wind stable conditions or when meandering is highly prevalent. The range will depend on the source size relative to the length scale of atmospheric turbulence as well as downwind distance.

5. Further work with the clipped-normal distribution should be pursued rather than the log-normal distribution. The clipped normal is likely the most applicable over a wider range of conditions.

   It should be noted that the exponential and clipped-normal models require only estimates of $\overline{c}$ and unconditional intensity or variance to determine the peak concentrations while the log-normal requires conditional intensity, intermittency and $\overline{c}$. This reduces the requisite equation set as developed by Wilson for the log-normal model.

6. The modelling systems created should be evaluated against a wider range of full-scale data sets which include convective conditions.

REFERENCES

Barry, P.J., 1975: **Stochastic Properties of Atmospheric Diffusivity. Atomic Energy of Canada Limited**, AECL-5012, Chalk River Nuclear Laboratories.

Chatwin P.C. and Sullivan P.J., 1979: "The Basic Structure of Clouds of Diffusing Contaminant", In **Mathematical Modelling of Turbulent Diffusion in the Environment**, ed. C. J. Harris, 3-31, Academic Press.

Chatwin P.C. and Sullivan P.J., 1990: "A Simple and Unifying Physical Interpretation of Scalar Fluctuation Measurements From Many Turbulent Shear Flows", **J. Fluid Mech.**, 212: 533-556.

Csanady, G.T., 1967: "Concentration Fluctuations in Turbulent Diffusion", **J. Atmos. Sci.**, 24:21-28.

Csanady, G.T., 1973: **Turbulent Diffusion in the Environment**, D. Reidel, Dordrecht, Holland.

Dinar, N., Kaplan, H. and Kleiman, M., 1988: "Characterization of Concentration Fluctuations of a Surface Plume in a Neutral Boundary Layer", **Boundary Layer Met.**, 45:157-175.

Durbin, P.A., 1980: "A Stochastic Model of Two Particle Dispersion and Concentration Fluctuations in Plumes", **Boundary-Layer Met.**, 22:335-350.

Energy Resources Conservation Board, 1990: **Field Measurement Program Atmospheric Dispersion Tracer Study and Stable Conditions and Meteorological Study**, ERCB Report 90-B Volume 1, Calgary.

Fackrell J.E. and Robbins A.G., 1982a: "Concentration Fluctuations and Fluxes in Plumes from Point Sources in a Turbulent Boundary-Layer", **J. Fluid Mech**, 117:1-26.

Fackrell J.E. and Robbins A.G., 1982b: "The Effect of Source Size on Concentration Fluctuations in Plumes", **Boundary-Layer Met.**, 22:335-350.

Fox, D.G., 1981: "Judging Air Quality Model Performance-A Summary of The AMS Workshop on Dispersion Model Performance", **Bull. Am. Meteor. Soc., 62:599-609.**

Gifford, F.A., 1972: "The Form of the Frequency Distribution of Air Pollution Concentrations", **Synp. on Statistical Aspects of Air Quality Data**, Chapill Hill, N.C.

Halitsky, J., 1961: "Single Camera Measurement of Smoke Plumes", **Inter. J. Air and Water Pol.**, 4:1147.

Hanna, S.R., 1984a: "Concentration Fluctuations in a Smoke Plume", **Atmos. Envlon.**, 18:1091-1106.

Hanna, S.R., 1984b: "The Exponential Probability Density Function and Concentration Fluctuations in Smoke Plumes", **Boundary Layer Met.**, 29:361-375.

Hanna, S.R., 1988: "Air Quality Model Evaluation and Uncertainty", **J. Air. Pollut. Control Ass.**, 38:406-412.

Kaplan, H. and Dinar, N., "A Stochastic Model for Dispersion and Concentration Distribution in Homogeneous Turbulence", **J. Fluid Mech.**, 190:121-140.

Lamb, R.G., 1982: "Diffusion in the Convective Boundary Layer", In **Atmospheric Turbulence and Air Pollution Modelling**, eds. F.T.M. Nieuwstadt and H. VonDop, 159-229, D. Reidel, Dordrecht, Holland.

Lee, J.T. and Stone, G.L., 1983: "The Use of Eulerian Initial Conditions in a Lagrangian Model of Turbulence Diffusion", **Sixth Symp. on Turb. and Diff.**, AMS, Boston, 12-17.

Lewellen, W.S. and Sykes, R.I., 1983: "On the Use of Concentration Variance Predictions as a Measure of Natural Uncertainty in Observed Concentration Samples", **Sixth Symp. on Turb. and Diff.**, AMS, Boston, 47-50.

Mage, D.T., 1975: "An Improved Statistical Model for Analysing Air Pollution Concentration Data", Paper 75-51.4, Presented at **68th Meeting of the Air Pollution Control Association.**

Mylne, K.R. and Mason, P.J., 1990: "Concentration Fluctuation Measurements in a Dispersing Plume at a Range of up to 1000 m", Submitted to **Q.J.R. Met. Soc.**

Ontario Ministry of the Environment, 1990: **Clean Air Program: Stopping Air Pollution at its Source**, Environment Ontario, Toronto.

Nappo, C.J., 1983: "Turbulent Parameters Derived From Smoke-Plume Photoanalysis", **Sixth Symp. on Turb. and Diff.**, AMS, Boston, 47-50.

Netterville, D.D.J., 1979: **Concentration Fluctuations in Plumes**, Env. Res. Monograph 1979-4, Syncrude Canada Ltd. Edmonton.

Pendergrass, W.R. and Rao, K.S., 1984: "Evaluation of the Pollution Episodic Model using RAPS Data", **NOAA Technical Memorandum ERL ARL-128**, EPA-600/3-84-087, USEPA, Research Triangle Park.

Ramsdell J.V. and Hinds W.T., 1971: "Concentration Fluctuations and Peak-To-Mean Concentration ratios in Plumes from a Ground-Level Continuous Point Source", **Atmos. Environ.** 5:483-495.

Rao, S.T., Sistla, G., Pagnotti, V., Petersen, W.B., Irwin, J.S. and Turner, D.B., 1985: "Evaluation of the Performance of RAM with Regional Air Pollution Study Data Base", **Atmos. Environ.**, 19:229-245.

Sawford, B.L., 1983: "The Effects Of Gaussian Particle-Pair Distribution Functions In the Statistical Theory of Concentration Fluctuations in Homogeneous Turbulence", **Q. Jl. R. Met. Soc.**, 190:339-354.

Sawford, B.L., 1987: "Conditional Concentration Statistics for Surface Plumes in the Atmospheric Boundary Layer", **Boundary Layer Met.**, 38:209-223.

Sykes, R.I., Lewellen, W.S. and Parker, S.F., 1984: "A Turbulent Transport Model for Concentration Fluctuations and Fluxes. **J. Fluid. Mech.**, 139: 193-218.

Venkatram, A. 1980: "Dispersion from an Elevated Source in a Convective Boundary Layer", **Atmos. Environ**, 15:447-452.

Venkatram A., 1984: "The Uncertainty in Estimating Dispersion in the Convective Boundary-Layer", **Atmos. Envion.**, 18:307-310.

Willmott, C.J., 1982: "Some Comments on the Evaluation of Model Performance", **Bull. Am. Meteor. Soc.**, 63:1309-1313.

Wilson, D.J., 1982: **Predicting Risk of Exposure to Peak Concentrations in Fluctuating Plumes**, Prepared for Alberta Environment by the University of Alberta.

Wilson, D.J., 1986: **Plume Dynamics and Concentration Fluctuations in Gas Emissions**, Prepared for Alberta Environment by the University of Alberta.

Wilson, D.J., Robbins A.G. and Fackrell J.E., 1982a: "Predicting the Spatial Distribution of Concentration Fluctuations From a Ground Level Source", **Atmos. Envion.**, 16:497-504.

Wilson, D.J., Robbins A.G. and Fackrell J.E., 1982b: "Concentration Fluctuations in an Elevated Plume: A Diffusion-Dissipation Approximation", **Atmos. Envion.**, 16:2581-2589.

Wilson, D.J. and Simms, B.W. 1985: **Exposure Time Effects on Concentration Fluctuations in Plumes**, Prepared for Alberta Environment by the University of Alberta.

Wilson, D.J. and Zelt, B.W., 1990: **Technical Basis for EXPOSURE-1 and SHELTER-1 Models for Predicting Outdoor, Indoor and Evacuation Exposures in Dispersing Toxic Gas Plumes**, University of Alberta, Department of Mechanical Engineering Report 73.

Wyngaard, J.C., 1982: " Boundary-Layer Modelling", In **Atmospheric Turbulence and Air Pollution Modelling**, eds. F.T.M. Nieuwstadt and H. VanDop, 69-106, D. Reidel, Dordrecht, Holland.